

Modeling and Verification of Distributed Generation and Voltage Regulation Equipment for Unbalanced Distribution Power Systems

**Annual Subcontract Report
June 2007**

M.W. Davis
*DTE Energy
Detroit, Michigan*

R. Broadwater
*Electrical Distribution Design, Inc.
Blacksburg, Virginia*

J. Hambrick
*Virginia Polytechnic Institute and State University
Blacksburg, Virginia*

**Subcontract Report
NREL/SR-581-41885
July 2007**



Modeling and Verification of Distributed Generation and Voltage Regulation Equipment for Unbalanced Distribution Power Systems

Annual Subcontract Report
June 2007

M.W. Davis
DTE Energy
Detroit, Michigan

R. Broadwater
Electrical Distribution Design, Inc.
Blacksburg, Virginia

J. Hambrick
Virginia Polytechnic Institute and State University
Blacksburg, Virginia

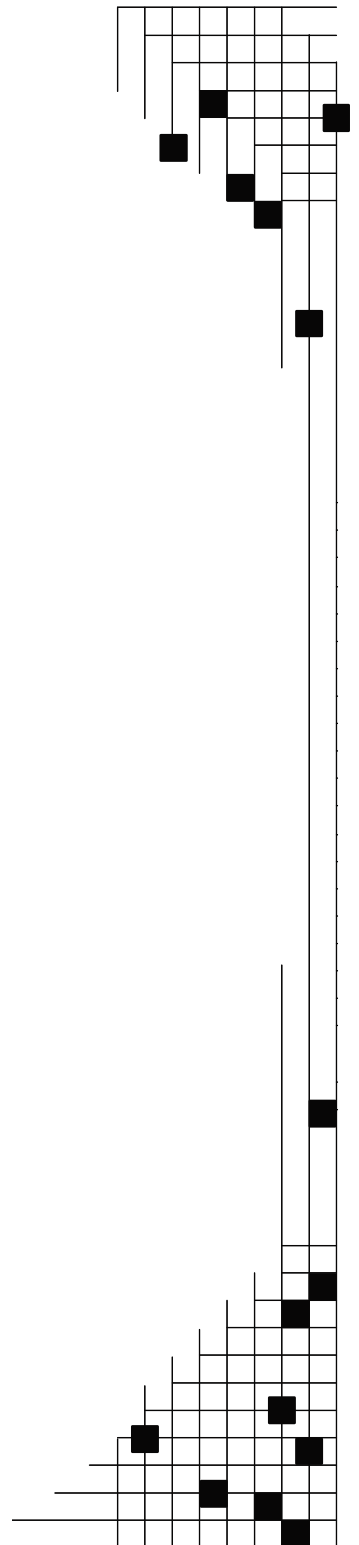
NREL Technical Monitor: T. Basso
Prepared under Subcontract No. ZAT-5-32616-06

National Renewable Energy Laboratory
1617 Cole Boulevard, Golden, Colorado 80401-3393
303-275-3000 • www.nrel.gov

Operated for the U.S. Department of Energy
Office of Energy Efficiency and Renewable Energy
by Midwest Research Institute • Battelle

Contract No. DE-AC36-99-GO10337

Subcontract Report
NREL/SR-581-41885
July 2007



The National Renewable Energy Laboratory is a national laboratory of the U.S. Department of Energy (DOE) managed by Midwest Research Institute for the U.S. Department of Energy under Contract Number DE-AC36-99GO10337. This report was prepared as an account of work sponsored by the California Energy Commission and pursuant to a M&O Contract with the United States Department of Energy (DOE). Neither Midwest Research Institute, nor the DOE, nor the California Energy Commission, nor any of their employees, contractors, or subcontractors, makes any warranty, express or implied, or assumes any legal liability or responsibility for the accuracy, completeness, or usefulness of any information, apparatus, product, or process disclosed, or represents that its use would not infringe privately owned rights. Reference herein to any specific commercial product, process, or service by trade name, trademark, manufacturer, or otherwise, does not necessarily constitute or imply its endorsement, recommendation, or favoring by Midwest Research Institute, or the DOE, or the California Energy Commission. The views and opinions of authors expressed herein do not necessarily state or reflect those of Midwest Research Institute, the DOE, or the California Energy Commission, or any of their employees, or the United States Government, or any agency thereof, or the State of California. This report has not been approved or disapproved by Midwest Research Institute, the DOE, or the California Energy Commission, nor has Midwest Research Institute, the DOE, or the California Energy Commission passed upon the accuracy or adequacy of the information in this report.

NOTICE

This report was prepared as an account of work sponsored by an agency of the United States government. Neither the United States government nor any agency thereof, nor any of their employees, makes any warranty, express or implied, or assumes any legal liability or responsibility for the accuracy, completeness, or usefulness of any information, apparatus, product, or process disclosed, or represents that its use would not infringe privately owned rights. Reference herein to any specific commercial product, process, or service by trade name, trademark, manufacturer, or otherwise does not necessarily constitute or imply its endorsement, recommendation, or favoring by the United States government or any agency thereof. The views and opinions of authors expressed herein do not necessarily state or reflect those of the United States government or any agency thereof.

Available electronically at <http://www.osti.gov/bridge>

Available for a processing fee to U.S. Department of Energy and its contractors, in paper, from:

U.S. Department of Energy
Office of Scientific and Technical Information
P.O. Box 62
Oak Ridge, TN 37831-0062
phone: 865.576.8401
fax: 865.576.5728
email: <mailto:reports@adonis.osti.gov>

Available for sale to the public, in paper, from:

U.S. Department of Commerce
National Technical Information Service
5285 Port Royal Road
Springfield, VA 22161
phone: 800.553.6847
fax: 703.605.6900
email: orders@ntis.fedworld.gov
online ordering: <http://www.ntis.gov/ordering.htm>

This publication received minimal editorial review at NREL



Printed on paper containing at least 50% wastepaper, including 20% postconsumer waste

Executive Summary

Introduction

An earlier study (Davis 2003) of the limits of distributed generation (DG) penetration indicated that DG generators in a wide range of sizes (rated in megavolt-amperes, or MVA) can be interconnected to a specific distribution circuit. The size limit is dependent on the system voltage, the location of DG on the circuit, system protection issues, voltage regulation issues, and other issues related to DG and circuit characteristics. This study showed that the size of the DG generator can be much larger if it is allowed to actively regulate voltage rather than operate at a fixed unity power factor.

Operating the DG generator at a fixed power factor has minimum effect on the traditional voltage regulation controls of a circuit because, as the system voltage changes, the field current of the DG synchronous generator is adjusted to bring the kilovolt-ampere reactance (kVAR) output back to zero (typically) and to maintain the desired kilowatt setpoint. Therefore, the only effect on system voltage is kilowatt injection at that point on the distribution circuit. However, if the DG synchronous generator is allowed to absorb or export VAR, voltage can be decreased or increased at that point on the circuit, and much larger kilowatt injections, and thus larger DG generators, can be installed on the circuit.

Some of the problems associated with interconnecting DG generators to a distribution circuit are related to the design of the circuit and its operation; others are related to the analytical tools used to evaluate DG operation. Distribution circuits are designed primarily for radial, one-way flow of power. Distribution line voltage regulators typically are designed to regulate voltage based on a unidirectional flow of power. When DG generators are interconnected to the circuit, two-way flows can result. Most of the load served on a distribution circuit is single-phase. However, most of the analytical tools used to evaluate circuit performance are based on balanced three-phase loads and balanced three-phase line circuit impedances.

Balanced three-phase power flow programs are used to calculate the voltage profile on the distribution circuit to determine whether DG generators are exceeding voltage limits. When that occurs, there is concern as to the accuracy of the resulting service voltages at individual single-phase loads on single-phase laterals, because only the three-phase portion of the circuit is modeled. American National Standards Institute (ANSI) Standard C84.1 voltage limits can be satisfied based on a three-phase balanced load/impedance analysis, but limits for single-phase loads can be exceeded.

This is a significant concern for a utility, because liability issues arise when a customer's equipment is damaged as a result of either high or low voltage on the circuit. Therefore, it is critically important to evaluate the effects of DG on the distribution circuit voltage profile to ensure that customers do not receive service voltages (voltages at the customer's billing meter) outside Range A or Range B of the ANSI C84.1 standard. This can be accomplished by using modeling and simulation tools that recognize single-phase loads, unsymmetrical distribution transformer connections, and unbalanced line impedances.

Purpose

The purpose of the project described in this report was to (1) develop models for an actual distribution circuit and all DG generator types (synchronous, induction, and inverter), recognizing unbalanced loading and unbalanced circuit impedances; (2) validate these models by comparing power flow simulations and voltage profiles with actual measured circuit data; and (3) determine the optimum generator operating conditions (e.g., P and Q) which provide the greatest improvement in terms of released capacity, reduced energy losses, and voltage regulation.

Project Objectives

The overall project objectives were fivefold: (1) develop a load model for an actual 13.2 kV distribution circuit that represents how the real and reactive load on the circuit changes when the voltage is raised or lowered with capacitor switching, distribution line voltage regulator step changes, and load tap changing (LTC) and DG voltage regulation; (2) develop models for overhead and underground distribution circuit line elements, transformers, shunt capacitors, step voltage regulators, and all DG generator types; (3) verify that the models are correct by comparing simulated data for power flow with actual measured circuit data; (4) determine the maximum DG generator size that can be interconnected to the circuit; and (5) determine the optimum generator operating conditions that will result in maximum released capacity savings, reduced energy losses, and improved voltage regulation. This annual report addresses objectives 2 and 3; the final report covers all five objectives.

Project Results

The circuit load was modeled using constant current, constant power, and a voltage-dependent current (VDC). The VDC model best represented the load characteristics of the circuit with a variance of only 2.0%. The percent variance of the constant power model, which is typically used, was 12.5%.

The VDC model that best represents how the load changes with changes in voltage is:

$$\frac{\% \Delta P}{\% \Delta V} = 1.26 ,$$

and

$$\frac{\% \Delta Q}{\% \Delta V} = 4.66 .$$

During heavy load conditions, with all voltage regulation equipment turned on, the circuit tag end voltage improvement was 14.87 V when compared with the case in which only the LTC transformer regulated the voltage. When the first step regulator was turned on, the tag end voltage improved by 4.11 V, and when the second regulator was turned on, the voltage increased another 11.34 V. With the first capacitor turned on, the voltage increased only 0.97 V; with the second turned on, the total voltage gain was 1.75 V; and with the third turned on, another 1.66 V rise occurred at the tag end. It may be necessary to operate DG generators to absorb VAR and thus prevent high voltages during light load conditions.

The highest unbalanced voltage, 1.52%, occurred during heavy load conditions with no LTC regulation. Since most synchronous generators trip when the unbalanced voltage is greater than 3%, unbalanced three-phase power flow studies should always be conducted on the circuit to ensure that the unbalance does not exceed 3% at the point of interconnection (not the point of common coupling). Adding LTC regulation during heavy load conditions lowered the maximum unbalance voltage to 1.44%; adding step regulators worsened the unbalanced voltage. When all three capacitors were turned on, the maximum unbalanced voltage was reduced to 1.31%. Turning on all regulation also lowered the maximum unbalanced voltage to 1.31%. During light load conditions, the voltage unbalance did not exceed 1.26%. A 13-utility survey on unbalanced voltage reported a maximum measured voltage unbalance of 5.94%. The high imbalances occurred on open delta transformer connections.

On many locations on the circuit, the current imbalance exceeded 20%. Most synchronous generators trip at between 10% and 20% current imbalance. Therefore, studies must be conducted to determine the current imbalance at the location where the DG generator might be sited; otherwise, it might never operate without tripping. The load imbalance at the substation reached 4% during heavy load conditions and 5.45% during light load conditions.

Models were developed for the following circuit elements:

- Line impedance
- Line voltage drop
- Line loss (the model was validated using unbalanced and balanced line configurations and unbalanced and balanced load conditions)
- Transformers (models were developed for three-phase and single-phase conditions and different loading combinations)
- Secondary and service impedance, voltage drop, and losses
- Shunt capacitors and step regulators
- Synchronous, induction and inverter generators.

The models were validated by measuring power quantities throughout the circuit on the peak day and comparing the measured data with simulation data. The percent variances between measured data and simulation data for phase currents at eight different nodes throughout the circuit were within 5.7%, and the highest phase voltage variance was only 1.5%.

Conclusions

The VDC model best represents how the real and reactive components of the load change with changes in voltage. This model, which had an error of only 2%, should always be used in place of the constant power model, which had an error of 12.5%.

Heavy load conditions produce the highest voltage unbalance, and adding voltage regulation equipment reduced the maximum percent voltage unbalance from 1.52% to 1.31%. Inverter-based generation was not sensitive to voltage or current unbalance, and it operated at a current imbalance of as much as 100%.

The models developed for the line elements, distribution equipment, and generation and the simulations conducted during peak load conditions compared favorably with actual phase currents, phase voltages, and power factors measured at eight locations throughout the circuit. However, it is essential to know the phasing of the loads on the circuit to obtain such a high degree of accuracy. The percent variance between simulated and measured data was less than 5.7% for phase currents and did not exceed 1.5% for phase voltages. These low variance values indicate that the models are accurate enough to represent the actual operation of a circuit under unbalanced load conditions. The only measured circuit data needed to perform accurate simulations are phase voltages and currents at the source of the circuit and at the regulators, capacitors, and DG generation locations.

Recommendations

The project has resulted in a number of recommendations; some of the major ones are:

- Always model distribution circuit loads with a voltage-dependent current. In addition, always use a validated unbalanced three-phase power flow to determine the percent unbalanced load and voltage during peak loads and at all the locations where DG generators are to be placed. Using a balanced three-phase power flow will not indicate unbalanced load and voltage where DG generators are to be installed, so a location could possibly be selected at which a synchronous DG generator would never operate because of circuit unbalance conditions.
- It is advisable to conduct a three-phase unbalanced power flow study of a circuit before installing a synchronous DG generator, because the unit might be installed at a place on the circuit where voltage unbalance causes the unit to trip (thus, it will never operate at that location). Furthermore, the current imbalance cannot exceed 20% or the synchronous DG generator will trip, and there are many places on the distribution circuit where the current imbalance exceeds 20%.
- Adding both LTC voltage regulation equipment and switched capacitors reduces the percent voltage unbalance. Adding DG generators to the circuit improves the voltage regulation of the circuit when they are allowed to produce and absorb VAR. Larger units can be installed if they are allowed to regulate voltage.
- Future research should include developing an optimal control algorithm that controls the substation transformer LTC, bidirectional step regulators, switched capacitors, and DG units. This could be accomplished for less than \$500,000, because the equipment is already installed on Milford Circuit 8103.

Benefits to California

Test data indicate that the models developed for this project accurately represent the operation of a distribution circuit. In addition, applying these models allows planners to select the sites on a circuit for distributed generation that allow the installed generators to perform as intended, resulting in the highest possible released capacity savings, the lowest energy losses, and the most improved voltage regulation.

Table of Contents

1.0 Introduction	1
2.0 Approach	2
3.0 Results for Model Development	3
3.1 Three-Phase Substation Transformer Models.....	3
3.2 Delta Wye-Grounded Three-Phase Substation Transformer.....	3
3.3 Three-Phase and Single-Phase Distribution Transformer Connections for the Distribution Circuit.....	5
3.4 Distribution Transformer Impedance.....	8
3.5 Distribution Transformer Voltage Drop.....	9
3.6 Distribution Transformer Losses.....	11
3.7 Line Impedance Model.....	13
3.8 Line Voltage Drop Model.....	16
3.9 Line Losses Model Validation.....	17
3.10 Secondary and Service Impedances and Voltage Drops.....	34
3.11 Secondary and Service Real Losses.....	37
3.12 Shunt Capacitor Models.....	38
3.13 Step Voltage Regulator Models.....	42
3.14 Synchronous Generator Model.....	42
3.15 Self-Excited Induction Generator Model.....	43
3.16 Inverter-Based Generator Model.....	47
4.0 Results for the Design of Field Voltage Regulation and Metering Equipment Used to Verify the Models	50
4.1 Voltage Regulation Equipment.....	50
4.2 Major System Protection Equipment.....	52
4.3 Metering Equipment and Accuracy of Measurements.....	53
5.0 Results for Distributed Generation Control Strategies Used in Field Verification	55
5.1 1000 kW Synchronous Generator.....	55
5.2 400 kW High-Speed Generator and Inverter.....	55
5.3 400 kW Self-Excited Induction Generator.....	55
5.4 Voltage Regulation Simulations and Field Verification Strategy 17.....	55
6.0 Results for Field Verification of Models	62
6.1 Circuit and Generation Measured Data.....	62
6.2 Bidirectional Voltage Regulator Measured Data.....	64
6.3 Circuit Equipment (Capacitors) and Customer Measured Data.....	64
6.4 Percent Variance Between Simulated and Field Measured Data.....	64
6.5 Summary of Variance Results.....	70
7.0 Conclusions and Recommendations	72
Conclusions.....	72
Recommendations.....	73
Benefits to California.....	73
8.0 References	74

List of Figures

Figure 1.	Delta wye-grounded three-phase transformer.....	3
Figure 2.	Four-wire wye-grounded overhead distribution line with multigrounded neutral	14
Figure 3.	Flat line spacing configuration.....	14
Figure 4.	Configuration, phase, and neutral spacings; phase and neutral sizes; and conductor types	18
Figure 5.	Line transposition and load.....	19
Figure 6.	Total line losses versus load imbalance for each line configuration	29
Figure 7.	Percent losses versus load imbalance for each line configuration.....	29
Figure 8.	Voltage imbalance versus load imbalance for each line configuration	30
Figure 9.	Sequence currents versus load imbalance for each line configuration	30
Figure 10.	Voltage imbalance versus current imbalance for equilateral spacing line.....	31
Figure 11.	Voltage imbalance versus current imbalance for nontransposed line.....	31
Figure 12.	Voltage imbalance versus current imbalance for transposed line.....	32
Figure 13.	Sequence currents versus current imbalance for equilateral spacing line.....	32
Figure 14.	Sequence currents versus current imbalance for nontransposed line.....	33
Figure 15.	Sequence currents versus current substance for transposed line	33
Figure 16.	Distribution transformer servicing secondaries and services.....	35
Figure 17.	Distribution service drop.....	36
Figure 18.	Steady-state synchronous machine model	42
Figure 19.	Two-phase primitive machine to be interconnected to an RLC load.....	43
Figure 20.	Stator direct axis with an R_{load} added.....	45
Figure 21.	RLC load R_L , L_L , and C_L connected to the self-excited capacitor C_S	46
Figure 22.	One line diagram of a 400 kW inverter-based generator and prime mover.....	48
Figure 23.	Voltage pullback curves.....	49
Figure 24.	Inverse time-current characteristic.....	49
Figure 25.	Milford Circuit DC 8103	51
Figure 26.	Milford Substation one line diagram	52
Figure 27.	DG control strategies for 1000 kW synchronous machine	56
Figure 28.	DG control strategies for 400 kW high-speed generator and inverter in current mode	57
Figure 29.	DG control strategies for 400 kW self-excited induction generator	58
Figure 30.	Daily circuit load profile and time stamps.....	63

List of Tables

Table 1.	Distribution Transformer No-Load (Core Losses) and Load (Copper Losses) ...	10
Table 2.	Evaluation of Equilateral Spacing Kilowatt Losses.....	23
Table 3.	Evaluation of Nontransposed kW Losses	25
Table 4.	Evaluation of Transposed kW Losses.....	27
Table 5.	The Effects of Circuit Spacing and Unbalanced Load on Percent kW Losses	34
Table 6.	Summary of Transformer, Secondary, and Service Voltage Drops.....	37
Table 7.	Comparison of Peak Day Real Losses	38
Table 8.	Voltage Regulation Equipment.....	50
Table 9.	Major System Protection Equipment.....	52
Table 10.	Measurement Locations and Data Collection	53
Table 11.	Accuracy of 3720 ACM.....	54
Table 12.	Matrix of Voltage Regulation Simulations and Control Strategy 17 for Field Verification	59
Table 13.	Test Dates and Data Collection Periods.....	62
Table 14.	Circuit and Generation Measured Data.....	65
Table 15.	Bidirectional Voltage Regulator Measured Data.....	66
Table 16.	Circuit Equipment and Customer Measured Data	67
Table 17.	Field Verification Data – 7/17/06 – DR Generation On.....	68
Table 18.	Field Verification Data – 7/29/06 – DR Generation On.....	69
Table 19.	Field Verification Data – 7/31/-6 – DR Generation Off.....	69
Table 20.	Percent Variance Between Actual and Simulated Currents, Voltages, and Power Factors.....	71

1.0 Introduction

An earlier study (Davis 2003) reported that the largest distributed generation (DG) power generator that can be installed on a distribution circuit (or DC) depends on (1) the circuit system voltage, (2) the location of the DG generator on the circuit, (3) the circuit configuration and characteristics, (4) system protection issues, (5) voltage regulation issues, and (6) DG characteristics. Larger DG units can be installed on circuits with higher system voltages and at substations with less effect on system protection and voltage regulation issues. In addition, installing DG generators that actively regulate voltage allows units of much larger sizes to be interconnected to a distribution circuit. This is so because high voltage conditions during light load conditions can be curtailed when DG units are absorbing volt-amperes reactive (VAR).

Earlier analyses were all evaluated using three-phase balanced power flows on distribution circuits with balanced loads. However, most distribution circuits have unbalanced load conditions, unbalanced line impedances, and unbalanced voltage conditions. In addition, there is no assurance that the results of studies in which balanced power flows are assumed actually represent what is happening on single-phase laterals of a three-phase circuit. The single-phase portion may serve upwards of 90% of the load on the circuit. Even if voltage limits are satisfied on the three-phase portion of the circuit, this does not mean that there are voltage limit violations on the single-phase loads. Installing DG generators on the circuit can add another level of complexity to an analysis of a distribution system, but it can also provide the added benefits of released capacity, lower energy losses, and improved voltage regulation.

The objectives of the project described in this report are as follows:

1. Select a distribution circuit and install DG generators to reduce overload and improve voltage regulation.
2. Develop models and run simulations to calculate voltage profiles on this distribution circuit with load tap changers (LTC), step regulators, capacitors, and DG units all regulating the voltage.
3. Install metering on the circuit and DG installations and compare actual measured data with data from the simulations.
4. Determine the maximum size of DG units and the optimum DG operating conditions that will provide the greatest released capacity, the lowest energy losses, and the most improved voltage regulation.

2.0 Approach

The approach to this project involves carrying out all of the following activities:

1. Develop a load model of a selected distribution circuit that represents how the circuit load changes with changes in voltage.
2. Develop circuit line elements and circuit equipment models.
3. Develop DG models for synchronous, induction, and inverter generation.
4. Model an entire 13.2 kV distribution circuit with all three-phase and single-phase loads connected to the correct phases of the distribution circuit.
5. Install a 1000 kW synchronous generator on the circuit, and install the appropriate metering equipment throughout the circuit and where the DG unit is installed to measure the power quantities of the circuit, including single-phase loads.
6. Validate the models by conducting a multitude of power flow simulations and comparing the data from these simulations to measured data for an actual circuit on the circuit peak day (with the DG unit both on and off).
7. Report the variance between the simulated data and actual measured power data.
8. Determine the largest DG units that can be installed on the circuit without violating voltage, thermal, and reverse power criteria.
9. Determine the optimum DG operating conditions that result in high released capacity, low energy losses, and improved voltage regulation.

3.0 Results for Model Development

This section describes the development of models for distributed generation and distribution circuit voltage regulation equipment for unbalanced power systems. Voltage regulation models were developed for the substation LTC transformer, bidirectional step regulator, capacitors, each of the DC transformer connections, and different loading combinations. Examples are given of how to calculate transformer impedances from test data, transformer voltage drop, and transformer losses. Models for line impedance, voltage drop, and losses as well as secondary and service drop impedances, voltage drop, and losses were also developed. Also included are models for a shunt capacitor for a wye-grounded connection and for synchronous, induction, and inverter-based generators.

3.1 Three-Phase Substation Transformer Models

Three-phase transformers are used at a distribution substation to transform the voltage from the subtransmission system (or, in some cases, the transmission system) to distribution circuit voltage levels. These three-phase transformers can feature high- or low-voltage fixed taps and LTC or under-load tap changing. The typical distribution circuit is a four-wire wye-multigrounded system fed from a delta wye-grounded three-phase substation transformer. However, there are also three-wire ungrounded delta distribution circuits, and they are normally fed from delta-delta three-phase substation transformers. The three-phase and single-phase connected transformers on the circuit feed the customer loads, which are three-phase or various combinations of single-phase and three-phase. In addition, single-phase transformers on the circuit feed single-phase loads.

3.2 Delta Wye-Grounded Three-Phase Substation Transformer

The delta wye-grounded transformer connection is shown in Figure 1.

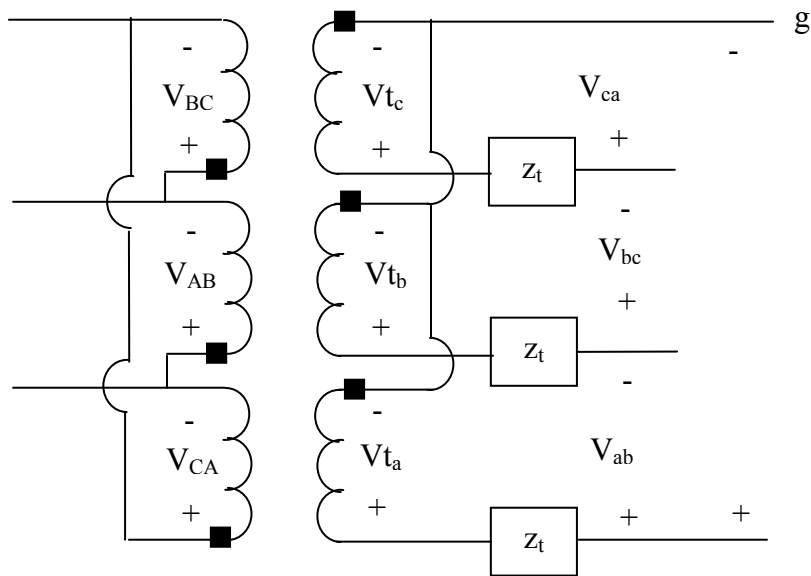


Figure 1. Delta wye-grounded three-phase transformer

From Figure 1, the primary side line-to-line voltages can be written as a function of the ideal secondary side voltages as:

$$\begin{bmatrix} V_{AB} \\ V_{BC} \\ V_{CA} \end{bmatrix} = \begin{bmatrix} 0 & -n_t & 0 \\ 0 & 0 & -n_t \\ -n_t & 0 & 0 \end{bmatrix} \cdot \begin{bmatrix} v_{ta} \\ v_{tb} \\ v_{tc} \end{bmatrix}, \quad \text{Equation 3.1}$$

where the turns ratio n_t is defined as

$$n_t = \frac{V_{LLHS}}{V_{LNLS}}. \quad \text{Equation 3.2}$$

The ideal secondary voltage can be written as a function of the secondary side line-to-neutral voltage, as follows:

$$V_{t_{abc}} = V_{LG_{abc}} + Z_{t_{abc}} I_{abc}, \quad \text{Equation 3.3}$$

where

$$Z_t = \begin{bmatrix} Z_t & 0 & 0 \\ 0 & Z_t & 0 \\ 0 & 0 & Z_t \end{bmatrix}. \quad \text{Equation 3.4}$$

The primary line-to-line voltage as a function of the secondary line-to-ground voltage, and the secondary current I_{abc} is

$$\begin{bmatrix} V_{AB} \\ V_{BC} \\ V_{CA} \end{bmatrix} = \begin{bmatrix} 0 & -n_t & 0 \\ 0 & 0 & -n_t \\ -n_t & 0 & 0 \end{bmatrix} \cdot \left(\begin{bmatrix} V_a \\ V_b \\ V_c \end{bmatrix} + \begin{bmatrix} z_t & 0 & 0 \\ 0 & z_t & 0 \\ 0 & 0 & z_t \end{bmatrix} \cdot \begin{bmatrix} I_a \\ I_b \\ I_c \end{bmatrix} \right). \quad \text{Equation 3.5}$$

To make the transformer model consistent with other system models and thus easier to calculate, the secondary side line-to-ground voltage should be expressed as a function of the primary side line-to-neutral voltage. This can be done using the theory of symmetrical components and algebraic manipulation. The resulting expression is as follows:

$$\begin{bmatrix} V_{AB} \\ V_{BC} \\ V_{CA} \end{bmatrix} = \begin{bmatrix} 1 & -1 & 0 \\ 0 & 1 & -1 \\ -1 & 0 & 1 \end{bmatrix} \cdot \begin{bmatrix} V_A \\ V_B \\ V_C \end{bmatrix}$$

$$\begin{bmatrix} 1 & -1 & 0 \\ 0 & 1 & -1 \\ -1 & 0 & 1 \end{bmatrix} \cdot \begin{bmatrix} V_A \\ V_B \\ V_C \end{bmatrix} = \begin{bmatrix} 0 & -n_t & 0 \\ 0 & 0 & -n_t \\ -n_t & 0 & 0 \end{bmatrix} \cdot \left(\begin{bmatrix} V_a \\ V_b \\ V_c \end{bmatrix} + \begin{bmatrix} z_t & 0 & 0 \\ 0 & z_t & 0 \\ 0 & 0 & z_t \end{bmatrix} \cdot \begin{bmatrix} I_a \\ I_b \\ I_c \end{bmatrix} \right)$$

$$\frac{1}{n_t} \begin{bmatrix} 0 & 0 & -1 \\ -1 & 0 & 0 \\ 0 & -1 & 0 \end{bmatrix} \cdot \begin{bmatrix} 1 & -1 & 0 \\ 0 & 1 & -1 \\ -1 & 0 & 1 \end{bmatrix} \cdot \begin{bmatrix} V_A \\ V_B \\ V_C \end{bmatrix} = \begin{bmatrix} V_a \\ V_b \\ V_c \end{bmatrix} + \begin{bmatrix} z_t & 0 & 0 \\ 0 & z_t & 0 \\ 0 & 0 & z_t \end{bmatrix} \cdot \begin{bmatrix} I_a \\ I_b \\ I_c \end{bmatrix}$$

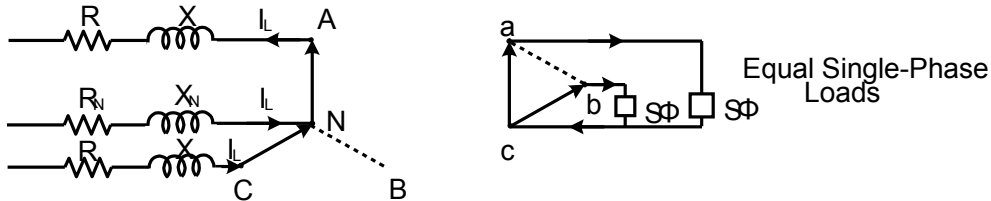
$$\begin{bmatrix} V_a \\ V_b \\ V_c \end{bmatrix} = \frac{1}{n_t} \begin{bmatrix} 1 & 0 & -1 \\ -1 & 1 & 0 \\ 0 & -1 & 1 \end{bmatrix} \cdot \begin{bmatrix} V_A \\ V_B \\ V_C \end{bmatrix} - \begin{bmatrix} z_t & 0 & 0 \\ 0 & z_t & 0 \\ 0 & 0 & z_t \end{bmatrix} \cdot \begin{bmatrix} I_a \\ I_b \\ I_c \end{bmatrix} . \quad \text{Equation 3.6}$$

3.3 Three-Phase and Single-Phase Distribution Transformer Connections for the Distribution Circuit

The following equations determine the voltage drop on the wye-grounded primary system feeding different transformer connections and three-phase and single-phase loading on these transformers. The factor $0.9 I_L$ in some of the equations below represents the portion of the neutral current in the neutral conductor, the remainder of which is the current in the earth.

Wye-Grounded Primary System Transformer Connections and Voltage Regulation

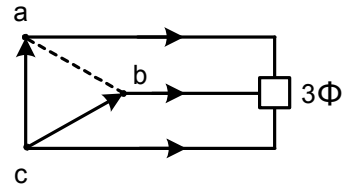
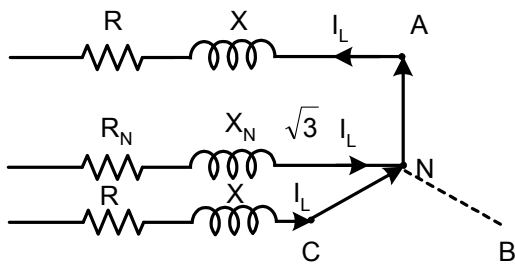
Case I



$$V_{R_{NA}} = I_L [R \cos \theta + X \sin \theta] + 0.9 I_L [R_N \cos (\theta - 60^\circ) + X_N \sin (\theta - 60^\circ)], \quad \text{Equation 3.7}$$

$$V_{R_{CN}} = I_L [R \cos \theta + X \sin \theta] + 0.9 I_L [R_N \cos (\theta + 60^\circ) + X_N \sin (\theta + 60^\circ)]. \quad \text{Equation 3.8}$$

Case II



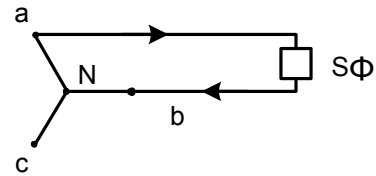
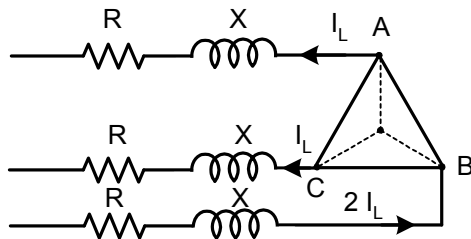
$$V_{R_{NA}} = I_L [R \cos(\theta - 30^\circ) + X \sin(\theta - 30^\circ)] + 0.9 \sqrt{3} I_L [R_N \cos(\theta - 60^\circ) + X_N \sin(\theta - 60^\circ)] .$$

Equation 3.9

$$V_{R_{CN}} = I_L [R \cos(\theta + 30^\circ) + X \sin(\theta + 30^\circ)] + 0.9 \sqrt{3} I_L [R_N \cos(\theta + 60^\circ) + X_N \sin(\theta + 60^\circ)] .$$

Equation 3.10

Case III



$$V_{R_{NA}} = I_L [R \cos(\theta - 60^\circ) + X \sin(\theta - 60^\circ)] .$$

Equation 3.11

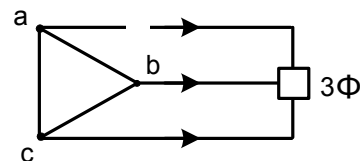
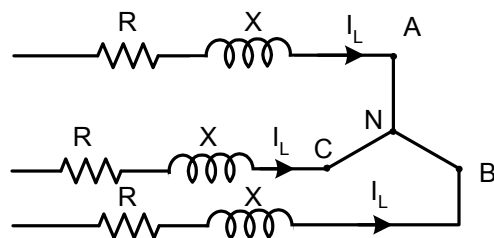
$$V_{R_{BN}} = 2 I_L (R \cos \theta + X \sin \theta) .$$

Equation 3.12

$$V_{R_{CN}} = I_L [R \cos(\theta + 60^\circ) + X \sin(\theta + 60^\circ)] .$$

Equation 3.13

Case IV



$$V_{R_{AN}} = I_L (R \cos \theta + X \sin \theta) \text{ on L-N Base Voltage .}$$

Equation 3.14

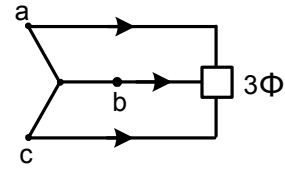
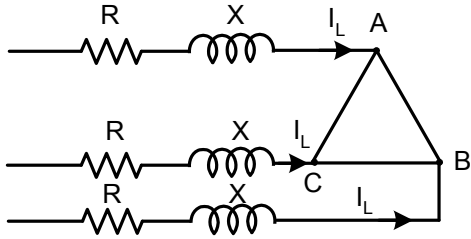
$$V_{R_{BN}} = I_L (R \cos \theta + X \sin \theta) \text{ on L-N Base Voltage .}$$

Equation 3.15

$$V_{R_{CN}} = I_L (R \cos \theta + X \sin \theta) \text{ on L-N Base Voltage .}$$

Equation 3.16

Case V



$$V_{R_{NA}} = I_L (R \cos \theta + X \sin \theta) .$$

Equation 3.17

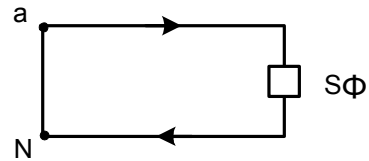
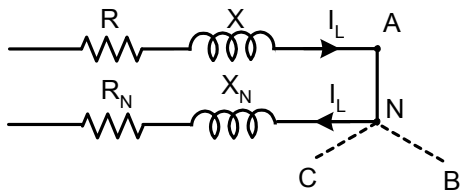
$$V_{R_{NB}} = I_L (R \cos \theta + X \sin \theta) .$$

Equation 3.18

$$V_{R_{NC}} = I_L (R \cos \theta + X \sin \theta) .$$

Equation 3.19

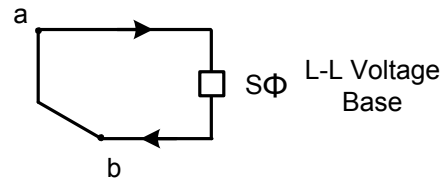
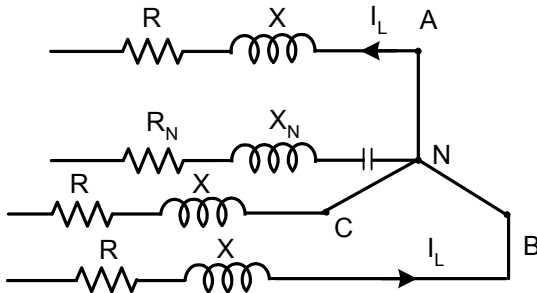
Case VI



$$V_{R_{NA}} = I_L [R + R_N] \cos \theta + (X + X_N) \sin \theta] .$$

Equation 3.20

Case VII



$$V_{R_{BA}} = 2 I_L (R \cos \theta + X \sin \theta) .$$

Equation 3.21

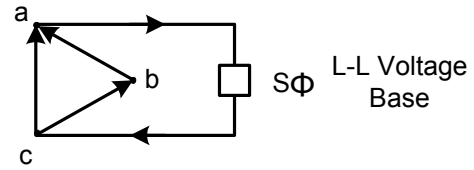
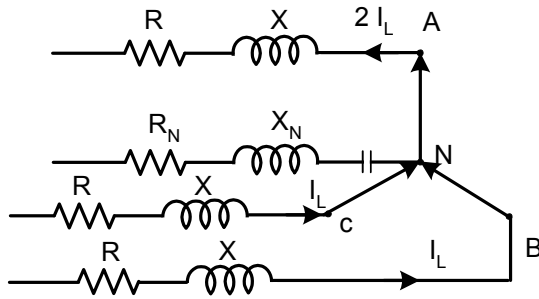
$$V_{R_{NA}} = I_L [R \cos (\theta - 30^\circ) + X \sin (\theta - 30^\circ)] .$$

Equation 3.22

$$V_{R_{BN}} = I_L [R \cos (\theta + 30^\circ) + X \sin (\theta + 30^\circ)] .$$

Equation 3.23

Case VIII

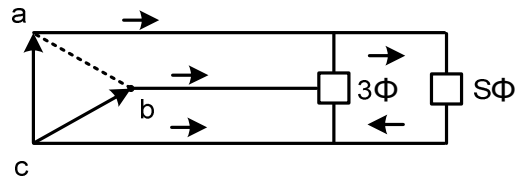
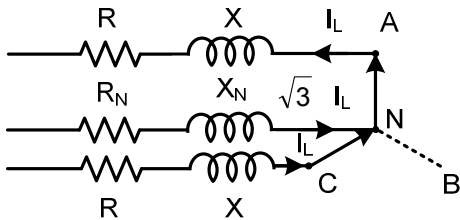


$$V_{R_{NA}} = 2 I_L (R \cos \theta + X \sin \theta) . \quad \text{Equation 3.24}$$

$$V_{R_{BN}} = I_L [R \cos (\theta + 60^\circ) + X \sin (\theta + 60^\circ)] . \quad \text{Equation 3.25}$$

$$V_{R_{CN}} = I_L [R \cos (\theta - 60^\circ) + X \sin (\theta - 60^\circ)] . \quad \text{Equation 3.26}$$

Case IX



$$V_{R_{NA3\Phi} + NA S\Phi} = I_{L3\Phi} [R \cos (\theta_{3\Phi} - 30^\circ) + X \sin (\theta_{3\Phi} - 30^\circ)] + 0.9 \sqrt{3} I_{L3\Phi} [R_N \cos (\theta_{3\Phi} - 60^\circ) + X_N \sin (\theta_{3\Phi} - 60^\circ)] + I_{LS\Phi} [R \cos \theta_{S\Phi} + X \sin \theta_{S\Phi}] + 0.9 I_{LS\Phi} [R_N \cos (\theta_{S\Phi} - 60^\circ) + X_N \sin (\theta_{S\Phi} - 60^\circ)] . \quad \text{Equation 3.27}$$

$$V_{R_{CN3\Phi}} = I_{L3\Phi} [R \cos (\theta_{3\Phi} + 30^\circ) + X \sin (\theta_{3\Phi} + 30^\circ)] + 0.9 \sqrt{3} I_{L3\Phi} [R_N \cos (\theta_{3\Phi} + 60^\circ) + X_N \sin (\theta_{3\Phi} + 60^\circ)] . \quad \text{Equation 3.28}$$

$$V_{R_{CA3\Phi} + CA S\Phi} = I_{L3\Phi} [R \cos (\theta + 60^\circ) + X \sin (\theta + 60^\circ) + I_{L3\Phi} [R \cos (\theta - 60^\circ) + X \sin (\theta - 60^\circ)] + I_{LS\Phi} [R \cos (\theta - 30^\circ) + X \sin (\theta - 30^\circ)] . \quad \text{Equation 3.29}$$

3.4 Distribution Transformer Impedance

The percent resistance and percent reactance of transformers can be determined from load losses (in watts [W]) and the percent impedance.

The percent Z is defined as

$$\% Z = \sqrt{\% R^2 + \% X^2} , \quad \text{Equation 3.30}$$

and percent R is determined from

$$\% R = \frac{\text{Load Losses (W)}}{10 \text{ kVA}} . \quad \text{Equation 3.31}$$

Using the 25 kVA transformer load losses in Table 1, then

$$\% R = \frac{397 \text{ W}}{(10)(25)} = 1.59 .$$

From Equation 3.3, the %R of Equation 3.31, and the %Z of Table 1, %X is determined as

$$\% X = \sqrt{\% Z^2 - \% R^2} ,$$
$$\% X = \sqrt{(2.58)^2 - (1.59)^2} = 2.03 .$$

3.5 Distribution Transformer Voltage Drop

The voltage drop can be determined when the R and X values, the load current, and the power factor are known. The actual R and X values (in ohms) are found from the %R and %X values as follows (showing the voltage drop for a 25 kVA transformer):

$$\text{Base Voltage} = 240 \text{ V} .$$

$$\text{Base kVA} = 25 \text{ kVA} .$$

$$\text{Base Current} = \frac{25,000}{240} = 104.17 \text{ A} .$$

$$\text{Base Z} = \frac{240}{104.17} = 2.30 \Omega .$$

Table 1. Distribution Transformer No-Load (Core Losses) and Load (Copper Losses)

Type	kVA	Phase	Sec. Volt	Pri. Volt	No-Load Losses (W)	Load Losses (W)	Tot. Losses (W)	% Z	% I _e
OH	15	S	120/240	4800/7620	34	280	314	2.58	0.51
OH	25	S	120/240	4800/7620	43	397	440	2.58	0.27
OH	50	S	120/240	4800/7620	103	564	667	1.97	0.76
OH	100	S	120/240	4800/7620	165	1150	1315	2.10	0.21
OH	167	S	120/240	4800/7620	267	1749	2016	2.37	0.33
PAD	75	3	120/208	4800x13200/7620	283	836	1119	2.43	0.78
PAD	150	3	120/208	13200/7620	328	2026	2354	2.37	0.34
PAD	300	3	120/208	13200/7620	639	3198	3837	2.50	0.55
PAD	500	3	120/208	4800x13200/7620	1140	4085	5225	3.45	0.46
PAD	1000	3	480Y/277	4160	1160	7601	8761	5.51	0.23
PAD	1500	3	480Y/277	4800x13200	1516	10294	11810	6.04	0.17
PAD	2000	3	480Y/277	4800x13200	1894	12933	14827	5.75	0.15
ISO	333	S	4800/8320	7620/13200	416	2937	3353	3.43	0.35
PAD	50	S	120/240	7620	107	675	782	1.92	0.30
PAD	100	S	120/240	7620	173	1074	1247	2.34	0.26
PAD	167	S	120/240	4800x13200/7620	231	1466	1697	2.72	0.20

$$\begin{aligned} \text{Actual R ohms} &= 1.59\% \times 2.30 \Omega \\ &= 0.0366 \Omega . \end{aligned}$$

$$\begin{aligned} \text{Actual X ohms} &= 2.0\% \times 2.30 \Omega \\ &= 0.0460 \Omega . \end{aligned}$$

$$\begin{aligned} \text{Actual Z ohms} &= 2.58\% \times 2.30 \Omega \\ &= 0.0593 \Omega . \end{aligned}$$

Assuming a power factor of 0.90 (25.84°), a load current of 1.40 times rated kVA, and a voltage of 105% of rated voltage, then the current would be

$$I = \frac{(104.17 \text{ A})}{1.05} \times 1.40 = 138.9 \text{ A} .$$

The approximate voltage drop is then

$$\begin{aligned} \Delta V &= IR \cos \theta + I X \sin \theta && \text{Equation 3.32} \\ &= (138.9) [(0.0366) (0.90) + (0.0460) (0.4358)] \\ &= (138.9) [0.03294 + 0.0200] . \end{aligned}$$

$$\Delta V = 7.36 \text{ V @ } 240 \text{ V.}$$

Equation 3.33

$$\Delta V @ 120 \text{ V} = 3.68 \text{ V}$$

The voltage drop can be reduced if a 50 kVA transformer is substituted for the 25 kVA transformer. The following shows the voltage drop for a 50 kVA transformer:

$$\text{Base Current} = 208.34 \text{ A.}$$

$$\text{Base } Z = \frac{240}{208.34} = 1.15 \Omega .$$

$$\begin{aligned} \text{Actual R ohms} &= 1.13\% \times 1.15 \Omega \\ &= 0.0130 \Omega . \end{aligned}$$

$$\begin{aligned} \text{Actual X ohms} &= 1.62\% \times 1.15 \Omega \\ &= 0.0187 \Omega . \end{aligned}$$

$$\begin{aligned} \text{Actual Z ohms} &= 1.97\% \times 1.15 \Omega \\ &= 0.0227 \Omega . \end{aligned}$$

Using a 0.90 power factor, 1.40 times rated current, and 105% voltage, the current is

$$I = \frac{208.34}{1.05} \times 1.40 = 277.8 \text{ A,}$$

and

$$\begin{aligned} \Delta V &= IR \cos \theta + I X \sin \theta \\ &= (277.8) [(0.0130) (0.90) + (0.0187) (0.4358)] \\ &= (277.8) [0.0117 + 0.00815]. \end{aligned}$$

$$\Delta V = 5.51 \text{ V @ } 240 \text{ V}$$

Equation 3.34

$$\Delta V @ 120 \text{ V} = 2.75 \text{ V}$$

3.6 Distribution Transformer Losses

The distribution transformer losses consist of load losses and no-load losses.

3.6.1 Load Losses

The load losses are proportional to the square of the load current. The test data shown in Table 1 are given at rated load current. The load losses at loads other than rated load are:

$$\text{Load Losses} = \left(\frac{I_{\text{load}}}{I_{\text{rated}}} \right)^2 (\text{load losses at rated load}), \quad \text{Equation 3.35}$$

$$= \left(\frac{kV_{\text{rated}}}{kV_{\text{actual}}} \frac{kVA_{\text{actual}}}{kVA_{\text{rated}}} \right)^2 (\text{load losses at rated load}). \quad \text{Equation 3.36}$$

For the 25 kVA transformer, the load losses at rated load are 397 W. But at peak load, the load may be as high as 140% to 200% of rated load. The load losses at 105% of rated voltage and 140% of rated load are from Equation 3.36.

$$\begin{aligned} \text{Load Losses} &= \left(\frac{7620}{(7620)(1.05)} \times \frac{(25)(1.40)}{25} \right)^2 (397) \\ &= (1.78)(397) \\ &= 706 \text{ W} . \end{aligned}$$

$$\text{Percent Load Losses} = \frac{\text{Load Loss (W)}}{(1.4)(VA_{\text{rated}})(\text{Cos } \theta)} \times 100 = \frac{\text{Load Loss (W)}}{(1.4)(10 \text{ kVA}_{\text{rated}})(\text{Cos } \theta)} . \quad \text{Equation 3.37}$$

For the 25 kVA transformer, the percent load losses can be calculated as follows:

$$\text{Percent Load Losses} = \frac{706}{(1.4)(10)(25)(0.90)} = 2.24\% .$$

3.6.2 No-Load Losses

The no-load losses are the core, dielectric, and copper losses caused by the excitation current, but the core losses due to hysteresis and eddy current losses are the most significant ones. From Table 1, the no-load losses for the 25 kVA transformer amount to 43 W. For operation above rated voltage, the no-load losses must be corrected. The correction factors are 1.15 at 105% of rated voltage and 1.30 at 110% of rated voltage. At 105% voltage,

$$\text{No-Load Losses} = (\text{Rated No-Load Losses})(\text{Voltage Correction}) \quad \text{Equation 3.38}$$

$$\text{No-Load Losses} = (43 \text{ W})(1.15) = 49.5 \text{ W} .$$

3.6.3 Total Losses

Adding the no-load losses corrected for voltage and load losses corrected for voltage and current gives the total percent losses of 2.40% for the 25 kVA transformer.

$$\text{Total Percent Losses} = \frac{706 + 49.5}{(1.4)(10)(25)(0.90)} = 2.40\% . \quad \text{Equation 3.39}$$

For the 50 kVA transformer, the percent load losses are

$$\begin{aligned} \text{Load Losses} &= \left(\frac{7620}{(7620)(1.05)} \times \frac{(50)(1.40)}{50} \right)^2 (564) \\ &= 1003 \text{ W} . \end{aligned}$$

$$\text{Percent Load Losses} = \frac{1003}{(1.4)(10)(50)(0.90)} = 1.59\% .$$

The percent no-load losses are calculated as follows:

$$\text{No-Load Losses} = (103)(1.15) = 118.5 \text{ W},$$

and the total percent losses are then

$$\text{Total Percent Losses} = \frac{1003 + 118.5}{(1.4)(10)(50)(0.90)} = 1.78\% . \quad \text{Equation 3.40}$$

3.7 Line Impedance Model

A four-wire wye grounded overhead line distribution circuit consisting of three-phase conductors and one neutral may be represented as a 4x4 matrix. Using Figure 2, the resultant 4x4 matrix using Kirckhoff's voltage law can be expressed as:

$$\begin{bmatrix} V_{A_S} \\ V_{B_S} \\ V_{C_S} \\ V_{N_S} \end{bmatrix} = \begin{bmatrix} V_{A_L} \\ V_{B_L} \\ V_{C_L} \\ V_{N_L} \end{bmatrix} + \begin{bmatrix} Z_A & Z_{AB} & Z_{AC} & Z_{AN} \\ Z_{BA} & Z_B & Z_{BC} & Z_{BN} \\ Z_{CA} & Z_{CB} & Z_C & Z_{CN} \\ Z_{NA} & Z_{NB} & Z_{NC} & Z_N \end{bmatrix} \cdot \begin{bmatrix} I_A \\ I_B \\ I_C \\ I_N \end{bmatrix} \quad \text{Equation 3.41}$$

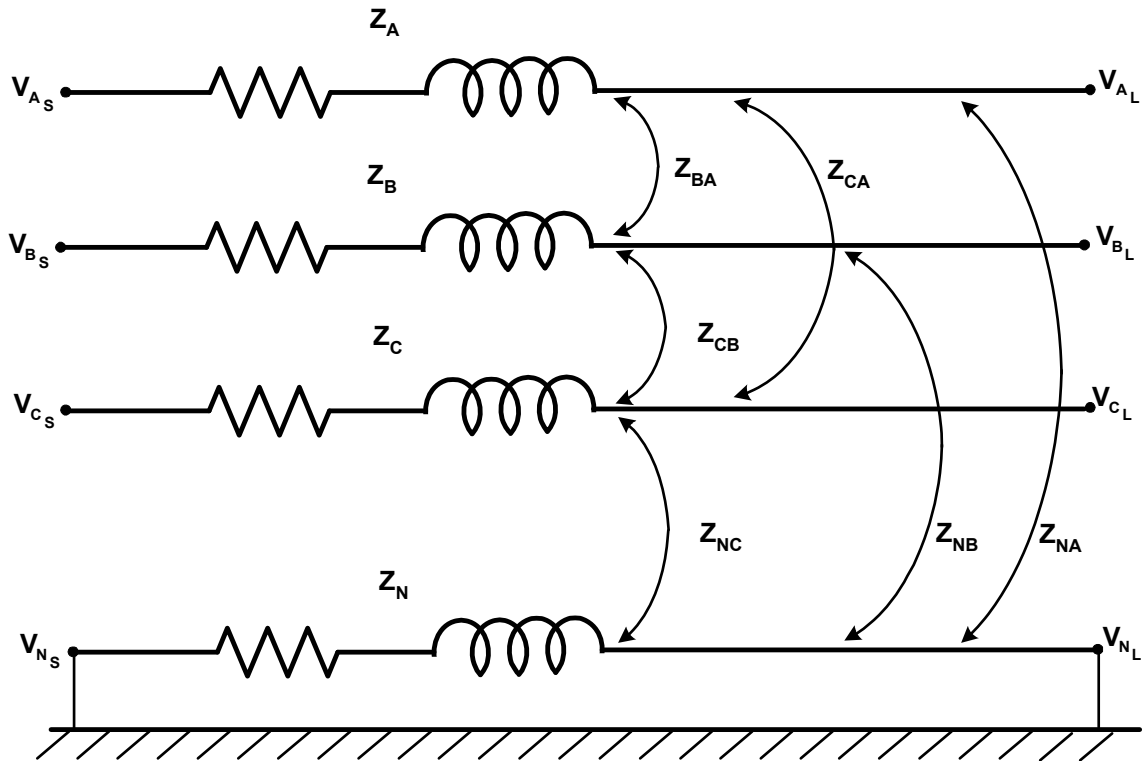


Figure 2. Four-wire wye-grounded overhead distribution line with multigrounded neutral

For a three-conductor cable with one neutral, the impedance matrix is

$$Z = \begin{bmatrix} Z_A & Z_{AB} & Z_{AC} & Z_{AN} \\ Z_{BA} & Z_B & Z_{BC} & Z_{BN} \\ Z_{CA} & Z_{CB} & Z_C & Z_{CN} \\ Z_{NA} & Z_{NB} & Z_{NC} & Z_N \end{bmatrix}$$

For the flat line configuration used in the Milford circuit in California, the line spacing is:

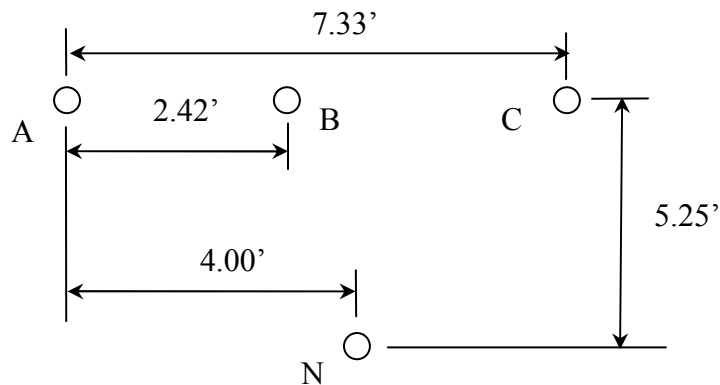


Figure 3. Flat line spacing configuration

The characteristics of the phase and neutral conductors are:

	A	B	C	N
Conductor	636 Al	636 Al	636 Al	1/0 ACSR
GMR (ft)	0.0294	0.0294	0.0294	0.006
Resistance (Ω /mi)	0.146	0.146	0.146	1.153

The diagonal and off-diagonal elements of the impedance matrix (Kersting 2004) are calculated using the following formulas.

$$z_{ii} = r_i + 0.09530 + j0.12134 [\ln(1/\text{GMR}_i) + 7.93402] \Omega/\text{mi}, \quad \text{Equation 3.42}$$

$$z_{ij} = 0.09530 + j0.12134 [\ln(1/D_{ij}) + 7.93402] \Omega/\text{mi}, \quad \text{Equation 3.43}$$

where

- r_i = resistance of the conductor, in Ω /mi
- D_{ij} = distance, in feet, from conductor i to conductor j
- GMR_i = geometric mean radius of the conductor, in feet
- 0.09530 = equivalent resistance of earth (100 Ω -m)
- 7.93402 = equivalent mutual inductive reactance between a conductor and earth at 60 Hz .

Note that the diagonal terms account for the self-inductance and resistance of the line and also contain expressions that take into account the effects of the earth return path. The off-diagonal elements account for the mutual inductance of the lines, and again take into account the effects of the earth return path.

For the flat line model of Figure 3, the impedance matrix is as follows:

$$Z = \begin{bmatrix} 0.2413 + j1.3907 & 0.0953 + j0.85548 & 0.0953 + j0.72101 & 0.0953 + j0.70949 \\ 0.0953 + j0.8554 & 0.2413 + j1.3907 & 0.0953 + j0.76963 & 0.0953 + j0.78573 \\ 0.0953 + j0.72101 & 0.0953 + j0.76963 & 0.2413 + j1.3907 & 0.0953 + j0.76267 \\ 0.0953 + j0.70949 & 0.0953 + j0.78573 & 0.0953 + j0.76267 & 1.2483 + j1.3907 \end{bmatrix} \quad \text{Equation 3.44}$$

The Kron reduction technique allows the 4x4 matrix above to be reduced to a more applicable 3x3 matrix, Z_{ABC} . This is accomplished in the following manner:

$$Z_{ij} = \begin{bmatrix} Z_A & Z_{AB} & Z_{AC} \\ Z_{BA} & Z_B & Z_{BC} \\ Z_{CA} & Z_{CB} & Z_C \end{bmatrix} = \begin{bmatrix} 0.2413 + j1.3907 & 0.0953 + j0.85548 & 0.0953 + j0.72101 \\ 0.0953 + j0.8554 & 0.2413 + j1.3907 & 0.0953 + j0.76963 \\ 0.0953 + j0.72101 & 0.0953 + j0.76963 & 0.2413 + j1.3907 \end{bmatrix}. \quad \text{Equation 3.45}$$

$$Z_{in} = \begin{bmatrix} z_{AN} \\ z_{BN} \\ z_{CN} \end{bmatrix} = \begin{bmatrix} 0.0953 + j0.70949 \\ 0.0953 + j0.78573 \\ 0.0953 + j0.76267 \end{bmatrix} . \quad \text{Equation 3.46}$$

$$Z_{nj} = [Z_{NA} \quad Z_{NB} \quad Z_{NC}] = [0.0953 + j0.70949 \quad 0.0953 + j0.78573 \quad 0.0953 + j0.76267] . \quad \text{Equation 3.47}$$

$$Z_N = z_N = 1.2483 + j1.5835 . \quad \text{Equation 3.48}$$

$$Z_{ABC} = Z_{ij} - Z_{in}Z_N^{-1}Z_{nj} = \begin{bmatrix} 0.3404 + j1.1566 & 0.0953 + j0.85548 & 0.0953 + j0.7210 \\ 0.0953 + j0.85548 & 0.2413 + j1.3907 & 0.0953 + j0.76963 \\ 0.0953 + j0.7210 & 0.0953 + j0.76963 & 0.2413 + j1.3907 \end{bmatrix} . \quad \text{Equation 3.49}$$

For a nontransposed line with a length of 6.25 mi (33,000 ft), the impedance matrix becomes

$$Z_{ABC} = \begin{bmatrix} 2.1275 + j7.2289 & 1.3100 + j3.7384 & 1.2750 + j2.9420 \\ 1.3100 + j3.7384 & 2.3108 + j6.9235 & 1.3689 + j3.0904 \\ 1.2750 + j2.9420 & 1.3689 + j3.0904 & 2.2530 + j7.0188 \end{bmatrix} . \quad \text{Equation 3.50}$$

3.8 Line Voltage Drop Model

The voltage drop for a given four-wire line segment is calculated using the impedance and matrix for that particular line segment.

$$V_S - V_L = Z_{ABC} I_{ABC} . \quad \text{Equation 3.51}$$

$$\Delta V = Z_{ABC} I_{ABC} . \quad \text{Equation 3.52}$$

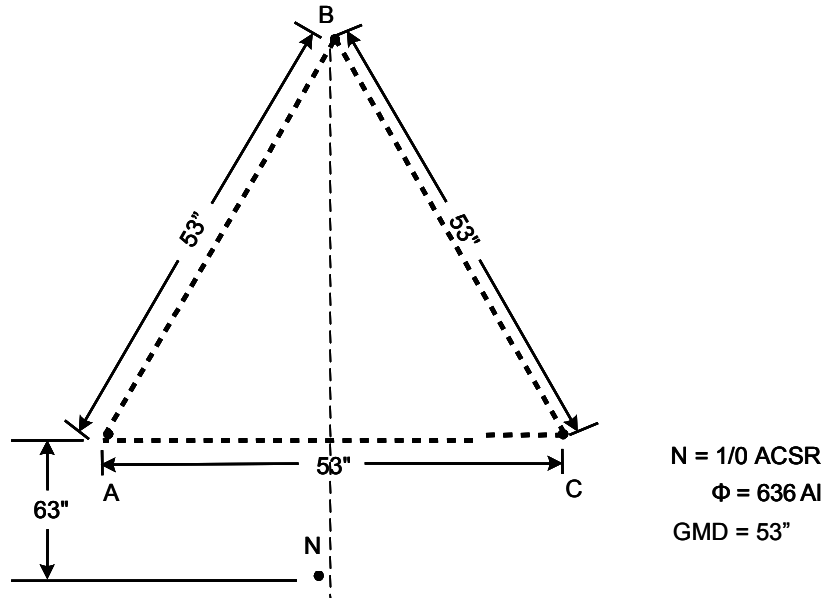
$$\begin{bmatrix} \Delta V_A \\ \Delta V_B \\ \Delta V_C \end{bmatrix} = \begin{bmatrix} z_A & z_{AB} & z_{AC} \\ z_{BA} & z_B & z_{BC} \\ z_{CA} & z_{CB} & z_C \end{bmatrix} \cdot \begin{bmatrix} I_A \\ I_B \\ I_C \end{bmatrix} . \quad \text{Equation 3.53}$$

The effects of the admittance matrix have been neglected because of the relatively short line length (6.25 mi).

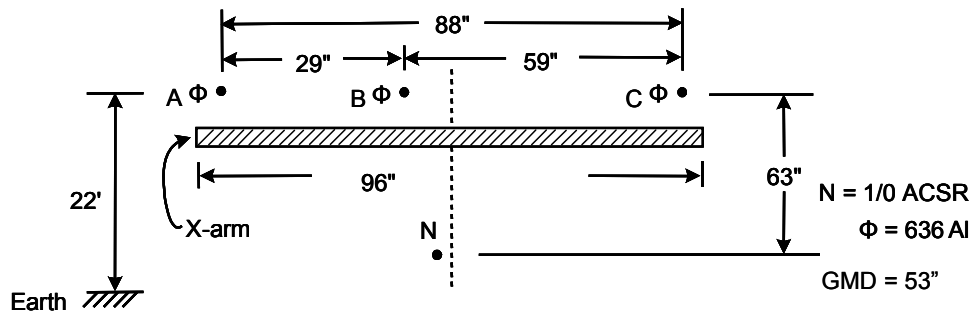
3.9 Line Losses Model Validation

To validate the line losses model, three line configurations and balanced and unbalanced load conditions were considered. These line configurations are shown in Figure 4. Figure 4(a) is a balanced impedance triangular or equilateral configuration with a high B phase. The geometric mean distance (GMD) of the phase spacings shown in Figure 4(a) is 53 in. (4.42 ft), which is the same GMD for the flat configuration of Figure 3. Figure 4(b) is the flat nontransposed line, and Figure 4(c) is the flat transposed line. The dimensions between phases, neutral, and ground are identical in Figure 4(b) and Figure 4(c), but the flat transposed line of Figure 4(c) has two transpositions.

Figure 5 shows the flat transposed line that consists of three line segments of 11,000 ft each for a total line length of 33,000 ft. The source is at node 0, and the two transpositions are shown at node 1 and node 2. The lump load of 9000 kVA at unity power factor is located at the end of the line at node 3.

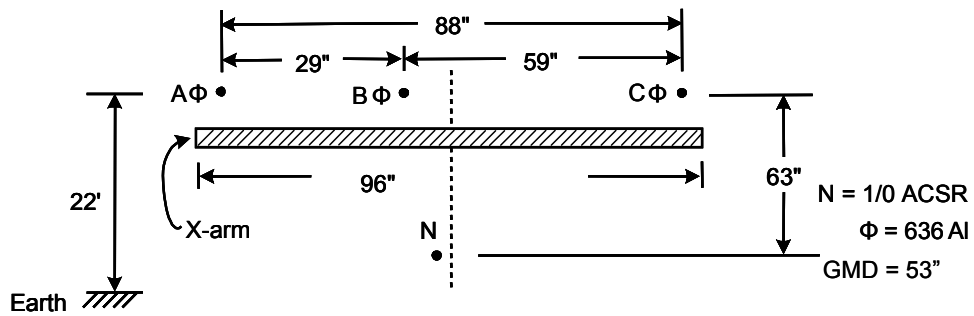


(a) Equilateral Spacing



(b) Flat Non-transposed

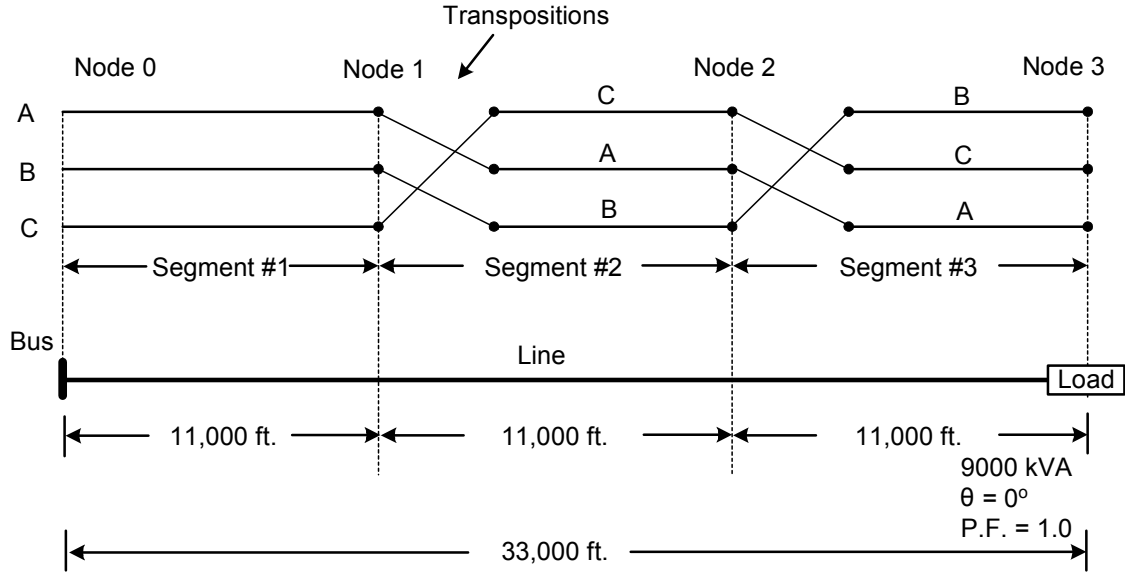
Note: Neutral to ground distance = $22' - 63'' = 201''$ (16.75')



(c) Flat Transposed

Note: Neutral to ground distance = $22' - 63'' = 201''$ (16.75')

Figure 4. Configuration, phase, and neutral spacings; phase and neutral sizes; and conductor types



Flat Transposed Line and Load Characteristics

Figure 5. Line transposition and load

This validation shows that, with balanced line impedance and balanced load, the kilowatt losses are equal in each phase, and the total kilowatt losses are the lowest. In addition, an example is given to explain that, even though the kilowatt losses per phase might not be correct because of the application of the Kron reduction process, which reduces a 4x4 matrix to a 3x3 matrix, the total losses are, in fact, correct. Table 2, Table 3, and Table 4 and the associated graphs provide a summary of balanced and unbalanced loading for the equilateral line spacing, nontransposed flat line spacing, and transposed flat line spacing configurations.

A *balanced* load of 3000 kW per phase, modeled using constant impedance and computed using a nominal voltage of 7.62 kV, is attached at the end of the nontransposed line at node 3. The load impedance matrix is

$$Z_{\text{load}} = \begin{bmatrix} 19.35 & 0 & 0 \\ 0 & 19.35 & 0 \\ 0 & 0 & 19.35 \end{bmatrix}, \quad \text{Equation 3.54}$$

where

$$Z_{\text{load},i} = \frac{(7.62 \text{ kV})^2}{3 \text{ MVA}} = 19.35. \quad \text{Equation 3.55}$$

Attaching the load to the end of the above nontransposed line yields

$$V_S = (Z_{\text{load}} + Z_{\text{ABC}}) I_{\text{ABC}}. \quad \text{Equation 3.56}$$

For a 13.2 kV line, the above load, and the 6.25-mi nontransposed line, solving for I_{ABC} gives

$$I_{ABC} = (Z_{load} + Z_{ABC})^{-1} V_S . \quad \text{Equation 3.57}$$

$$I_{ABC} = \begin{bmatrix} 358.4 \angle -10.2 \\ 377.8 \angle -130.2 \\ 371.3 \angle 108.4 \end{bmatrix} \text{ A} . \quad \text{Equation 3.58}$$

Note from the data for a nontransposed line in Table 3 at node 3, the magnitudes of phase currents are $I_A = 356.2$, $I_B = 375.9$, and $I_C = 372.0$. The data are based on the voltage-dependent current source model rather than the constant impedance model data in the matrix above.

The load end voltage V_{load} is, therefore,

$$V_{load} = V_S - Z_{ABC} I_{ABC} .$$

$$V_{load} = \begin{bmatrix} 6.94 \angle -10.2 \\ 7.31 \angle -130.2 \\ 7.19 \angle 108.4 \end{bmatrix} \text{ kV} . \quad \text{Equation 3.59}$$

The magnitudes of the phase voltages in kilovolts from Table 3 at node 3 are $V_A = 6.96$, $V_B = 7.31$, and $V_C = 7.24$, respectively. The power loss in the line is

$$P_{loss} = \text{Re}[S_{in}] - \text{Re}[S_{out}] = \begin{bmatrix} 200.5 \\ 71.6 \\ 102.8 \end{bmatrix} \text{ kW} . \quad \text{Equation 3.60}$$

The total loss for the line is 374.9 kW. This compares to $\Phi_A = 194.35$ kW, $\Phi_B = 72.47$ kW, and $\Phi_C = 84.29$ kW, for a total of 351.11 kW for the voltage-dependent current model. If the balanced load impedance matrix is replaced with an *unbalanced* load impedance matrix, the loss results may appear incorrect.

$$Z_{load} = \begin{bmatrix} 12.90 & 0 & 0 \\ 0 & 25.81 & 0 \\ 0 & 0 & 25.81 \end{bmatrix} . \quad \text{Equation 3.61}$$

The impedance matrix above corresponds to a heavily loaded A phase (4500 kW) relative to the B and C phases (2250 kW). The last line of Table 3 at node 0 shows the voltage magnitudes in kilovolts of $V_A = 7.620$, $V_B = 7.620$, and $V_C = 7.620$. Applying these balanced voltages and unbalanced loads for each phase, then

$$Z_A = \frac{(7620)^2}{4500 \times 10^3} = 12.90,$$

$$Z_B = \frac{(7620)^2}{2250 \times 10^3} = 25.81, \text{ and}$$

$$Z_C = \frac{(7620)^2}{2250 \times 10^3} = 25.81.$$

Repeating the procedure above to find the line losses yields

$$P_{\text{loss}} = \text{Re}[S_{\text{in}}] - \text{Re}[S_{\text{out}}] = \begin{bmatrix} 516.0 \\ -164.4 \\ 57.0 \end{bmatrix} \text{ kW}. \quad \text{Equation 3.62}$$

The total losses for the line amount to 408.6 kW. The phase losses from the spreadsheet data for the nontransposed case are 131.8, 390.5, and -117.4, corresponding to a heavily loaded B phase (4500 kW) in the simulation case, or a total of 404.96 kW. It is obvious in this unbalanced case that the phase loss calculations do not represent the actual losses in each phase; however, the total line loss is correct. The inclusion of the effects of the earth and neutral in the 3x3 impedance matrix is the reason for the dubious phase loss numbers. To obtain correct losses for the individual phases, the I^2R losses should be calculated. First, the earth and neutral currents should be found.

$$I_N = Z_{Nt} I_{ABC} = 60.6 \angle 157.5 \text{ A}, \quad \text{Equation 3.63}$$

where

$$Z_{Nt} I_{ABC} = -Z_{Nj} I_{nj}. \quad \text{Equation 3.64}$$

The earth current is found as follows:

$$I_E = -(I_A + I_B + I_C + I_N) = 127.9 \angle 126.4 \text{ A}. \quad \text{Equation 3.65}$$

Next, the I^2R losses for each phase, earth, and neutral are calculated:

$$P_{\text{lossA}} = |I_A|^2 R_A = 209.1 \text{ kW} \quad \text{Equation 3.66}$$

$$P_{\text{lossB}} = |I_B|^2 R_B = 88.4 \text{ kW} \quad \text{Equation 3.67}$$

$$P_{\text{lossC}} = |I_C|^2 R_C = 75.0 \text{ kW} \quad \text{Equation 3.68}$$

$$P_{\text{lossE}} = |I_E|^2 R_E = 9.7 \text{ kW} \quad \text{Equation 3.69}$$

$$P_{\text{lossN}} = |I_N|^2 R_N = 26.4 \text{ kW}. \quad \text{Equation 3.70}$$

When the losses are summed from the I^2R calculations, the result is 408.6. This exactly matches the total line loss calculated previously. There is a slight difference between the amount for total losses in the Table 3 spreadsheet data, 404.96 kW, and the total losses amount of 408.6 kW shown above, because the spreadsheet data are for a voltage-dependent current model and the total losses above are based on a constant impedance model.

Table 2. Evaluation of Equilateral Spacing Kilowatt Losses

Spot Load (kW)			kW Losses			Total kW Losses	kVar Losses			Total kVar Losses	kW Flow			Total kW Flow
ΦA	ΦB	ΦC	ΦA	ΦB	ΦC		ΦA	ΦB	ΦC		ΦA	ΦB	ΦC	
3000.00	3000.00	3000.00	117.17	117.02	116.89	351.08	515.76	515.74	515.68	1547.18	2758.79	2759.06	2759.28	8277.13
3150.00	2925.00	2925.00	143.85	94.42	113.39	351.66	568.41	507.63	472.37	1548.41	2856.88	2713.97	2703.31	8274.16
3300.00	2850.00	2850.00	171.35	72.44	109.62	353.41	622.80	498.63	430.76	1552.19	2951.53	2666.94	2646.96	8265.43
3450.00	2775.00	2775.00	199.93	51.43	104.92	356.28	677.99	489.86	390.41	1558.26	3041.81	2619.49	2589.48	8250.78
3600.00	2700.00	2700.00	228.92	31.27	100.01	360.20	734.23	480.24	351.94	1566.41	3128.22	2570.23	2531.83	8230.28
3750.00	2625.00	2625.00	258.85	11.66	94.75	365.26	792.19	470.22	314.54	1576.95	3211.81	2519.64	2472.90	8204.35
3900.00	2550.00	2550.00	289.23	-6.96	89.03	371.30	850.71	459.93	278.75	1589.39	3291.28	2468.02	2413.32	8172.62
4050.00	2475.00	2475.00	320.05	-24.56	82.79	378.28	909.51	449.56	244.49	1603.56	3366.43	2415.58	2352.90	8134.91
4200.00	2400.00	2400.00	351.17	-41.40	76.48	386.25	969.41	438.57	211.70	1619.68	3438.52	2361.61	2291.72	8091.85
4350.00	2325.00	2325.00	382.50	-57.46	70.17	395.21	1030.43	426.96	180.38	1637.77	3507.79	2306.09	2229.77	8043.65
4500.00	2250.00	2250.00	414.10	-72.43	63.39	405.06	1091.39	415.48	150.55	1657.42	3572.73	2249.97	2166.85	7989.55

Node 0															
Voltage			Sequence Voltages (V)				V2/V1	Current			Sequence Currents			Imbalance	
ΦA	ΦB	ΦC	V0	V1	V2	ΦA		ΦB	ΦC	I0	I1	I2	I2/I1	PF	
7.62	7.62	7.62	0	7620.91	0.11	0.0%	368.22	368.25	368.28	0.02	368.24	0.01	0.0%	0.0%	
7.62	7.62	7.62	0	7620.91	0.11	0.0%	382.16	362.23	360.04	6.44	368.12	8.39	2.3%	4.0%	
7.62	7.62	7.62	0	7620.91	0.11	0.0%	395.74	355.95	351.85	12.85	367.78	16.63	4.5%	8.0%	
7.62	7.62	7.62	0	7620.91	0.11	0.0%	408.87	349.61	343.58	19.24	367.2	24.7	6.7%	11.0%	
7.62	7.62	7.62	0	7620.91	0.11	0.0%	421.56	343.04	335.36	25.53	366.38	32.61	8.9%	15.0%	
7.62	7.62	7.62	0	7620.91	0.11	0.0%	433.99	336.27	327.06	31.87	365.35	40.37	11.0%	19.0%	
7.62	7.62	7.62	0	7620.91	0.11	0.0%	445.97	329.36	318.74	38.14	364.09	47.97	13.2%	22.0%	
7.62	7.62	7.62	0	7620.91	0.11	0.0%	457.5	322.35	310.36	44.35	362.59	55.41	15.3%	26.0%	
7.62	7.62	7.62	0	7620.91	0.11	0.0%	468.72	315.12	301.96	50.54	360.88	62.69	17.4%	30.0%	
7.62	7.62	7.62	0	7620.91	0.11	0.0%	479.63	307.68	293.51	56.72	358.97	69.83	19.5%	0.33	
7.62	7.62	7.62	0	7620.91	0.11	0.0%	490.12	300.16	284.99	62.84	356.83	76.81	21.5%	0.37	

Node 1															
Voltage			Sequence Voltages (V)				V2/V1	Current			Sequence Currents			Imbalance	
ΦA	ΦB	ΦC	V0	V1	V2	ΦA		ΦB	ΦC	I0	I1	I2	I2/I1	PF	
7.44	7.44	7.44	0.1	7444.34	0.08	0.0%	368.22	368.25	368.28	0.02	368.24	0.01	0.0%	0.0%	
7.42	7.46	7.45	27.28	7444.34	10.95	0.1%	382.16	362.23	360.04	6.44	368.12	8.39	2.3%	4.0%	
7.39	7.48	7.46	54.31	7444.22	21.65	0.3%	395.74	355.95	351.85	12.85	367.78	16.63	4.5%	8.0%	
7.36	7.5	7.47	81.21	7444.01	32.15	0.4%	408.87	349.61	343.58	19.24	367.2	24.7	6.7%	11.0%	
7.33	7.52	7.48	107.71	7443.74	42.43	0.6%	421.56	343.04	335.36	25.53	366.38	32.61	8.9%	15.0%	
7.3	7.54	7.49	134.43	7443.41	52.52	0.7%	433.99	336.27	327.06	31.87	365.35	40.37	11.0%	19.0%	
7.27	7.56	7.5	160.86	7443.01	62.4	0.8%	445.97	329.36	318.74	38.14	364.09	47.97	13.2%	22.0%	
7.25	7.58	7.51	187.04	7442.55	72.06	1.0%	457.5	322.35	310.36	44.35	362.59	55.41	15.3%	26.0%	
7.22	7.59	7.52	213.13	7442.05	81.53	1.1%	468.72	315.12	301.96	50.54	360.88	62.69	17.4%	30.0%	
7.19	7.61	7.53	239.13	7441.52	90.81	1.2%	479.63	307.68	293.51	56.72	358.97	69.83	19.5%	0.33	
7.16	7.63	7.54	264.96	7440.9	99.88	1.3%	490.12	300.16	284.99	62.84	356.83	76.81	21.5%	0.37	

Node 2															
Voltage			Sequence Voltages (V)				V2/V1	Current			Sequence Currents			Imbalance	
ΦA	ΦB	ΦC	V0	V1	V2	ΦA		ΦB	ΦC	I0	I1	I2	I2/I1	PF	
7.29	7.29	7.3	0.19	7294.81	0.15	0.0%	368.23	368.27	368.29	0.02	368.26	0.01	0.0%	0.0%	
7.24	7.33	7.31	54.55	7294.79	21.95	0.3%	382.18	362.24	360.05	6.44	368.13	8.39	2.3%	3.0%	
7.19	7.37	7.33	108.61	7294.48	43.37	0.6%	395.76	355.97	351.86	12.85	367.79	16.63	4.5%	7.0%	
7.13	7.41	7.34	162.42	7293.96	64.36	0.9%	408.89	349.63	343.59	19.24	367.21	24.7	6.7%	10.0%	
7.08	7.45	7.36	215.42	7293.28	84.91	1.2%	421.58	343.05	335.37	25.52	366.39	32.61	8.9%	13.0%	
7.03	7.48	7.37	268.87	7292.42	105.1	1.4%	434.01	336.28	327.07	31.87	365.37	40.37	11.0%	17.0%	
6.98	7.52	7.39	321.72	7291.4	124.86	1.7%	445.99	329.38	318.74	38.14	364.11	47.97	13.2%	20.0%	
6.92	7.56	7.41	374.07	7290.21	144.19	2.0%	457.52	322.36	310.37	44.35	362.61	55.41	15.3%	23.0%	
6.87	7.6	7.42	426.25	7288.9	163.12	2.2%	468.74	315.14	301.96	50.54	360.9	62.69	17.4%	26.0%	
6.82	7.63	7.44	478.26	7287.49	181.69	2.5%	479.65	307.7	293.52	56.71	358.99	69.83	19.5%	0.29	
6.77	7.67	7.46	529.91	7285.88	199.83	2.7%	490.14	300.18	284.99	62.84	356.84	76.81	21.5%	0.32	

Node 3															
Voltage			Sequence Voltages (V)				V2/V1	Current			Sequence Currents			Imbalance	
ΦA	ΦB	ΦC	V0	V1	V2	ΦA		ΦB	ΦC	I0	I1	I2	I2/I1	PF	
7.17	7.17	7.17	0.29	7174.03	0.24	0.0%	368.24	368.27	368.3	0.02	368.26	0.01	0.0%	0.0%	
7.1	7.23	7.19	81.83	7173.95	32.96	0.5%	382.19	362.25	360.06	6.44	368.14	8.39	2.3%	3.0%	
7.02	7.29	7.21	162.92	7173.39	65.08	0.9%	395.77	355.97	351.86	12.85	367.8	16.63	4.5%	6.0%	
6.95	7.35	7.23	243.63	7172.45	96.57	1.3%	408.9	349.63	343.59	19.24	367.22	24.7	6.7%	9.0%	
6.88	7.4	7.25	323.12	7171.2	127.4	1.8%	421.59	343.06	335.38	25.52	366.4	32.61	8.9%	12.0%	
6.8	7.46	7.27	403.29	7169.63	157.69	2.2%	434.02	336.29	327.07	31.87	365.37	40.37	11.0%	15.0%	
6.73	7.51	7.29	482.57	7167.75	187.32	2.6%	446	329.38	318.75	38.14	364.11	47.97	13.2%	17.0%	
6.66	7.57	7.31	561.09	7165.55	216.31	3.0%	457.53	322.37	310.37	44.35	362.62	55.4	15.3%	20.0%	
6.59	7.63	7.34	639.36	7163.11	244.72	3.4%	468.75	315.14	301.96	50.54	360.91	62.69	17.4%	23.0%	
6.52	7.68	7.36	717.38	7160.47	272.57	3.8%	479.67	307.7	293.52	56.71	358.99	69.83	19.5%	0.26	
6.44	7.74	7.38	794.85	7157.47	299.78	4.2%	490.16	300.18	284.99	62.84	356.85	76.81	21.5%	0.28	

kVar Flow			Total kVar Flow	kW Native Load			Total kW Load	kVar Native Load			Total kVar Load
ΦA	ΦB	ΦC		ΦA	ΦB	ΦC		ΦA	ΦB	ΦC	
513.61	513.62	513.49	1540.72	2641.63	2642.04	2642.39	7926.06	-2.15	-2.12	-2.20	-6.47
566.39	505.01	469.93	1541.33	2713.03	2619.55	2589.92	7922.50	-2.03	-2.62	-2.44	-7.09
620.16	496.25	428.61	1545.02	2780.18	2594.50	2537.33	7912.01	-2.64	-2.38	-2.15	-7.17
675.99	487.17	388.05	1551.21	2841.88	2568.05	2484.56	7894.49	-2.00	-2.70	-2.36	-7.06
732.12	478.01	349.25	1559.38	2899.30	2538.95	2431.82	7870.07	-2.11	-2.23	-2.69	-7.03
789.55	467.89	312.28	1569.72	2952.96	2507.99	2378.15	7839.10	-2.65	-2.33	-2.26	-7.24
847.92	457.62	276.52	1582.06	3002.05	2474.98	2324.28	7801.31	-2.78	-2.31	-2.23	-7.32
907.62	447.15	241.84	1596.61	3046.38	2440.15	2270.11	7756.64	-1.89	-2.41	-2.65	-6.95
967.68	436.16	208.98	1612.82	3087.35	2403.01	2215.24	7705.60	-1.73	-2.42	-2.72	-6.87
1027.84	424.65	177.97	1630.46	3125.30	2363.54	2159.60	7648.44	-2.58	-2.31	-2.41	-7.30
1089.67	412.92	147.93	1650.52	3158.63	2322.40	2103.46	7584.49	-1.73	-2.56	-2.61	-6.90

Plot Information:

kW			Node 1			Node 2			Node 3		
Node 0	Total kW	Losses /	Node 1	Node 2	Node 3	I0	I1	I2			
I2/I1	Losses	kW Flow	V1/V2	V1/V2	V1/V2						
0.0%	351.08	4.2%	0.0%	0.0%	0.0%	0.02	368.24	0.01			
2.3%	351.66	4.3%	0.1%	0.3%	0.5%	6.44	368.12	8.39			
4.5%	353.41	4.3%	0.3%	0.6%	0.9%	12.85	367.78	16.63			
6.7%	356.28	4.3%	0.4%	0.9%	1.3%	19.24	367.20	24.70			
8.9%	360.20	4.4%	0.6%	1.2%	1.8%	25.53	366.38	32.61			
11.0%	365.26	4.5%	0.7%	1.4%	2.2%	31.87	365.35	40.37			
13.2%	371.30	4.5%	0.8%	1.7%	2.6%	38.14	364.09	47.97			
15.3%	378.28	4.7%	1.0%	2.0%	3.0%	44.35	362.59	55.41			
17.4%	386.25	4.8%	1.1%	2.2%	3.4%	50.54	360.88	62.69			
19.5%	395.21	4.9%	1.2%	2.5%	3.8%	56.72	358.97	69.83			
21.5%	405.06	5.1%	1.3%	2.7%	4.2%	62.84	356.83	76.81			

Note: "PF" in Table 2, Table 3, and Table 4 is the percent power flow imbalance (kVA).

Table 3. Evaluation of Nontransposed kW Losses

Spot Load (kW)			kW Losses			Total kW Losses	kVar Losses			Total kVar Losses	kW Flow			Total kW Flow
ΦA	ΦB	ΦC	ΦA	ΦB	ΦC		ΦA	ΦB	ΦC		ΦA	ΦB	ΦC	
3000.00	3000.00	3000.00	194.35	72.47	84.29	351.11	468.69	504.08	571.12	1543.89	2673.63	2820.78	2777.24	8271.65
2925.00	3150.00	2925.00	191.64	101.18	59.82	352.64	421.45	558.63	560.65	1540.73	2617.99	2918.11	2734.33	8270.43
2850.00	3300.00	2850.00	187.85	130.92	36.35	355.12	376.15	614.45	549.88	1540.48	2561.96	3010.91	2690.10	8262.97
2775.00	3450.00	2775.00	183.15	161.60	13.77	358.52	332.63	671.65	538.71	1542.99	2505.32	3099.54	2644.44	8249.30
2700.00	3600.00	2700.00	177.65	193.08	-7.92	362.81	290.90	730.13	527.13	1548.16	2448.06	3184.09	2597.33	8229.48
2625.00	3750.00	2625.00	171.40	225.19	-28.66	367.93	250.97	789.76	515.15	1555.88	2390.15	3264.58	2548.82	8203.55
2550.00	3900.00	2550.00	164.51	257.80	-48.44	373.87	212.83	850.44	502.77	1566.04	2331.59	3341.09	2498.88	8171.56
2475.00	4050.00	2475.00	157.03	290.77	-67.24	380.56	176.49	912.05	490.01	1578.55	2272.37	3413.67	2447.55	8133.59
2400.00	4200.00	2400.00	149.06	323.97	-85.02	388.01	141.95	974.51	476.88	1593.34	2212.46	3482.4	2394.83	8089.69
2325.00	4350.00	2325.00	140.67	357.27	-101.76	396.18	109.20	1037.72	463.38	1610.30	2151.87	3547.33	2340.72	8039.92
2250.00	4500.00	2250.00	131.84	390.48	-117.36	404.96	78.33	1101.20	449.63	1629.16	2090.66	3608.08	2285.35	7984.09

Node 0															
Voltage			Sequence Voltages (V)				V2/V1	Current			Sequence Currents			Imbalance	
ΦA	ΦB	ΦC	V0	V1	V2	ΦA		ΦB	ΦC	I0	I1	I2	I2/I1	PF	
7.6200	7.6200	7.6200	0	7620.91	0.11	0.0%	356.11	375.94	371.99	3.24	367.98	9.3	2.5%	0.03	
7.62	7.62	7.62	0	7620.91	0.11	0.0%	347.9	389.79	366.19	9.06	367.9	15.93	4.3%	0.06	
7.62	7.62	7.6200	0	7620.91	0.11	0.0%	339.73	403.15	360.22	15.38	367.57	23.48	6.4%	0.1	
7.62	7.62	7.6200	0	7620.91	0.11	0.0%	331.58	416.08	354.06	21.72	367.01	31.17	8.5%	0.13	
7.62	7.62	7.6200	0	7620.91	0.11	0.0%	323.45	428.57	347.7	28.05	366.2	38.8	10.6%	0.17	
7.62	7.62	7.6200	0	7620.91	0.11	0.0%	315.32	440.64	341.15	34.34	365.14	46.31	12.7%	0.2	
7.62	7.62	7.6200	0	7620.91	0.11	0.0%	307.19	452.3	334.41	40.59	363.85	53.68	14.8%	0.24	
7.62	7.62	7.6200	0	7620.91	0.11	0.0%	299.04	463.56	327.47	46.8	362.32	60.9	16.8%	0.28	
7.62	7.62	7.62	0	7620.91	0.11	0.0%	290.89	474.41	320.35	52.97	360.56	67.97	18.9%	0.31	
7.62	7.62	7.62	0	7620.91	0.11	0.0%	282.71	484.88	313.04	59.1	358.57	74.88	20.9%	0.35	
7.6200	7.62	7.62	0	7620.91	0.11	0.0%	274.51	494.92	305.56	65.15	356.34	81.62	22.9%	0.38	

Node 1															
Voltage			Sequence Voltages (V)				V2/V1	Current			Sequence Currents			Imbalance	
ΦA	ΦB	ΦC	V0	V1	V2	ΦA		ΦB	ΦC	I0	I1	I2	I2/I1	PF	
7.38	7.49	7.46	17.54	7442.93	56.3	0.8%	356.11	375.94	371.99	3.24	367.98	9.3	2.5%	0.03	
7.39	7.46	7.48	42.54	7442.11	46.62	0.6%	347.9	389.79	366.19	9.06	367.9	15.93	4.3%	0.06	
7.39	7.43	7.5	71.6	7441.23	37.83	0.5%	339.73	403.15	360.22	15.38	367.57	23.48	6.4%	0.1	
7.4	7.4	7.52	101.14	7440.28	30.53	0.4%	331.58	416.08	354.06	21.72	367.01	31.17	8.5%	0.13	
7.41	7.37	7.54	130.7	7439.27	25.77	0.3%	323.45	428.57	347.7	28.05	366.2	38.8	10.6%	0.17	
7.42	7.34	7.57	160.16	7438.22	24.81	0.3%	315.32	440.64	341.15	34.34	365.14	46.31	12.7%	0.2	
7.43	7.3	7.59	189.47	7437.11	27.84	0.4%	307.19	452.3	334.41	40.59	363.85	53.68	14.8%	0.24	
7.43	7.27	7.61	218.59	7435.97	33.64	0.5%	299.04	463.56	327.47	46.8	362.32	60.9	16.8%	0.28	
7.44	7.24	7.63	247.53	7434.78	40.92	0.6%	290.89	474.41	320.35	52.97	360.56	67.97	18.9%	0.31	
7.45	7.21	7.65	276.27	7433.56	48.93	0.7%	282.71	484.88	313.04	59.1	358.57	74.88	20.9%	0.35	
7.46	7.18	7.67	304.7	7432.31	57.25	0.8%	274.51	494.92	305.56	65.15	356.34	81.62	22.9%	0.38	

Node 2															
Voltage			Sequence Voltages (V)				V2/V1	Current			Sequence Currents			Imbalance	
ΦA	ΦB	ΦC	V0	V1	V2	ΦA		ΦB	ΦC	I0	I1	I2	I2/I1	PF	
7.16	7.39	7.33	35.08	7291.9	112.7	1.5%	356.14	375.94	372	3.24	367.99	9.29	2.5%	0.04	
7.17	7.33	7.38	85.08	7290.1	93.32	1.3%	347.93	389.8	366.2	9.06	367.91	15.91	4.3%	0.06	
7.18	7.27	7.42	143.2	7288.13	75.74	1.0%	339.76	403.16	360.23	15.37	367.59	23.47	6.4%	0.09	
7.19	7.21	7.46	202.27	7285.99	61.12	0.8%	331.61	416.08	354.07	21.72	367.02	31.16	8.5%	0.13	
7.21	7.15	7.5	261.4	7283.7	51.56	0.7%	323.47	428.58	347.71	28.04	366.21	38.79	10.6%	0.16	
7.22	7.09	7.54	320.31	7281.26	49.59	0.7%	315.34	440.65	341.16	34.34	365.16	46.3	12.7%	0.19	
7.24	7.03	7.59	378.92	7278.69	55.61	0.8%	307.21	452.31	334.41	40.59	363.87	53.67	14.7%	0.22	
7.25	6.98	7.63	437.17	7276	67.19	0.9%	299.07	463.57	327.48	46.8	362.34	60.89	16.8%	0.25	
7.27	6.92	7.67	495.05	7273.19	81.75	1.1%	290.91	474.43	320.36	52.97	360.58	67.96	18.8%	0.28	
7.28	6.86	7.71	552.53	7270.27	97.75	1.3%	282.73	484.9	313.05	59.09	358.59	74.87	20.9%	0.31	
7.3	6.8	7.75	609.38	7267.27	114.39	1.6%	274.52	494.94	305.57	65.15	356.36	81.61	22.9%	0.34	

Node 3															
Voltage			Sequence Voltages (V)				V2/V1	Current			Sequence Currents			Imbalance	
ΦA	ΦB	ΦC	V0	V1	V2	ΦA		ΦB	ΦC	I0	I1	I2	I2/I1	PF	
6.96	7.31	7.24	52.62	7169.53	169.1	2.4%	356.17	375.94	372	3.24	368	9.27	2.5%	0.05	
6.97	7.23	7.3	127.61	7166.6	140.03	2.0%	347.95	389.79	366.2	9.05	367.92	15.9	4.3%	0.07	
6.99	7.14	7.37	214.79	7163.34	113.65	1.6%	339.78	403.16	360.23	15.37	367.6	23.47	6.4%	0.09	
7	7.06	7.43	303.4	7159.76	91.71	1.3%	331.63	416.08	354.07	21.71	367.03	31.15	8.5%	0.12	
7.02	6.98	7.49	392.08	7155.89	77.36	1.1%	323.49	428.58	347.71	28.04	366.22	38.78	10.6%	0.15	
7.04	6.9	7.55	480.44	7151.74	74.38	1.0%	315.36	440.65	341.16	34.33	365.17	46.29	12.7%	0.18	
7.05	6.82	7.62	568.36	7147.34	83.38	1.2%	307.23	452.32	334.41	40.58	363.88	53.66	14.7%	0.2	
7.07	6.74	7.68	655.73	7142.68	100.74	1.4%	299.08	463.57	327.48	46.8	362.35	60.89	16.8%	0.23	
7.09	6.66	7.74	742.55	7137.8	122.56	1.7%	290.92	474.43	320.36	52.96	360.59	67.95	18.8%	0.25	
7.11	6.58	7.8	828.77	7132.71	146.57	2.1%	282.74	484.9	313.05	59.09	358.6	74.86	20.9%	0.28	
7.14	6.5	7.86	914.04	7127.42	171.52	2.4%	274.54	494.94	305.57	65.14	356.37	81.6	22.9%	0.31	

kVar Flow			Total kVar Flow	kW Native Load			Total kW Load	kVar Native Load			Total kVar Load
ΦA	ΦB	ΦC		ΦA	ΦB	ΦC		ΦA	ΦB	ΦC	
465.92	501.64	569.08	1536.64	2479.28	2748.31	2692.95	7920.54	-2.78	-2.43	-2.04	-7.25
419.06	555.98	558.44	1533.48	2426.36	2816.93	2674.51	7917.80	-2.39	-2.66	-2.21	-7.26
373.75	611.81	547.65	1533.21	2374.11	2879.99	2653.75	7907.85	-2.40	-2.63	-2.23	-7.26
330.22	669.05	536.47	1535.74	2322.17	2937.94	2630.67	7890.78	-2.41	-2.60	-2.24	-7.25
288.48	727.55	524.87	1540.90	2270.41	2991.02	2605.25	7866.68	-2.42	-2.58	-2.26	-7.26
248.53	787.22	512.87	1548.62	2218.75	3039.39	2577.47	7835.61	-2.44	-2.54	-2.28	-7.26
210.38	847.92	500.48	1558.78	2167.09	3083.29	2547.33	7797.71	-2.45	-2.52	-2.30	-7.27
174.03	909.56	487.70	1571.29	2115.34	3122.90	2514.79	7753.03	-2.46	-2.48	-2.31	-7.25
139.48	972.05	474.55	1586.08	2063.40	3158.43	2479.85	7701.68	-2.47	-2.47	-2.33	-7.27
106.72	1035.28	461.04	1603.04	2011.20	3190.07	2442.48	7643.75	-2.48	-2.44	-2.35	-7.27
75.60	1099.26	447.30	1622.16	1958.82	3217.60	2402.71	7579.13	-2.73	-1.94	-2.32	-6.99

Plot Information:

kW			Node 1			Node 2			Node 3		
Node 0	Total kW	Losses /	Node 1	Node 2	Node 3	I0	I1	I2			
I2/I1	Losses	kW Flow	V1/V2	V1/V2	V2/V1						
2.5%	351.11	4.2%	0.8%	1.5%	2.4%	3.24	367.98	9.30			
4.3%	352.64	4.3%	0.6%	1.3%	2.0%	9.06	367.90	15.93			
6.4%	355.12	4.3%	0.5%	1.0%	1.6%	15.38	367.57	23.48			
8.5%	358.52	4.3%	0.4%	0.8%	1.3%	21.72	367.01	31.17			
10.6%	362.81	4.4%	0.3%	0.7%	1.1%	28.05	366.20	38.80			
12.7%	367.93	4.5%	0.3%	0.7%	1.0%	34.34	365.14	46.31			
14.8%	373.87	4.6%	0.4%	0.8%	1.2%	40.59	363.85	53.68			
16.8%	380.56	4.7%	0.5%	0.9%	1.4%	46.80	362.32	60.90			
18.9%	388.01	4.8%	0.6%	1.1%	1.7%	52.97	360.56	67.97			
20.9%	396.18	4.9%	0.7%	1.3%	2.1%	59.10	358.57	74.88			
22.9%	404.96	5.1%	0.8%	1.6%	2.4%	65.15	356.34	81.62			

Note: "PF" in Table 2, Table 3, and Table 4 is the percent power flow imbalance (kVA).

Table 4. Evaluation of Transposed kW Losses

Spot Load (MW)			kW Losses			Total kW Losses	kVar Losses			Total kVar Losses	kW Flow			Total kW Flow
ΦA	ΦB	ΦC	ΦA	ΦB	ΦC		ΦA	ΦB	ΦC		ΦA	ΦB	ΦC	
3000.00	3000.00	3000.00	117.05	117.04	117.06	351.15	515.80	515.77	515.79	1547.36	2758.93	2758.99	2759.00	8276.92
3150.00	2925.00	2925.00	144.46	91.77	115.41	351.64	570.85	508.10	469.82	1548.77	2854.89	2716.82	2702.11	8273.82
3300.00	2850.00	2850.00	172.80	67.30	112.99	353.09	627.40	500.00	425.46	1552.86	2946.78	2673.22	2644.53	8264.53
3450.00	2775.00	2775.00	201.93	43.65	109.86	355.44	685.35	491.46	382.72	1559.53	3034.65	2628.21	2586.23	8249.09
3600.00	2700.00	2700.00	231.72	20.86	106.09	358.67	744.55	482.47	341.61	1568.63	3118.54	2581.78	2527.21	8227.53
3750.00	2625.00	2625.00	262.04	-1.04	101.75	362.75	804.88	473.04	302.13	1580.05	3198.50	2533.96	2467.46	8199.92
3900.00	2550.00	2550.00	292.76	-22.01	96.92	367.67	866.23	463.17	264.30	1593.70	3274.59	2484.74	2406.97	8166.30
4050.00	2475.00	2475.00	323.76	-42.03	91.64	373.37	928.50	452.87	228.11	1609.48	3346.87	2434.14	2345.73	8126.74
4200.00	2400.00	2400.00	354.91	-61.08	85.99	379.82	991.58	442.13	193.57	1627.28	3415.40	2382.16	2283.73	8081.29
4350.00	2325.00	2325.00	386.12	-79.12	80.03	387.03	1055.39	430.97	160.70	1647.06	3480.26	2328.81	2220.98	8030.05
4500.00	2250.00	2250.00	417.26	-96.12	73.83	394.97	1119.83	419.41	129.49	1668.73	3541.49	2274.10	2157.48	7973.07

Node 0															
Voltage			Sequence Voltages (V)				V2/V1	Current			Sequence Currents			Imbalance	
ΦA	ΦB	ΦC	V0	V1	V2	ΦA		ΦB	ΦC	I0	I1	I2	I2/I1	PF	
7.62	7.62	7.62	0	7620.91	0.11	0.0%	368.23	368.24	368.24	0	368.23	0	0.0%	0	
7.62	7.62	7.62	0	7620.91	0.11	0.0%	381.96	362.61	359.83	6.43	368.11	8.38	2.3%	0.04	
7.62	7.62	7.62	0	7620.91	0.11	0.0%	395.27	356.79	351.42	12.82	367.74	16.59	4.5%	0.07	
7.62	7.62	7.62	0	7620.91	0.11	0.0%	408.16	350.78	343	19.18	367.13	24.63	6.7%	0.11	
7.62	7.62	7.62	0	7620.91	0.11	0.0%	420.63	344.57	334.58	25.5	366.28	32.5	8.9%	0.15	
7.62	7.62	7.62	0	7620.91	0.11	0.0%	432.71	338.18	326.15	31.78	365.19	40.21	11.0%	0.18	
7.62	7.62	7.62	0	7620.91	0.11	0.0%	444.38	331.59	317.7	38.03	363.86	47.74	13.1%	0.22	
7.62	7.62	7.62	0	7620.91	0.11	0.0%	455.67	324.82	309.22	44.25	362.29	55.12	15.2%	0.25	
7.62	7.62	7.62	0	7620.91	0.11	0.0%	466.58	317.85	300.71	50.42	360.49	62.33	17.3%	0.29	
7.62	7.62	7.62	0	7620.91	0.11	0.0%	477.12	310.7	292.17	56.55	358.47	69.38	19.4%	0.33	
7.62	7.62	7.62	0	7620.91	0.11	0.0%	487.29	303.37	283.59	62.65	356.22	76.27	21.4%	0.36	

Node 1															
Voltage			Sequence Voltages (V)				V2/V1	Current			Sequence Currents			Imbalance	
ΦA	ΦB	ΦC	V0	V1	V2	ΦA		ΦB	ΦC	I0	I1	I2	I2/I1	PF	
7.36	7.5	7.47	25.23	7444.34	60.26	0.8%	368.23	368.24	368.24	0	368.23	0	0.0%	0	
7.33	7.53	7.48	53.13	7445.92	64.24	0.9%	381.96	362.61	359.83	6.43	368.11	8.38	2.3%	0.04	
7.31	7.55	7.49	81.93	7447.38	69.72	0.9%	395.27	356.79	351.42	12.82	367.74	16.59	4.5%	0.07	
7.28	7.57	7.5	110.8	7448.72	76.26	1.0%	408.16	350.78	343	19.18	367.13	24.63	6.7%	0.11	
7.25	7.6	7.5	139.58	7449.95	83.52	1.1%	420.63	344.57	334.58	25.5	366.28	32.5	8.9%	0.15	
7.22	7.62	7.51	168.23	7451.06	91.24	1.2%	432.71	338.18	326.15	31.78	365.19	40.21	11.0%	0.18	
7.19	7.64	7.52	196.72	7452.07	99.22	1.3%	444.38	331.59	317.7	38.03	363.86	47.74	13.1%	0.22	
7.17	7.67	7.53	225.04	7452.99	107.34	1.4%	455.67	324.82	309.22	44.25	362.29	55.12	15.2%	0.25	
7.14	7.69	7.54	253.18	7453.81	115.52	1.5%	466.58	317.85	300.71	50.42	360.49	62.33	17.3%	0.29	
7.11	7.71	7.55	281.14	7454.54	123.67	1.7%	477.12	310.7	292.17	56.55	358.47	69.38	19.4%	0.33	
7.08	7.73	7.56	308.91	7455.2	131.77	1.8%	487.29	303.37	283.59	62.65	356.22	76.27	21.4%	0.36	

Node 2															
Voltage			Sequence Voltages (V)				V2/V1	Current			Sequence Currents			Imbalance	
ΦA	ΦB	ΦC	V0	V1	V2	ΦA		ΦB	ΦC	I0	I1	I2	I2/I1	PF	
7.27	7.38	7.24	25.24	7294.81	60.31	0.8%	368.26	368.24	368.25	0	368.24	0.02	0.0%	0.01	
7.21	7.42	7.25	81.75	7295.27	47.15	0.6%	381.99	362.62	359.83	6.43	368.12	8.39	2.3%	0.02	
7.16	7.47	7.26	140.47	7295.49	42.66	0.6%	395.3	356.8	351.42	12.82	367.76	16.6	4.5%	0.05	
7.1	7.51	7.28	199.18	7295.5	48.7	0.7%	408.19	350.79	343.01	19.18	367.15	24.64	6.7%	0.09	
7.05	7.55	7.29	257.64	7295.3	61.82	0.8%	420.67	344.58	334.59	25.5	366.29	32.52	8.9%	0.12	
6.99	7.6	7.31	315.82	7294.91	78.2	1.1%	432.74	338.18	326.15	31.79	365.2	40.22	11.0%	0.15	
6.93	7.64	7.32	373.65	7294.34	95.91	1.3%	444.42	331.6	317.7	38.03	363.87	47.76	13.1%	0.18	
6.88	7.68	7.34	431.15	7293.6	114.1	1.6%	455.71	324.82	309.22	44.25	362.31	55.13	15.2%	0.21	
6.82	7.73	7.35	488.3	7292.7	132.4	1.8%	466.62	317.86	300.71	50.42	360.51	62.34	17.3%	0.24	
6.77	7.77	7.37	545.08	7291.65	150.59	2.1%	477.16	310.71	292.16	56.55	358.48	69.39	19.4%	0.27	
6.72	7.81	7.38	601.49	7290.47	168.59	2.3%	487.34	303.37	283.58	62.65	356.24	76.29	21.4%	0.3	

Node 3															
Voltage			Sequence Voltages (V)				V2/V1	Current			Sequence Currents			Imbalance	
ΦA	ΦB	ΦC	V0	V1	V2	ΦA		ΦB	ΦC	I0	I1	I2	I2/I1	PF	
7.17	7.17	7.17	0.02	7174.03	0.06	0.0%	368.26	368.24	368.27	0	368.25	0.02	0.0%	0.01	
7.1	7.24	7.19	88.72	7173.81	32.68	0.5%	381.99	362.62	359.85	6.42	368.13	8.39	2.3%	0.03	
7.02	7.3	7.2	176.95	7173.18	64.7	0.9%	395.3	356.8	351.44	12.81	367.76	16.6	4.5%	0.05	
6.94	7.37	7.22	264.74	7172.14	96.06	1.3%	408.19	350.79	343.03	19.17	367.15	24.64	6.7%	0.08	
6.86	7.43	7.24	352.03	7170.74	126.76	1.8%	420.67	344.58	334.61	25.49	366.3	32.51	8.9%	0.11	
6.79	7.5	7.25	438.83	7168.98	156.81	2.2%	432.75	338.18	326.17	31.78	365.21	40.21	11.0%	0.14	
6.71	7.56	7.27	525.1	7166.88	186.21	2.6%	444.42	331.6	317.71	38.03	363.88	47.75	13.1%	0.16	
6.63	7.62	7.29	610.86	7164.47	214.97	3.0%	455.72	324.82	309.23	44.24	362.31	55.13	15.2%	0.19	
6.56	7.69	7.31	696.09	7161.77	243.1	3.4%	466.63	317.86	300.72	50.41	360.52	62.34	17.3%	0.22	
6.48	7.75	7.33	780.78	7158.78	270.59	3.8%	477.17	310.71	292.18	56.55	358.49	69.39	19.4%	0.24	
6.41	7.81	7.35	864.92	7155.53	297.47	4.2%	487.34	303.37	283.59	62.64	356.24	76.28	21.4%	0.27	

kVar Flow			Total kVar Flow	kW Native Load			Total kW Load	kVar Native Load			Total kVar Load
ΦA	ΦB	ΦC		ΦA	ΦB	ΦC		ΦA	ΦB	ΦC	
513.41	513.32	513.39	1540.12	2641.88	2641.94	2641.95	7925.77	-2.40	-2.45	-2.40	-7.25
568.47	505.63	467.41	1541.51	2710.43	2625.05	2586.70	7922.18	-2.37	-2.47	-2.41	-7.25
625.05	497.51	423.04	1545.60	2773.98	2605.92	2531.54	7911.44	-2.35	-2.48	-2.43	-7.26
683.03	488.95	380.29	1552.27	2832.72	2584.56	2476.37	7893.65	-2.32	-2.51	-2.43	-7.26
742.25	479.94	339.17	1561.36	2886.82	2560.92	2421.12	7868.86	-2.30	-2.52	-2.44	-7.26
802.62	470.50	299.68	1572.80	2936.46	2534.99	2365.71	7837.16	-2.27	-2.55	-2.45	-7.27
863.99	460.61	261.83	1586.43	2981.83	2506.75	2310.05	7798.63	-2.24	-2.56	-2.47	-7.27
926.29	450.29	225.63	1602.21	3023.12	2476.17	2254.09	7753.38	-2.22	-2.58	-2.47	-7.27
989.39	439.53	191.09	1620.01	3060.49	2443.24	2197.74	7701.47	-2.19	-2.60	-2.49	-7.28
1053.22	428.35	158.21	1639.78	3094.14	2407.93	2140.95	7643.02	-2.17	-2.62	-2.49	-7.28
1117.68	416.77	126.99	1661.44	3124.24	2370.22	2083.65	7578.11	-2.15	-2.64	-2.50	-7.29

Plot Information:

kW			Node 1 V1/V2	Node 2 V1/V2	Node 3 V1/V2	I0	I1	I2
Node 0 I2/I1	Total kW Losses	Losses / kW Flow						
0.0%	351.15	4.2%	0.8%	0.8%	0.0%	0.00	368.23	0.00
2.3%	351.64	4.3%	0.9%	0.6%	0.5%	6.43	368.11	8.38
4.5%	353.09	4.3%	0.9%	0.6%	0.9%	12.82	367.74	16.59
6.7%	355.44	4.3%	1.0%	0.7%	1.3%	19.18	367.13	24.63
8.9%	358.67	4.4%	1.1%	0.8%	1.8%	25.50	366.28	32.50
11.0%	362.75	4.4%	1.2%	1.1%	2.2%	31.78	365.19	40.21
13.1%	367.67	4.5%	1.3%	1.3%	2.6%	38.03	363.86	47.74
15.2%	373.37	4.6%	1.4%	1.6%	3.0%	44.25	362.29	55.12
17.3%	379.82	4.7%	1.5%	1.8%	3.4%	50.42	360.49	62.33
19.4%	387.03	4.8%	1.7%	2.1%	3.8%	56.55	358.47	69.38
21.4%	394.97	5.0%	1.8%	2.3%	4.2%	62.65	356.22	76.27

Note: "PF" in Table 2, Table 3, and Table 4 is the percent power flow imbalance (kVA).

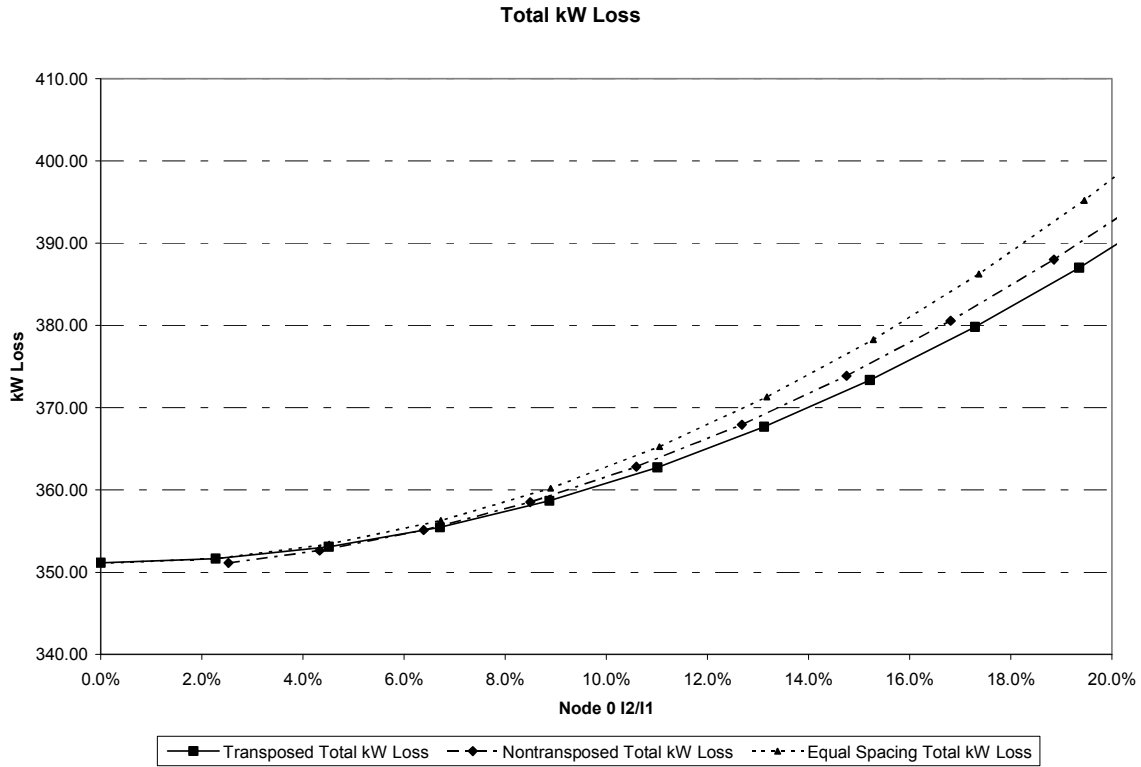


Figure 6. Total line losses versus load imbalance for each line configuration

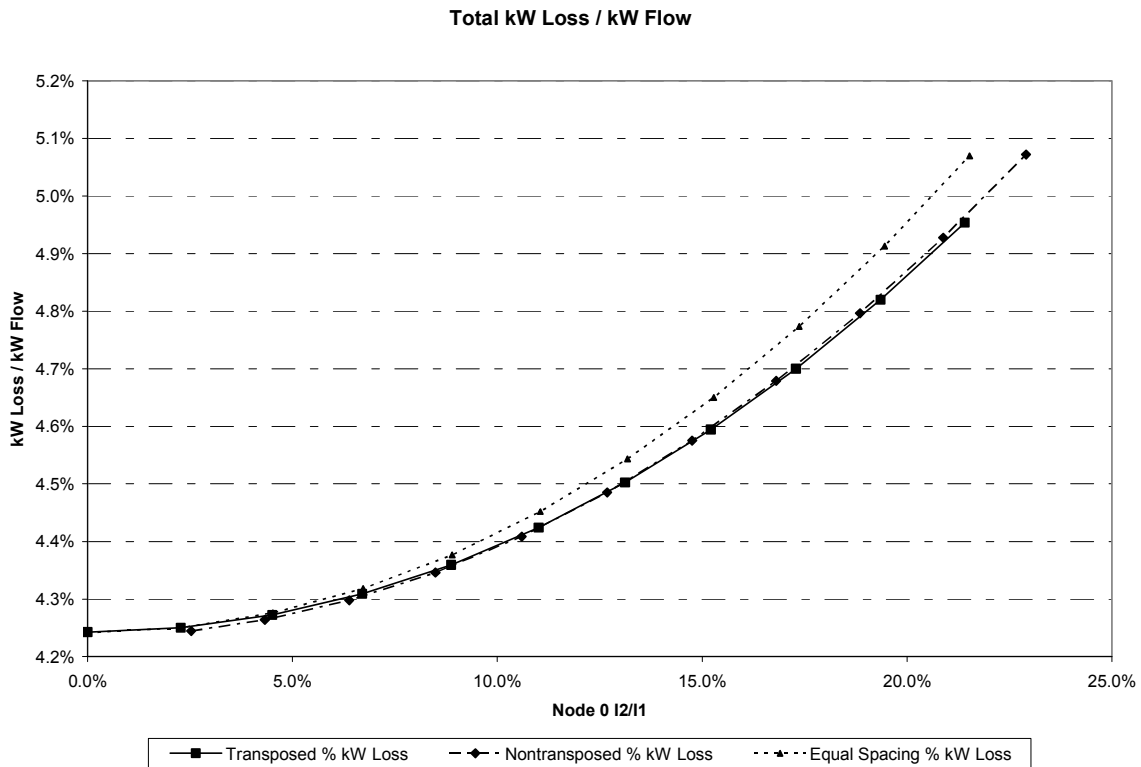


Figure 7. Percent losses versus load imbalance for each line configuration

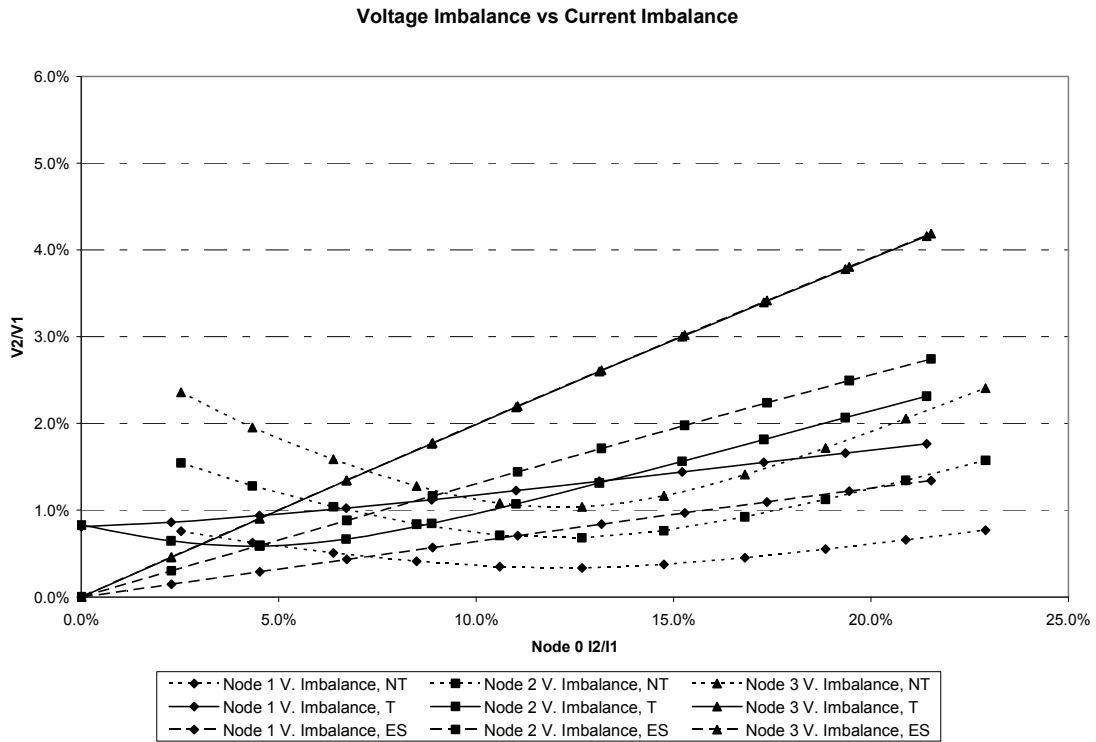


Figure 8. Voltage imbalance versus load imbalance for each line configuration

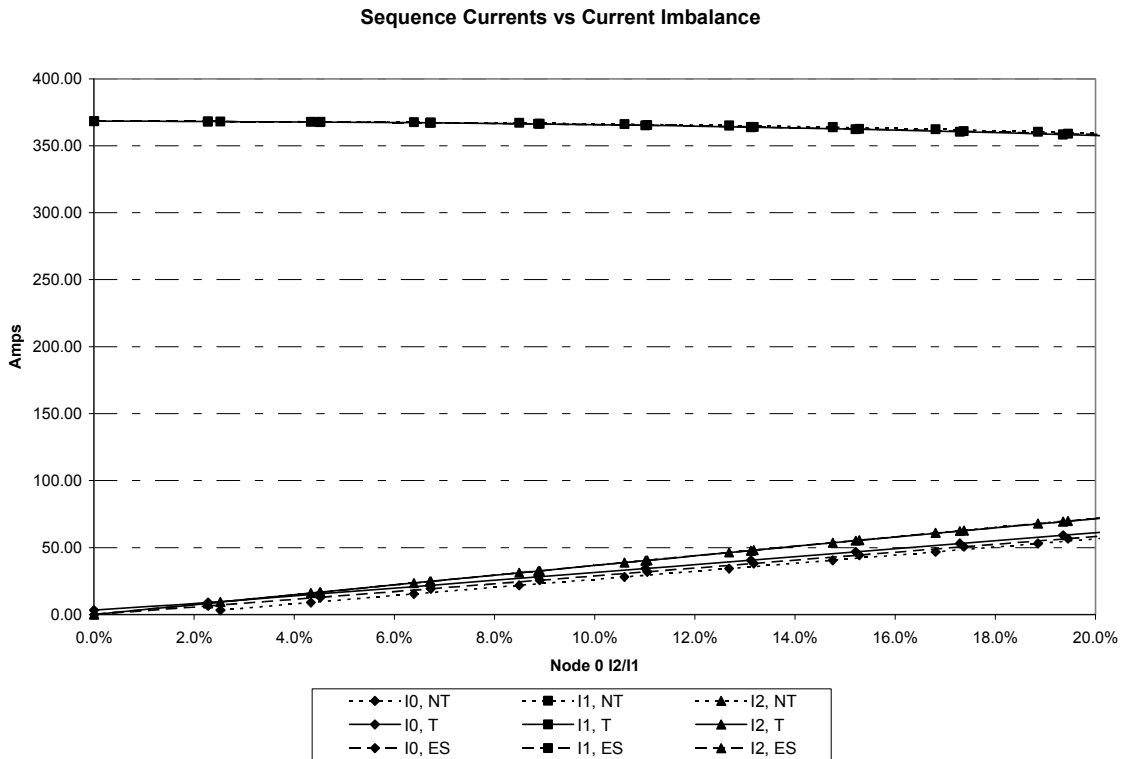


Figure 9. Sequence currents versus load imbalance for each line configuration

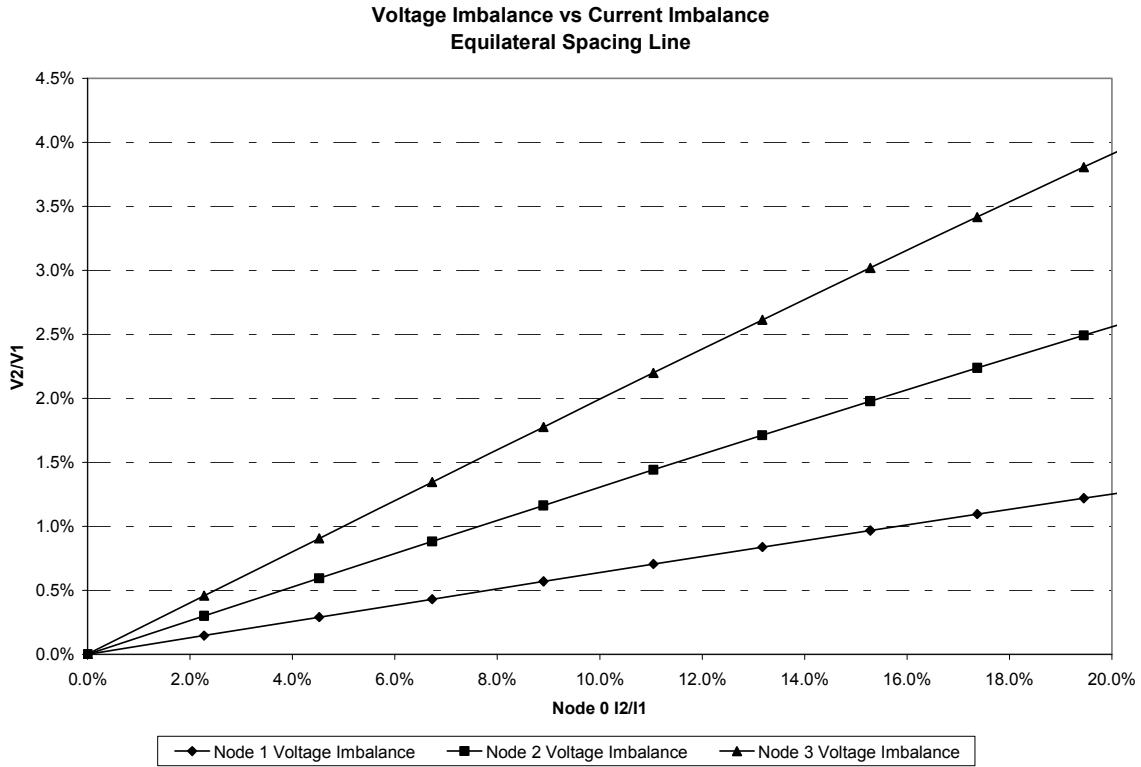


Figure 10. Voltage imbalance versus current imbalance for equilateral spacing line

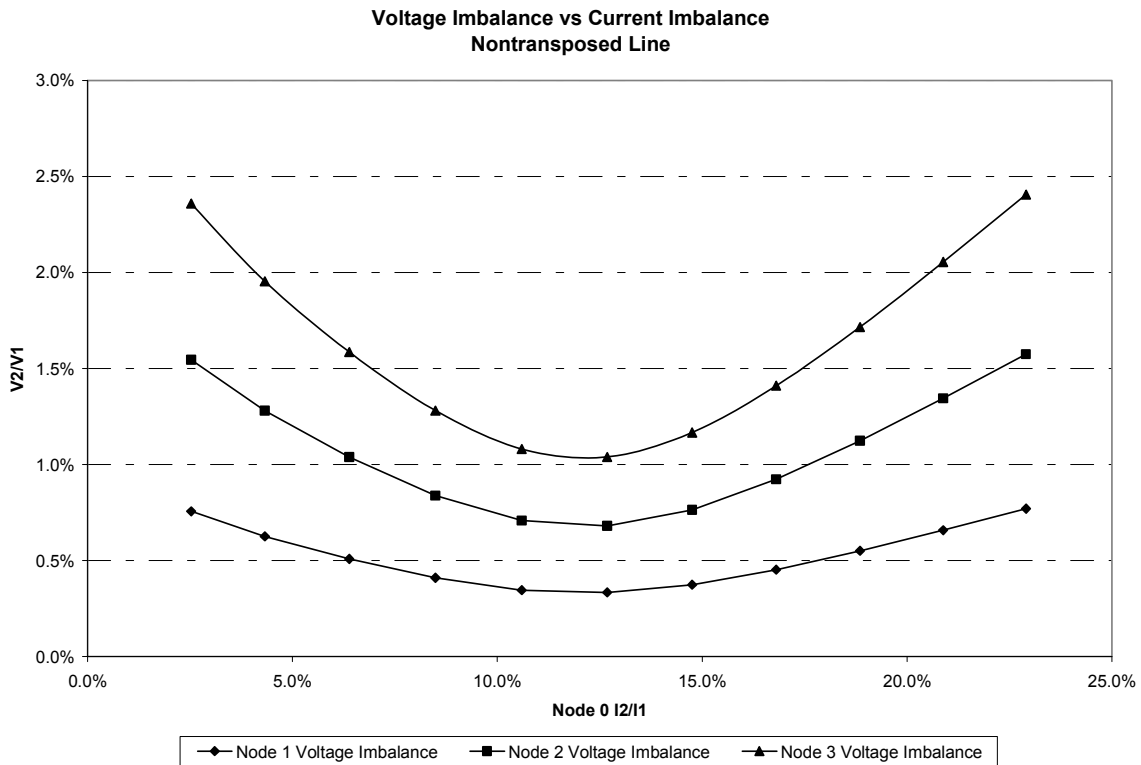


Figure 11. Voltage imbalance versus current imbalance for nontransposed line

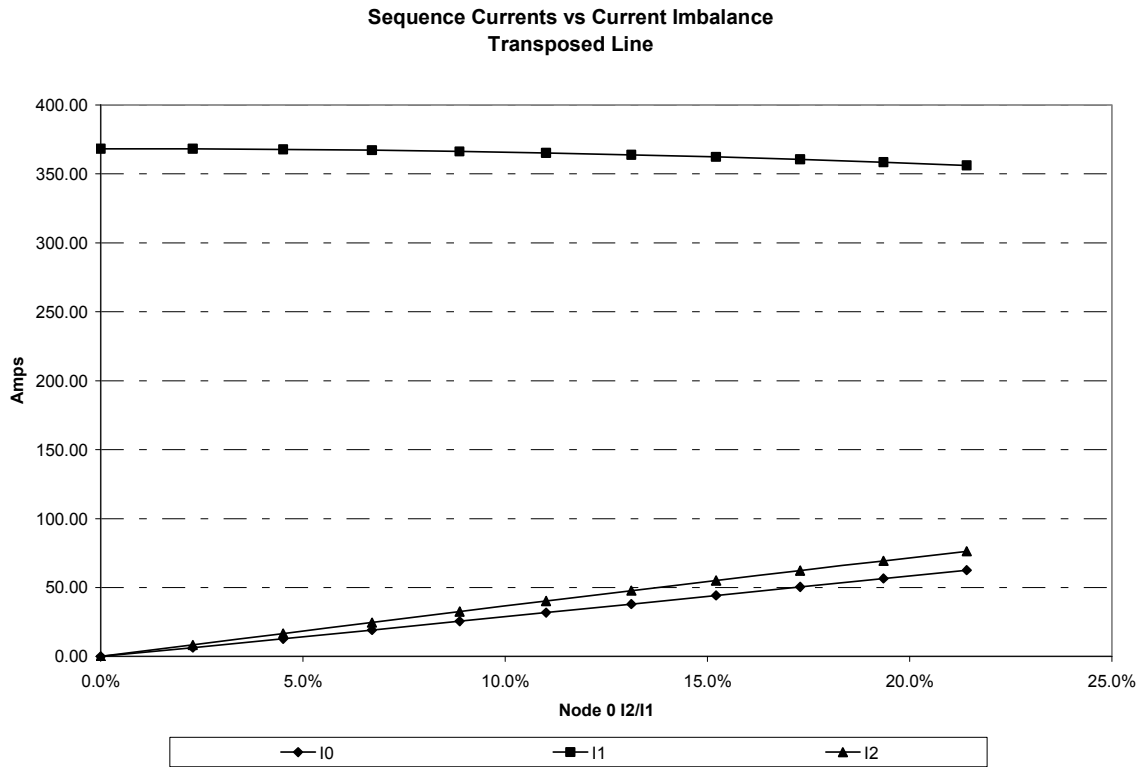


Figure 12. Voltage imbalance versus current imbalance for transposed line

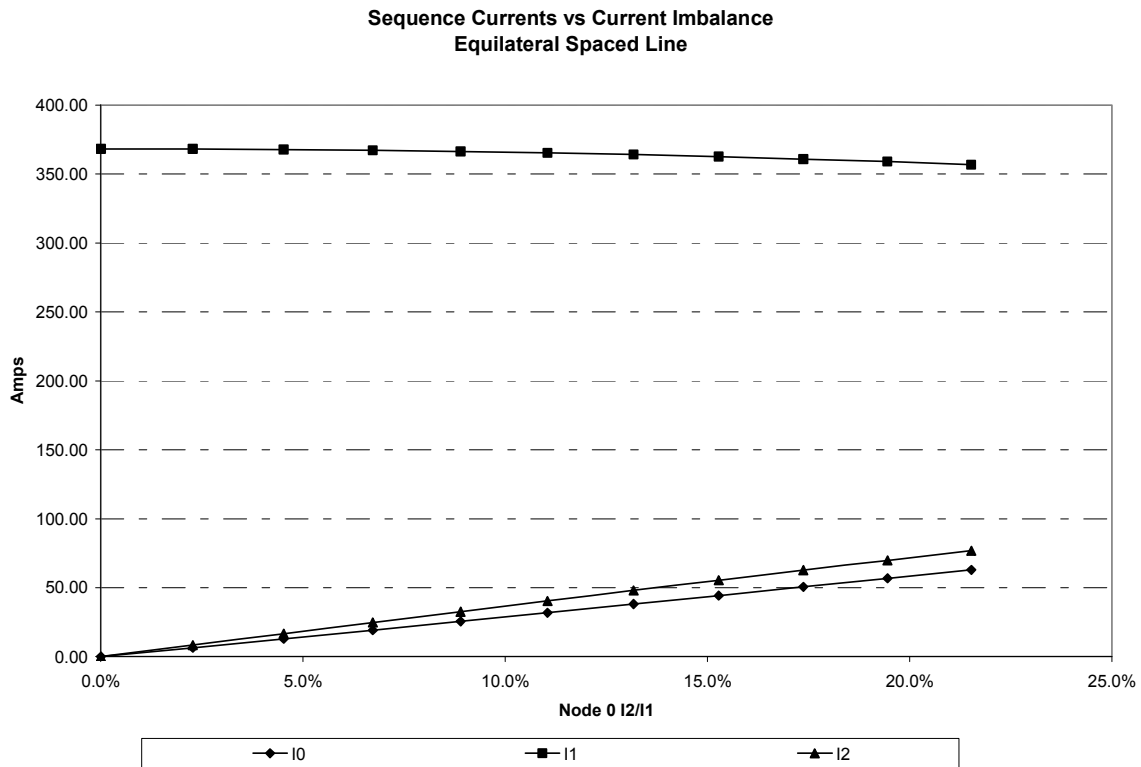


Figure 13. Sequence currents versus current imbalance for equilateral spacing line

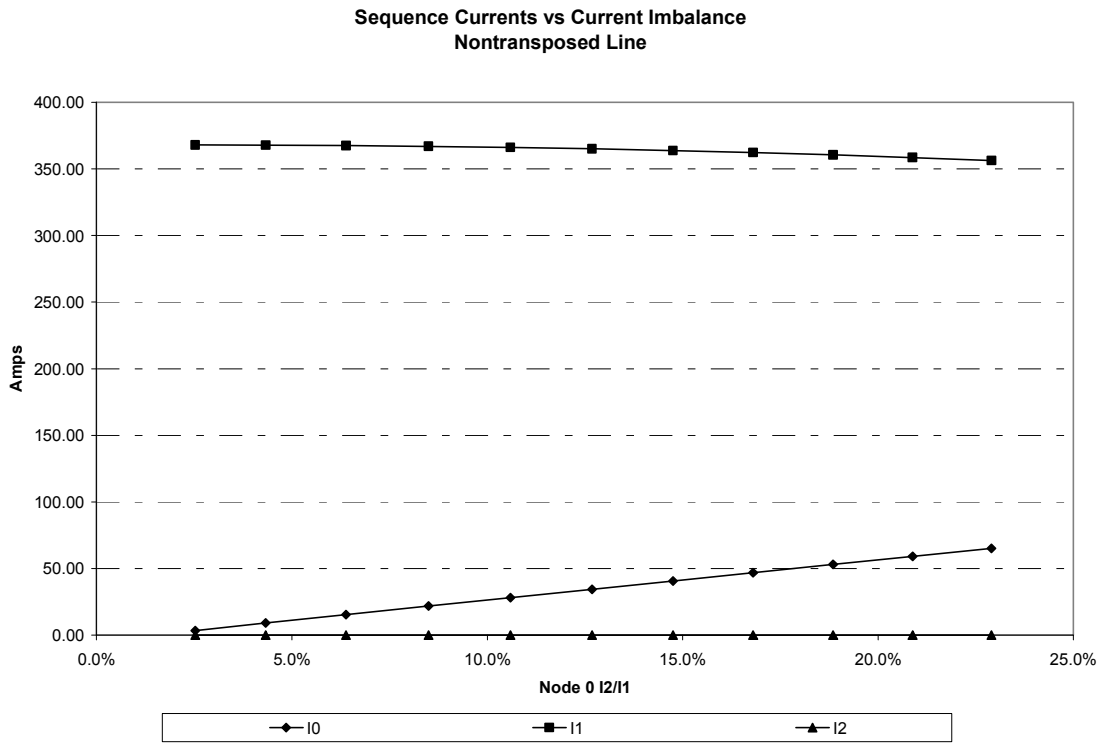


Figure 14. Sequence currents versus current imbalance for nontransposed line

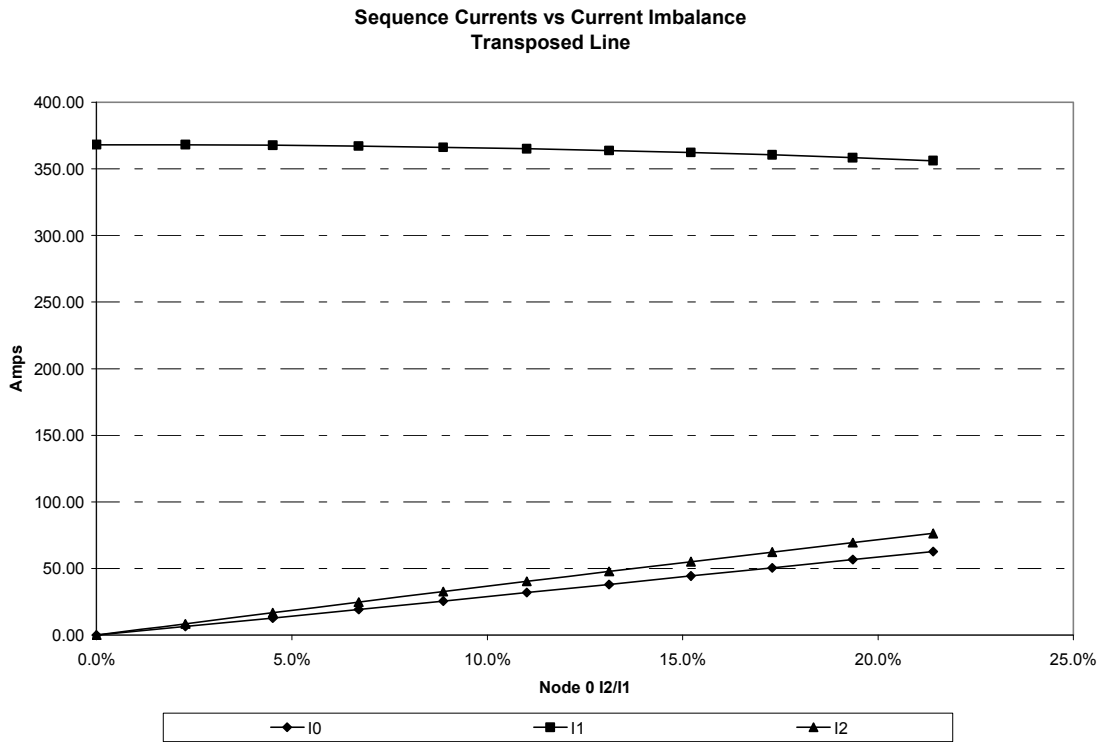


Figure 15. Sequence currents versus current substance for transposed line

Table 5. The Effects of Circuit Spacing and Unbalanced Load on Percent kW Losses

Equilateral Spacing								
	Balanced Load			Total	Unbalanced Load			Total
	$I_2/I_1 = 0\%$				$I_2/I_1 = 21.5\%$			
	ΦA	ΦB	ΦC		ΦA	ΦB	ΦC	
ΦI 's	368.22	368.25	368.28		490.12	300.16	284.99	
kW Losses	117.17	117.02	116.89	351.08	414.10	-72.43	63.39	405.06
% Losses				4.2%				5.10%
Native Load kW				7926				7584
Flat Non-Transposed								
	Balanced Load			Total	Unbalanced Load			Total
	$I_2/I_1 = 2.5\%$				$I_2/I_1 = 22.9\%$			
	ΦA	ΦB	ΦC		ΦA	ΦB	ΦC	
ΦI 's	356.11	375.94	371.99		274.51	494.92	305.56	
kW Losses	194.35	72.47	84.29	351.11	131.84	390.48	-117.36	404.96
% Losses				4.2%				5.10%
Native Load kW				7920				7579
Flat Transposed								
	Balanced Load			Total	Unbalanced Load			Total
	$I_2/I_1 = 0\%$				$I_2/I_1 = 21.4\%$			
	ΦA	ΦB	ΦC		ΦA	ΦB	ΦC	
ΦI 's	368.23	368.24	368.24		487.29	303.37	283.59	
kW Losses	117.05	117.04	117.06	351.15	417.26	-96.12	73.83	394.97
% Losses				4.2%				5.0%
Native Load kW				7925				7578

- Notes
- (1) Balanced loads result is less losses
 - (2) kW losses are greater for the non-transposed line than for transposed because % I_2/I_1 is greater for the non-transposed.
 - (3) Unbalanced load is 4500 kW on Phase A, 2250 kW on Phase B, and 2250 kW on Phase C. Balanced load is 3000 kW on each of the three-phases.

Table 5 presents a summary of the effects of circuit spacing and unbalanced load on percent losses. For the balanced load of 3000 kW on each phase (total load = 9,000 kW), the percent real losses, 4.2%, are the same for the equilateral spacing line, the flat nontransposed line, and the flat transposed line. For the unbalanced loads of 4500 kW on Phase A, 2250 kW on Phase B, and 2250 kW on Phase C, the percent losses are 5.10% for the equilateral and flat nontransposed configurations and 5.0% for the flat transposed configuration.

3.10 Secondary and Service Impedances and Voltage Drops

Secondary and service impedances and voltage drops can be represented as follows.

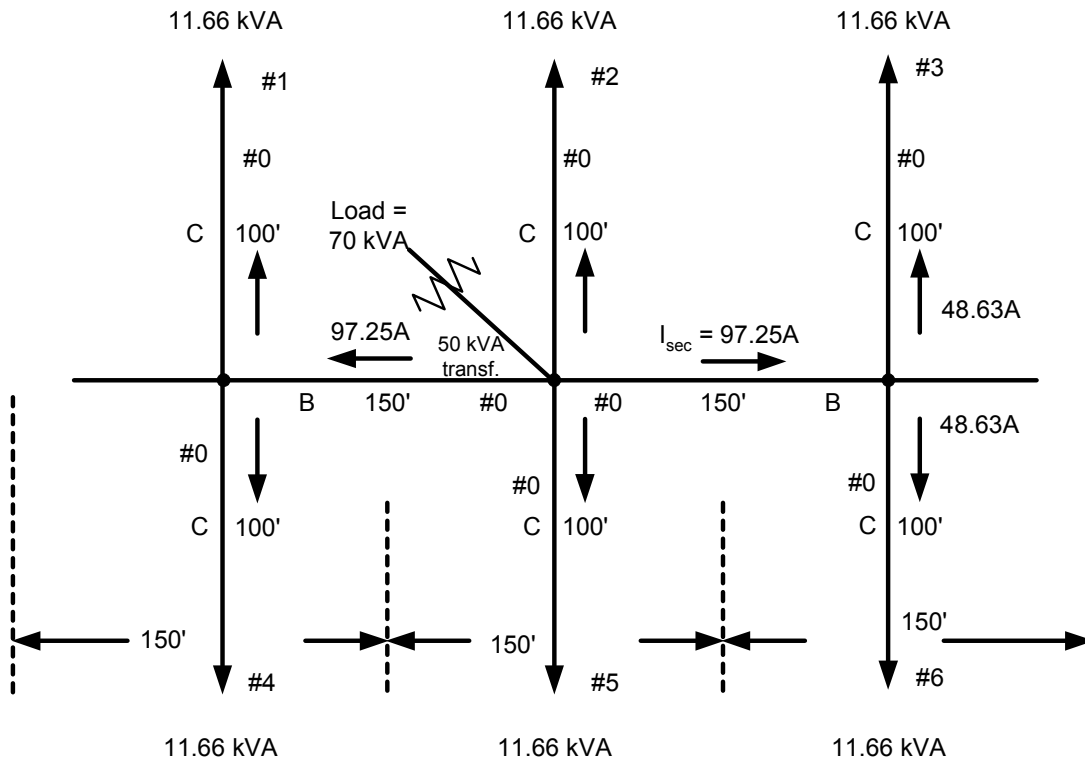


Figure 16. Distribution transformer servicing secondaries and services

Transformer Size = 50 kVA

D_m = maximum coincident total demand on the transformer

D_m = 70 kVA of load and losses

$\cos \theta = 0.90$

$$I_{\text{sec.}} = \frac{1}{2} \left[\frac{70 \text{ kVA} - 2(11.66 \text{ kVA})}{240 \text{ V}} \right] = \frac{1}{2} \left[\frac{46.68 \text{ kVA}}{240 \text{ V}} \right] = 97.25 \text{ A} .$$

$$I_{\text{service}} = \frac{1}{2} (97.25 \text{ A}) = 48.63 \text{ A} .$$

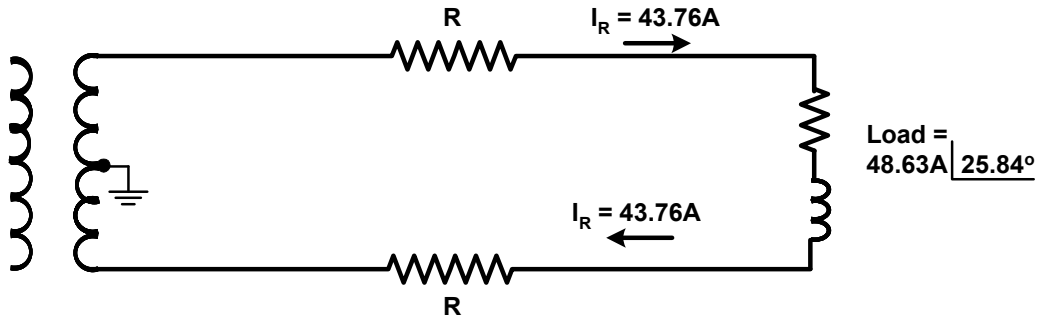


Figure 17. Distribution service drop

The R and X values for the #0 triplex secondary and service are

$$R = 0.211 \Omega/1000 \text{ ft}$$

$$X = 0.031 \Omega/1000 \text{ ft}.$$

The voltage drops in secondary B are

$$\Delta V = 2 (I R \cos \theta + I X \sin \theta) \quad \text{Equation 3.71}$$

$$= 2 [97.25 (0.211 \Omega/1000 \text{ ft} \times 150 \text{ ft}) 0.90 + 97.25 (0.031 \Omega/1000 \text{ ft} \times 150 \text{ ft}) .436]$$

$$= 2 (2.770 + 0.197).$$

$$\Delta V = 5.93 \text{ V @ } 240 \text{ V or } 2.97 \text{ V @ } 120 \text{ V base ,} \quad \text{Equation 3.72}$$

and the drops in the services C are

$$\Delta V = 2 [48.63 (0.211 \Omega/1000 \text{ ft} \times 100 \text{ ft}) 0.90 + 48.63 (0.031 \Omega/1000 \text{ ft} \times 100 \text{ ft}) 0.436]$$

$$= 2 (0.920 + 0.067)$$

$$\Delta V = 1.97 \text{ V @ } 240 \text{ V or } 0.99 \text{ V @ } 120 \text{ V base .} \quad \text{Equation 3.73}$$

The voltage drop for customer #2 and customer #5 is only 0.99 V, but for customers #1, #3, #4, and #6, it is 3.96 V (2.97 + 0.99).

Table 6. Summary of Transformer, Secondary, and Service Voltage Drops

	25 kVA N = 3 No Secondary	50 kVA N = 2 No Secondary	N = 4 Secondary
Transformer	3.68	2.75	2.75
Secondary	--	--	2.97
Service	<u>0.99</u>	<u>0.99</u>	<u>0.99</u>
Total	4.67	3.74	6.71

3.11 Secondary and Service Real Losses

Service drop real losses are determined as follows.

The resistance of #0 aluminum service drops for 100 ft is

$$R_{\text{service}} = 2 (0.211 \Omega/1000 \text{ ft} \times 100 \text{ ft}) = 0.0422 \Omega . \quad \text{Equation 3.74}$$

The resistance is doubled because of the forward and return path of the current.

$$I_{\text{service}}^2 R_{\text{service}} = (48.63)^2 (0.0422) = 99.80 \text{ W per service drop} . \quad \text{Equation 3.75}$$

$$\text{Service Drop Total Real Losses} = (6) (99.80 \text{ W}) = 598.8 \text{ W}, \quad \text{Equation 3.76}$$

Secondary real losses are determined as follows.

$$R_{\text{secondary}} = 2 (0.211 \Omega/1000 \text{ ft} \times 150 \text{ ft}) = 0.0633 \Omega , \quad \text{Equation 3.77}$$

$$I_{\text{sec.}}^2 R_{\text{secondary}} = (97.25)^2 (0.0633) = 598.7 \text{ W per secondary}. \quad \text{Equation 3.78}$$

$$\text{Secondary Total Real Losses} = 2 (598.7 \text{ W}) = 1197.3 \text{ W}. \quad \text{Equation 3.79}$$

$$\begin{aligned} \text{Total Service and Secondary Real Losses} &= 598.8 + 1197.3, & \text{Equation 3.80} \\ &= 1796.1 \text{ W}. \end{aligned}$$

$$\text{Percent Real Losses} = \frac{1.796 \text{ kW}}{(1.4) (50 \text{ kVA}) (0.90)} \times 100 = 2.9\% . \quad \text{Equation 3.81}$$

Note that we must add kW losses for each circuit element and divide by total kW flow to obtain the total circuit percent losses; percent losses cannot be added for each element.

The peak day (July 17, 2006) real power losses for the Milford substation transformer, the Milford Distribution Circuit 8103 primary, overhead and padmount transformers, and secondary and services are summarized in Table 7.

The percent real losses shown in the first column are for the 4.8 kV Hickory Distribution Circuit (Davis, Krupa, and Diedzic 1983). (See also Note 1 in Table 7.) These are actual measured losses and total 5.2%, excluding the substation transformer. The next two columns represent the percent real losses for Milford DC 8103. The second column depicts calculated losses based on the average peak loading of the transformers and services, and a lumped load representing the peak circuit load placed at the midpoint to calculate the primary losses. The third column shows the calculated losses determined from the simulation of the circuit for the peak load hour on July 17, 2006.

Table 7. Comparison of Peak Day Real Losses

	Percent Losses		
	Hickory DC	Milford DC 8103	Milford DC 8103
Transmission	--	3.5	--
Subtransmission	--	4.5	--
Substation Transformer	0.70	0.729	0.702
Primary	3.1 ⁽¹⁾	3.82 ⁽²⁾	3.59 ⁽³⁾
O.H. & UG Transformers	1.3 ⁽¹⁾	1.22 ⁽²⁾	1.50 ⁽³⁾
Secondary & Services	0.8 ⁽¹⁾	0.95 ⁽⁴⁾	0.89 ⁽⁴⁾ 0.31 ⁽⁵⁾
Total Circuit Losses	5.2	5.99	5.98 ⁽⁴⁾ 5.4 ⁽⁵⁾
Total System Losses	13.9	14.72	14.68 14.10

Notes:

- (1) Data [3] are taken from "The Economics of Load Management on the Design and Operation of Distribution System," Murray W. Davis, Theodore J. Krupa, and M. J. Diedzic (March 1983).
- (2) Approximate, based on average loading of transformers and services and lump load placed at midpoint for the primary losses.
- (3) Distribution Engineering Workstation.
- (4) #4 MXAT Services used.
- (5) #0 MXAT Services used.

3.12 Shunt Capacitor Models

When capacitors are connected in parallel, $kVAR = kVAR_1 + kVAR_2 + kVAR_3 + \dots$,

and when connected in series,

$$kVAR = \frac{1}{\frac{1}{kVAR_1} + \frac{1}{kVAR_2} + \frac{1}{kVAR_3} + \dots}$$

The capacitive reactance (in ohms) is

$$X_C = \frac{1}{2 \pi f C \times 10^{-6}} , \quad \text{Equation 3.82}$$

where 1 μf is 2653 Ω at 60 Hz, or

$$X_C = \frac{2653}{C} , \text{ where } C \text{ is } 1 \mu\text{f}.$$

From Equation 3.82, C is then

$$C = \frac{10^6}{2 \pi f X_C} . \quad \text{Equation 3.83}$$

Now, X_C can be defined in terms of voltage and VAR:

$$\text{kVAR} = \text{kV } I_X, \text{ where } I_X = \frac{V}{X_C} .$$

Since $\text{kV} = \frac{V}{1000}$, then

$$\text{kVAR} = \frac{\text{kV}^2 1000}{X_C} , \text{ and}$$

$$X_C = \frac{\text{kV}^2 1000}{\text{kVAR}} . \quad \text{Equation 3.84}$$

The capacitance C in microfarads can be determined in terms of voltage and VAR by substituting Equation 3.82 into Equation 3.84 and solving for C:

$$C = \frac{1000 \text{kVAR}}{\text{kV}^2 2 \pi f} . \quad \text{Equation 3.85}$$

If the capacitance C and voltage are known, then kVAR can be found from Equation 3.85:

$$\text{kVAR} = \frac{\text{kV}^2 2 \pi f C}{1000} . \quad \text{Equation 3.86}$$

Equations 3.84, 3.85, and 3.86 are the most commonly used. Two examples follow.

The ohms per phase for a 300 kVAR, three-phase 4.8 kV delta-connected capacitor bank is

$$\text{kVAR}/\Phi = \frac{300 \text{ kVAR}}{3} = 100 \text{ kVAR} .$$

The line-to-line voltage applied across each capacitor is 4.8 kV. Applying Equation 3.84,

$$X_C = \frac{4.8^2 (1000)}{100} = 230.4 \Omega .$$

The capacitance from Equation 3.85 is

$$C = \frac{(1000)(100)}{(4.8)^2 (377)} = 11.51 \mu\text{f} .$$

The ohms per phase for a 600 kVAR, three-phase 13.2 kV wye-connected capacitor bank is

$$\text{kVAR}/\Phi = \frac{600}{3} = 200 \text{ kVAR} .$$

The voltage across each capacitor is $\frac{13.2 \text{ kV}}{\sqrt{3}}$; therefore, using Equation 3.84 results in

$$X_C = \frac{(7.620)^2 1000}{200} = 290.3 \Omega ,$$

and the capacitance is

$$C = \frac{(1000)(200)}{(7.620)^2 (377)} = 9.14 \mu\text{f} .$$

Capacitor models can be developed using Equation 3.84, which is repeated below.

$$X_C = \frac{\text{kV}^2 1000}{\text{kVAR}} .$$

The susceptance B_C is the reciprocal of X_C ; therefore, B_C from Equation 3.84 becomes

$$B_C = \frac{1}{X_C} = \frac{\text{kVAR}}{\text{kV}^2 1000} , \quad \text{Equation 3.87}$$

where kVAR is the kVAR per phase, and kV is the applied voltage across the capacitor. For a wye-connected capacitor bank,

$$B_C = \frac{1}{X_C} = \frac{\text{kVAR}}{\text{kV}_{LN}^2 1000}, \quad \text{Equation 3.88}$$

and for a delta-connected capacitor bank,

$$B_C = \frac{1}{X_C} = \frac{\text{kVAR}}{\text{kV}_{LL}^2 1000}. \quad \text{Equation 3.89}$$

The line currents for the wye-connected bank are written from Equation 3.88:

$$V_{AN} = I_{C_A} j X_A$$

$$I_{C_A} = \frac{V_{AN}}{j X_A} = V_{AN} j B_A \quad \text{Equation 3.90}$$

$$I_{C_B} = V_{BN} j B_B \quad \text{Equation 3.91}$$

$$I_{C_C} = V_{CN} j B_C. \quad \text{Equation 3.92}$$

For the delta-connected bank, the phase currents are

$$I_{C_{AB}} = V_{AB} j B_{AB} \quad \text{Equation 3.93}$$

$$I_{C_{BC}} = V_{BC} j B_{BC} \quad \text{Equation 3.94}$$

$$I_{C_{CA}} = V_{CA} j B_{CA}, \text{ and} \quad \text{Equation 3.95}$$

the line currents are

$$I_{C_A} = I_{C_{AB}} - I_{C_{CA}} \quad \text{Equation 3.96}$$

$$I_{C_B} = I_{C_{BC}} - I_{C_{AB}} \quad \text{Equation 3.97}$$

$$I_{C_C} = I_{C_{CA}} - I_{C_{BC}}. \quad \text{Equation 3.98}$$

In matrix form, Equations 3.96, 3.97, and 3.98 can be written as

$$\begin{bmatrix} I_{C_A} \\ I_{C_B} \\ I_{C_C} \end{bmatrix} = \begin{bmatrix} 1 & 0 & -1 \\ -1 & 1 & 0 \\ 0 & -1 & 1 \end{bmatrix} \bullet \begin{bmatrix} I_{C_{AB}} \\ I_{C_{BC}} \\ I_{C_{CA}} \end{bmatrix} . \quad \text{Equation 3.99}$$

3.13 Step Voltage Regulator Models

Both Type A and Type B step voltage regulators are modeled. The relationship between the source voltage V_S and load voltage V_L for the single-phase step voltage regulator is:

$$V_S = a_r V_L, \quad \text{Equation 3.100}$$

where a_r is defined as

$$a_r = 1 \mp \frac{\text{Total \% Range}}{\# \text{ of Steps}} \times \text{Tap} \quad \text{Equation 3.101}$$

with the following sign convention:

	Type A	Type B
Raise	+	-
Lower	-	+

The relationship between source current and load current for the single-phase step voltage regulator is

$$I_S = \frac{1}{a_r} I_L . \quad \text{Equation 5.102}$$

3.14 Synchronous Generator Model

The Distribution Engineering Workstation uses two models to represent the synchronous machine, one for power flow and another for transient analysis. Since this study does not involve transient analysis, only the power flow model will be considered. The following is a graphical representation of the power flow synchronous machine model.

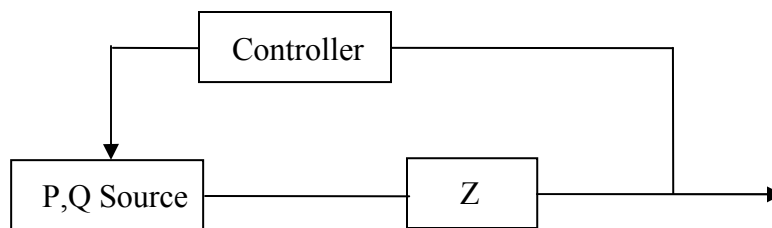


Figure 18. Steady-state synchronous machine model

As shown in Figure 18, the synchronous machine model used in power flow consists of a real and reactive power source along with the impedance Z (in this case, the synchronous impedance). The controller takes measurements from machine terminals—specifically, voltage magnitude and power factor—and allows the machine to operate in two different modes: constant P with power factor control, or constant P and constant Q .

The model takes into account the minimum and maximum generation limits of the machine, and the controller adjusts the P, Q source based on the control mode. For example, if the machine is in constant P with power factor control mode, the controller will maintain real rated power while varying the reactive power within the machine limits in an attempt to hold constant the power factor at the point of measurement.

3.15 Self-Excited Induction Generator Model

A self-excited induction generator (SEIG) can be represented as a two-phase primitive machine with stator windings fixed and rotor windings rotating. The currents i_{ds} and i_{qs} are the stator currents, and i_{dr} and i_{qr} are the rotor currents in the direct and quadrature axes, respectively. Figure 19 shows the mechanical angular speed of the rotor as $\omega = d\theta/dt$.

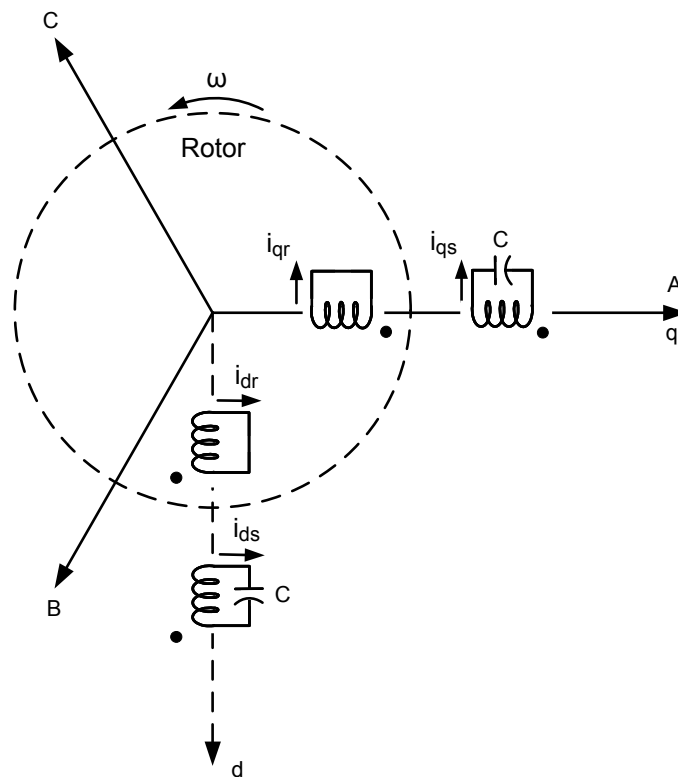


Figure 19. Two-phase primitive machine to be interconnected to an RLC load

A SEIG with capacitor added is represented in Equation 3.103. The voltage drop across the capacitor for the direct axis is v_{Cd} , and for the quadrature axis, it is v_{Cq} . The term $1/pC$ represents this voltage drop, since

$$v = \frac{1}{C} \int i dt ,$$

$$p = d/dt , \text{ and}$$

$$\frac{1}{p} = \int^t dt .$$

$$\begin{bmatrix} v_{ds} \\ v_{qs} \\ v_{dr} \\ v_{qr} \end{bmatrix} = \begin{bmatrix} R_1 + L_1 p + \frac{1}{pC} & 0 & Mp & 0 \\ 0 & R_1 + L_1 p + \frac{1}{pC} & 0 & Mp \\ Mp & \omega M & R_2 + L_2 p & \omega L_2 \\ -\omega M & Mp & -\omega L_2 & R_2 + L_2 p \end{bmatrix} \begin{bmatrix} i_{ds} \\ i_{qs} \\ i_{dr} \\ i_{qr} \end{bmatrix} .$$

Equation 3.103

Equation 3.103 represents the *no-load* condition, and the turns ratio is assumed to be unity; therefore, if needed, the ratio must be included when referring the rotor parameters to the stator.

The mutual inductance M varies with the relative position between the stator and rotor. R_1 and R_2 are the stator and rotor resistances, and L_1 and L_2 are their inductances. The additional voltage drop due to the mutual flux is

$$\phi_m = Mi, \text{ and}$$

$$v = \frac{d \phi_m}{dt} = M \frac{di}{dt} + \frac{idM}{dt} .$$

$$= Mpi + ipM$$

Equation 3.104

There is a nonlinear relationship between the magnetizing reactance and the magnetizing current; therefore, the mutual inductance M varies continuously. The term Mpi represents the current variation due to the stator and the term ipM is the variation due to the rotation of the rotor.

3.15.1 Resistive Load

When a resistive load R is added in parallel with the self-excitation capacitor C , then the voltage across this R load is the same as the voltage across the capacitor. When referring to the direct axis stator of Figure 19, we see that the addition of the load resistor changes the equivalent circuit to that of Figure 20.

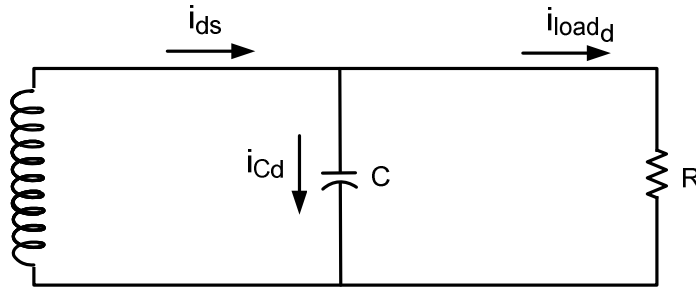


Figure 20. Stator direct axis with an R_{load} added

Since $v_{load\ d} = v_{Cd} = R i_{load\ d}$, and

Equation 3.105

$$i_{Cd} = C \frac{d v_{Cd}}{dt} = C p v_{Cd}, \text{ then}$$

$$i_{Cd} = C p R i_{load\ d}.$$

Because

$$i_{ds} = i_{Cd} + i_{load\ d}, \text{ therefore}$$

$$i_{ds} = R C p i_{load\ d} + i_{load\ d}, \text{ and}$$

$$= i_{load\ d} (R C p + 1).$$

Equation 3.106

From Equation 3.105,

$$i_{load\ d} = \frac{i_{ds}}{R C p + 1}.$$

Equation 3.107

Substituting Equation 3.107 into Equation 3.105 results in

$$v_{load\ d} = \frac{R i_{ds}}{R C p + 1}.$$

Equation 3.108

The quadrature load voltage is obtained in a similar manner as

$$v_{load\ q} = \frac{R i_{qs}}{R C p + 1}.$$

Equation 3.109

Now, Equation 3.103 can be rewritten with the addition of the *resistive load* R from Equations 3.108 and 3.109 as

$$\begin{bmatrix} v_{ds} \\ v_{qs} \\ v_{dr} \\ v_{qr} \end{bmatrix} = \begin{bmatrix} R_1 + L_1 p + \frac{R}{RCp+1} & 0 & Mp & 0 \\ 0 & R_1 + L_1 p + \frac{R}{RCp+1} & 0 & Mp \\ Mp & \omega M & R_2 + L_2 p & \omega L_2 \\ -\omega M & Mp & -\omega L_2 & R_2 + L_2 p \end{bmatrix} \begin{bmatrix} i_{ds} \\ i_{qs} \\ i_{dr} \\ i_{qr} \end{bmatrix}$$

Equation 3.110

3.15.2 Resistance-Inductance-Capacitance Load

When a resistance and an inductance load R_L and L_L is added in parallel with the self-excitation capacitor C_s or a combination of this excitation capacitor and other capacitors C_L on the circuit in parallel, then C in the following equations considers this combination of capacitors (see Figure 21).

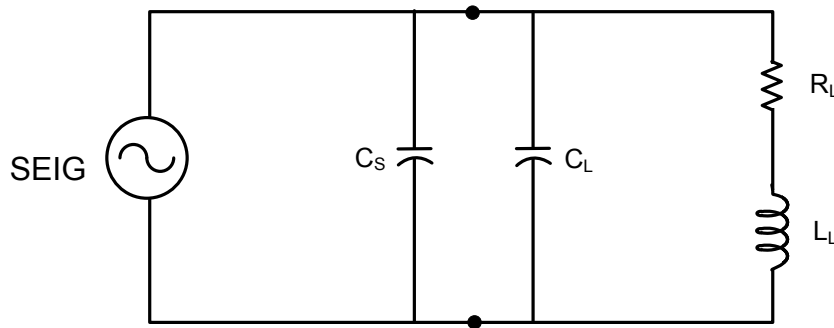


Figure 21. RLC load R_L , L_L , and C_L connected to the self-excited capacitor C_s

Since $v_{load\ d} = Ri_{load\ d}$ from Equation 3.105, then $v_{load\ d}$ with load inductance added is

$$v_{load\ d} = Ri_{load\ d} + L p i_{load\ d}, \quad \text{Equation 3.111}$$

and

$$i_{Cd} = Cp v_{load\ d} = (RCp + LCp^2) i_{load\ d}. \quad \text{Equation 3.112}$$

Now, from Equation 3.112,

$$i_{ds} = i_{Cd} + i_{load\ d} = (RCp + LCp^2) i_{load\ d} + i_{load\ d}, \quad \text{Equation 3.113}$$

and

$$i_{\text{load } d} = \frac{i_{ds}}{RCp + LCp^2 + 1}. \quad \text{Equation 3.114}$$

From Equation 3.111,

$$v_{\text{load } d} = Ri_{\text{load } d} + Lpi_{\text{load } d}, \quad \text{and}$$

$$v_{\text{load } d} = (R + Lp) i_{\text{load } d}. \quad \text{Equation 3.115}$$

Substituting $i_{\text{load } d}$ from Equation 3.114 into Equation 3.115 results in

$$v_{\text{load } d} = \frac{R + Lp}{RCp + LCp^2 + 1} i_{ds}. \quad \text{Equation 3.116}$$

The quadrature load voltage would become

$$v_{\text{load } q} = \frac{R + Lp}{RCp + LCp^2 + 1} i_{qs}. \quad \text{Equation 3.117}$$

Equation 3.103 can be rewritten with the addition of resistance load R , inductive load L , and capacitive load C using Equation 3.117.

Equation 3.118 is the impedance matrix for a single self-excited induction generator serving an RLC load. Note that the variation in the magnetizing reactance due to the magnetizing current must be included and corrected, as shown in the development of Equation 3.104.

$$\begin{bmatrix} v_{ds} \\ v_{qs} \\ v_{dr} \\ v_{qr} \end{bmatrix} = \begin{bmatrix} R_1 + L_1 p + \left(\frac{R + Lp}{RCp + LCp^2 + 1} \right) & 0 & Mp & 0 \\ 0 & R_1 + L_1 p + \left(\frac{R + Lp}{RCp + LCp^2 + 1} \right) & 0 & Mp \\ Mp & \omega M & R_2 + \frac{L_2}{p} & \omega L_2 \\ -\omega M & Mp & -\omega L_2 & R_2 + L_2 p \end{bmatrix} \begin{bmatrix} i_{ds} \\ i_{qs} \\ i_{dr} \\ i_{qr} \end{bmatrix}$$

$$\text{Equation 3.118}$$

3.16 Inverter-Based Generator Model

The 400 kW, 500 kVA inverter-based generator consists of a high-speed a-c generator driven by a 440 kW twin spool gas turbine engine. Figure 22 is a simplified one-line diagram of the 400 kW, 60 Hz generator and inverter.

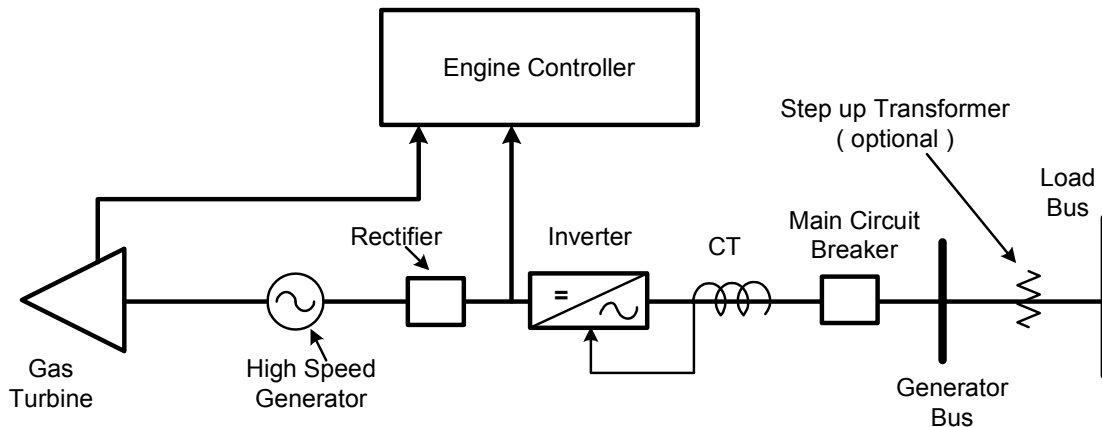


Figure 22. One line diagram of a 400 kW inverter-based generator and prime mover

The unit has seamless transfer capability where it can be operating in a current source mode parallel to the external power supply with only 10% load and switch without outage to deliver power in the voltage source mode to an islanded load. This generating unit has a continuous overload capability of 110% of rated load at any power factor from -0.8 to 0.8, and it can follow load steps of 25% up or down while maintaining frequency to less than ± 0.1 Hz. The voltage total harmonic distortion is less than 2%, and it can handle 100% load imbalance. During short circuits, it can deliver 200% of rated current for about 8 seconds.

The inverter model is represented by the voltage pullback curves given in Figure 23. The unit can deliver 1.10 per unit current (602 A root-mean-square [rms]) at 1.0 per unit rated voltage (277 V rms) and 2.0 per unit current at 0.56 per unit voltage. The inverse time current characteristic is given in Figure 24.

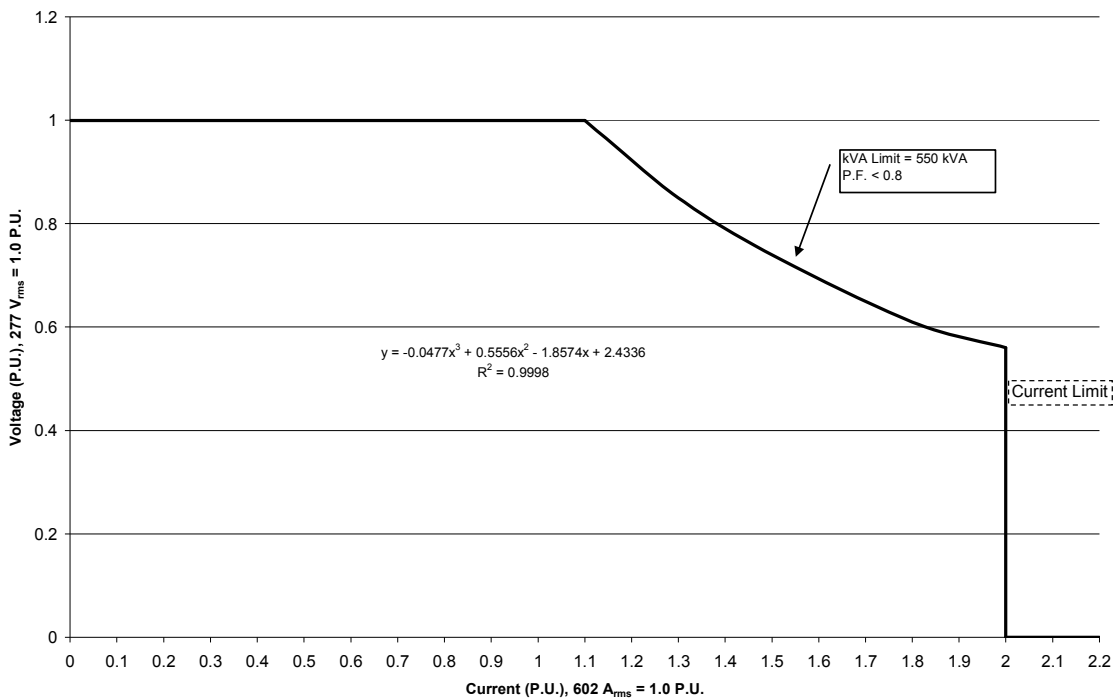


Figure 5.22 Voltage Pullback Curves

Figure 23. Voltage pullback curves

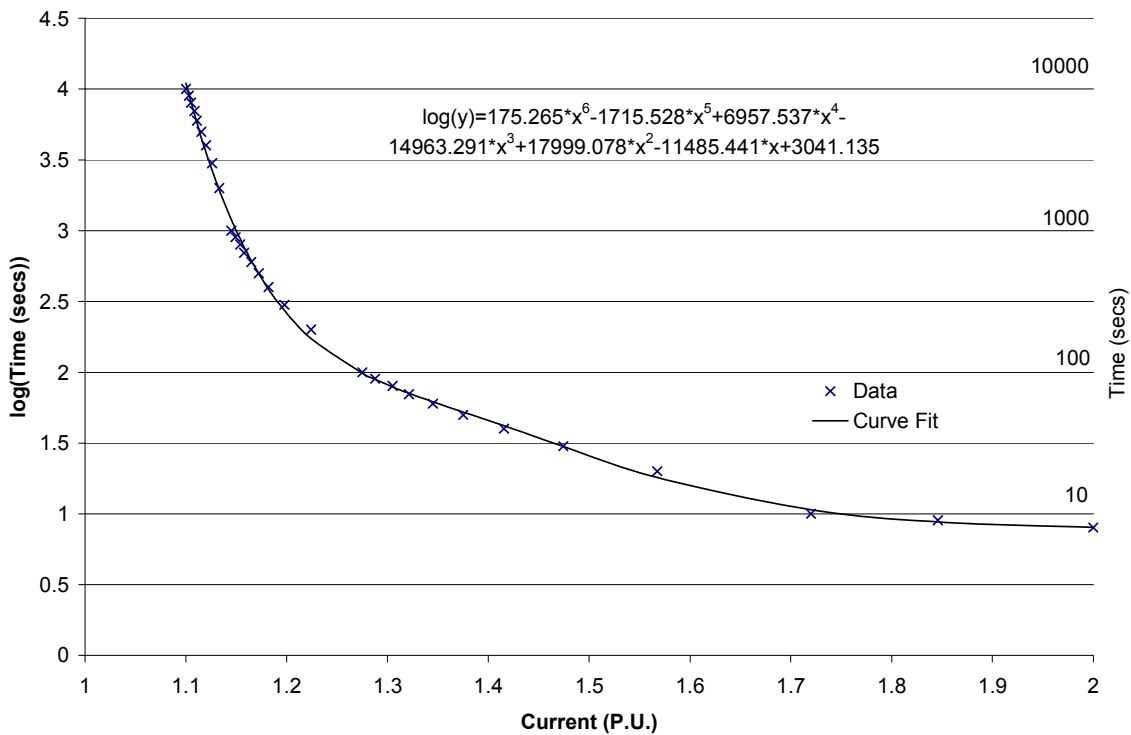


Figure 24. Inverse time-current characteristic

4.0 Results for the Design of Field Voltage Regulation and Metering Equipment Used to Verify the Models

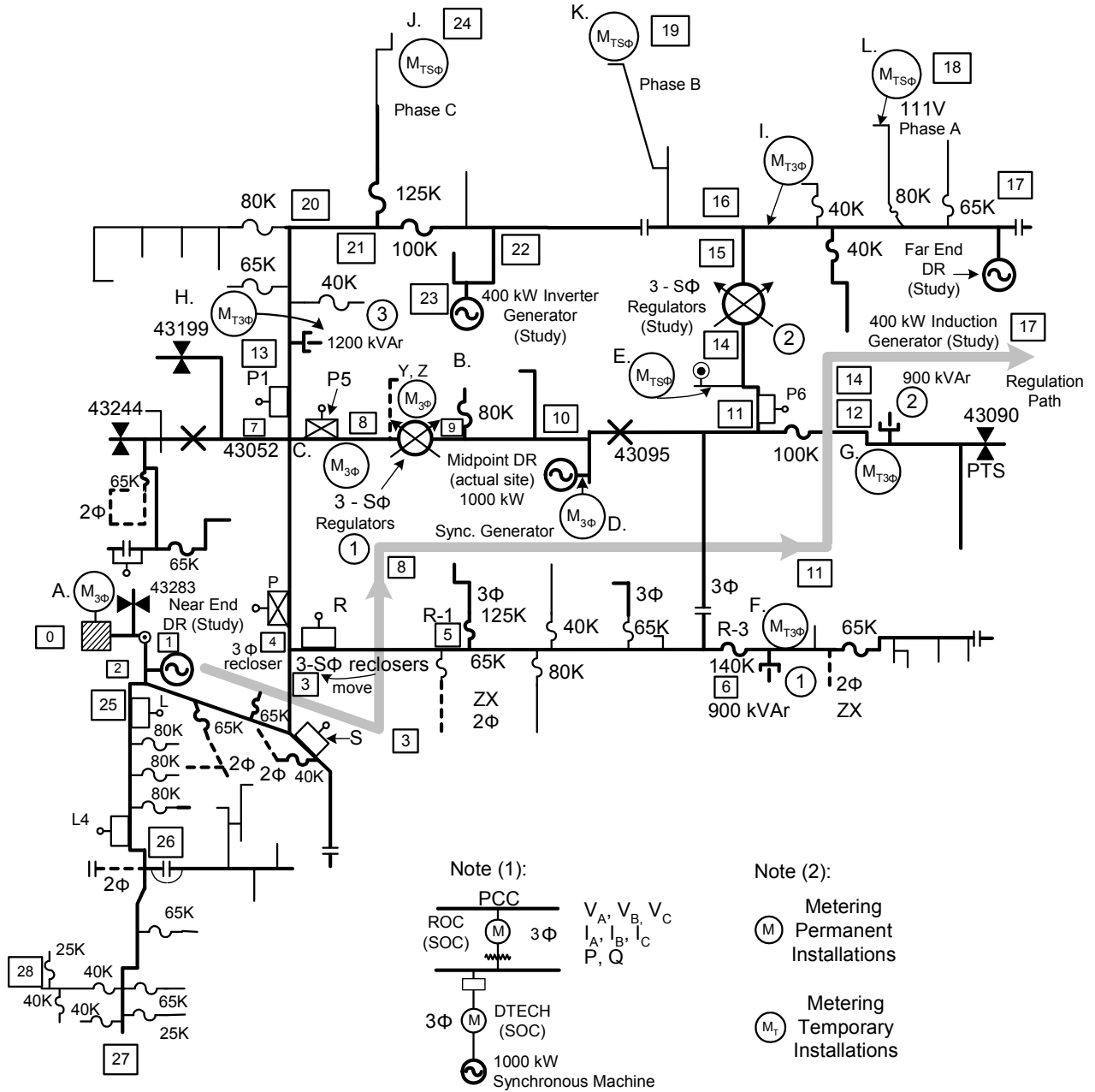
This section defines the equipment installed on the Milford DC 8103 for controlling voltage and the metering equipment used to validate the models developed in Section 3.0.

4.1 Voltage Regulation Equipment

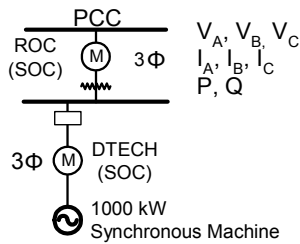
Figure 25 shows the locations of the voltage regulation equipment on the Milford Circuit DC 8103. Table 8 describes this equipment.

Table 8. Voltage Regulation Equipment

Location	Description
A.	10 MVA delta-wye transformer #1 Z = 7.02%, 41.57 kV/13.8 kV, 0, ± 2.5 , ± 5.0 high side setting = 0, low side setting = 0, LTC ± 16 steps $\pm 10\%$, $a_N = 3$ (see Figure 26)
B.	3 – 167 kVA single-phase step voltage regulators, 32 steps
D.	1000 kW synchronous generator, 1050 kW power prime mover, rated output = 1312 kVA @ P.F. = 0.8, 1800 rpm, 480 V, 60 Hz, voltage regulation $\pm 5\%$.
F.	(1) 900 kVAR 3 Φ capacitor Y-connected, neutral grounded
G.	(2) 900 kVAR 3 Φ capacitor Y-connected, neutral grounded
H.	(3) 1200 kVAR 3 Φ capacitor Y-connected, neutral grounded



Note (1):



Note (2):

- Metering Permanent Installations (M)
- Metering Temporary Installations (MT)

Note (3): Nodes where low voltage, high voltage, highest unbalance voltage, highest unbalanced load and nodes where actual values exceed pre-set values (criteria violations) may be different than the nodes indicated above.

Note (4): The LTC voltage regulator is gang operated using the C phase as reference.

Note (5): The "P" reclosure data is sent to midpoint DR consisting of $I_{A'}, I_{B'}, I_{C'}$, $V_{CN'}, V_{BN'}, V_{CN'}$, kW_A, kW_B, kW_C , $kVAr_A, kVAr_B, kVAr_C$

Figure 25. Milford Circuit DC 8103

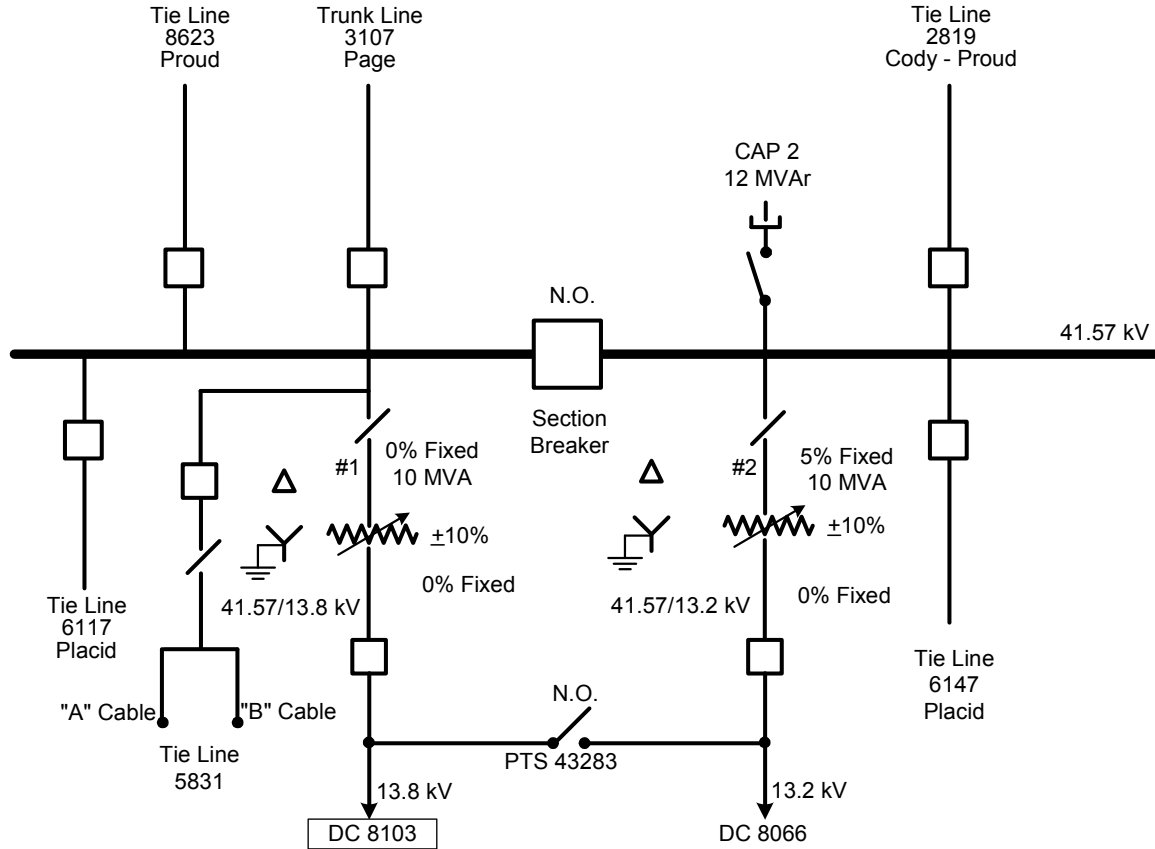


Figure 26. Milford Substation one line diagram

4.2 Major System Protection Equipment

The major system protection equipment shown in Table 9 consists of three-phase and single-phase reclosers and single-phase sectionalizers.

Table 9. Major System Protection Equipment

Location	Description of Major System Protection Equipment
1. R	3 – 3 Φ reclosers – 280A vacuum V4L, 2A, 2D
2. P	1 – 3 Φ recloser – 680A vacuum VWE, R, C
3. P5	3 – S Φ reclosers – 280A vacuum V4L, 2A, 2D
4. P1	3 – S Φ reclosers – 280A vacuum V4L, 2A, 2D
5. S	3 – S Φ reclosers – 140A vacuum V4L, 1A, 3D
6. L	3 – S Φ reclosers – 140A vacuum V4L, 1A, 3D
7. L4	3 – S Φ sectionalizers – 140A hydraulic
8. P6	3 – S Φ reclosers – 140A V4L, 2A, 2D

Table 10. Measurement Locations and Data Collection

Permanent Metering Locations					
Temporary Metering Locations					
A.	Substation	M3 Φ	V_{AN}, V_{BN}, V_{CN}	I_A, I_B, I_C	P, Q, P.F.
B.	Regulators (1)	M3 Φ	V_{AN}, V_{BN}, V_{CN}	I_A, I_B, I_C	P, Q, P.F.
D.	1000 kW Sync. DR	M3 Φ	V_{AN}, V_{BN}, V_{CN}	I_A, I_B, I_C	P, Q, P.F.
Temporary Metering Locations					
F.	900 kVAR capacitor	$M_{T\ 3\ \Phi}$	V_{AN}, V_{BN}, V_{CN}	I_A, I_B, I_C	
G.	900 kVAR capacitor	$M_{T\ 3\ \Phi}$	V_{AN}, V_{BN}, V_{CN}	I_A, I_B, I_C	
H.	1200 kVAR capacitor	$M_{T\ 3\ \Phi}$	V_{AN}, V_{BN}, V_{CN}	I_A, I_B, I_C	
I.	3 Φ circuit tag end	$M_{T\ 3\ \Phi}$		I_A, I_B, I_C	
K.L.	Single-phase tag ends	$M_{T\ S\ \Phi}$	V_{AN}	V_{BN}	

4.3 Metering Equipment and Accuracy of Measurements

4.3.1 Substation Metering

The substation metering consists of the ION 7600 Power Measurements Meter, which measures the three-phase voltages, the three line currents, and the phase power factors and calculates kW per phase and total kW, kVAR per phase and total kVAR, kVA per phase and total kVA, and the unbalanced voltage and unbalanced current. The integration period is 15 minutes. The accuracy of the metered data is 0.1% for voltage, 0.1% for current, +0.01 Hz for frequency, and 0.5% for power factor. The kW, kVAR, and kVA accuracy is Class 0.2.

4.3.2 Synchronous Generator Metering

The generator metering is a 3720 ACM meter, which measures the three-phase voltages, the three line currents, three-phase kW, three-phase kVAR, three-phase kVA, power factor, frequency, and circuit load, including generation. The data are 30-second samples integrated over 5 minutes. The data are 5-minute samples averaged over 15 minutes. The accuracy of the measured data is given in Table 11.

Table 11. Accuracy of 3720 ACM

Parameter	Accuracy
Current	0.2%
kW	0.4%
kVAR	0.4%
kVA	0.4%
Voltage	0.2%
Power Factor	1.0%
Frequency	0.05 Hz

4.3.3 Capacitor Location Metering

The metering at the capacitor locations (nodes F, G, and H) is the Line Tracker LT40 from Grid Sense. These metering devices measure the three-phase voltages and three line currents. Voltage is sampled at 600 samples per second; current is sampled at 1200 samples per second. The accuracy of the current measurement is $\pm 5\%$. The integration period is 15 minutes.

4.3.4 Voltage Regulator Location Metering

The CL-6 control of the voltage regulators at location B measures the load and source phase voltages, line currents, phase kW, phase kVAR, phase kVA, and phase power factor. The data are integrated over 15 minutes, and the accuracy is Class 1 metering, or 1.0% for all power quantities (i.e., voltage, current, kW, kVAR, and kVA).

4.3.5 Single-Phase Voltage Customer Metering

The Rustrak was used to measure voltage and current. The accuracy is 0.25% for voltage and 0.5% for current. Each stated accuracy is in percent of reading. The integration period is 15 minutes.

5.0 Results for Distributed Generation Control Strategies Used in Field Verification

This section defines the generation equipment voltage regulation capability and the control strategies used to regulate the voltage on the Milford Circuit DC 8103.

5.1 1000 kW Synchronous Generator

The voltage regulation control capabilities for the 1000 kW synchronous generator located at the midpoint on the circuit node D are given in Figure 27.

5.2 400 kW High-Speed Generator and Inverter

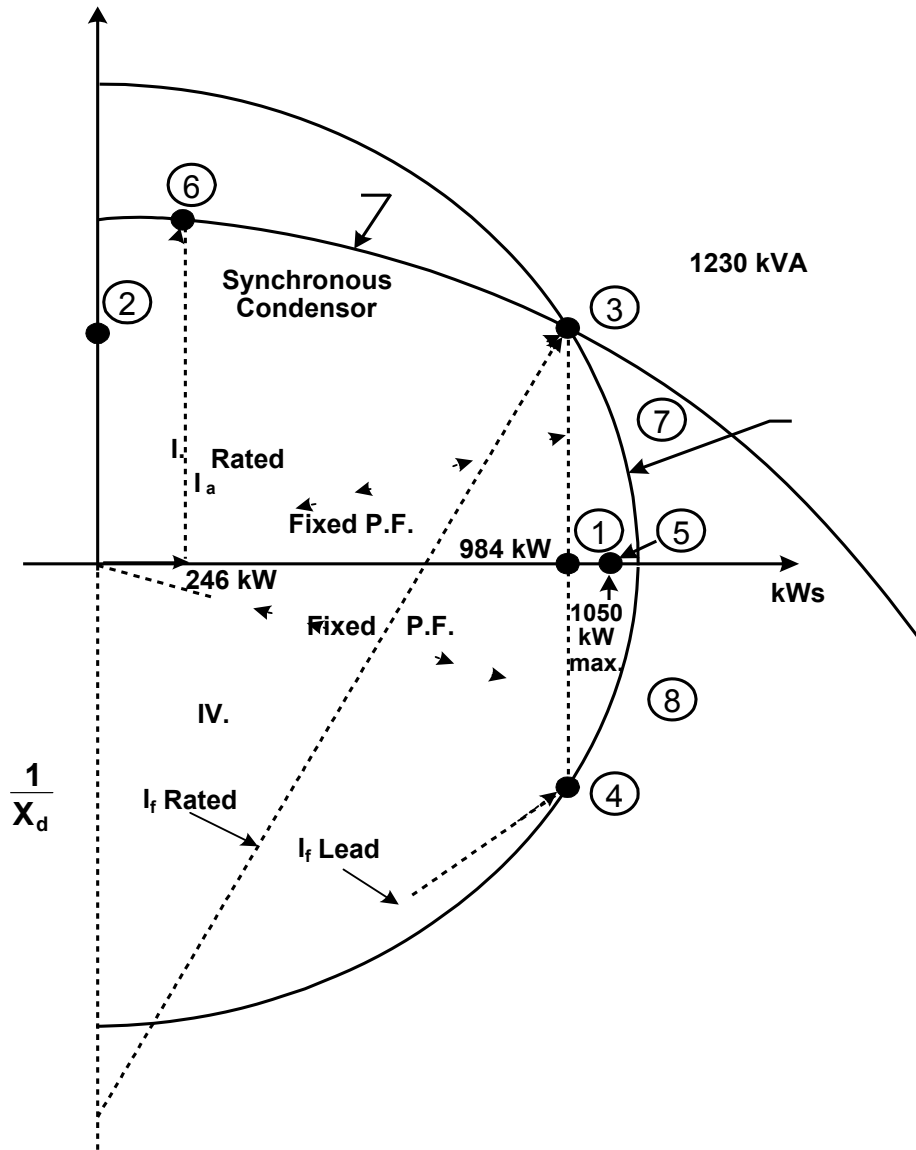
The voltage regulation control capability for the 400 kW high-speed generator and inverter is shown in Figure 28.

5.3 400 kW Self-Excited Induction Generator

The voltage regulation control capability for the 400 kW self-excited induction generator is displayed in Figure 29.

5.4 Voltage Regulation Simulations and Field Verification Strategy 17

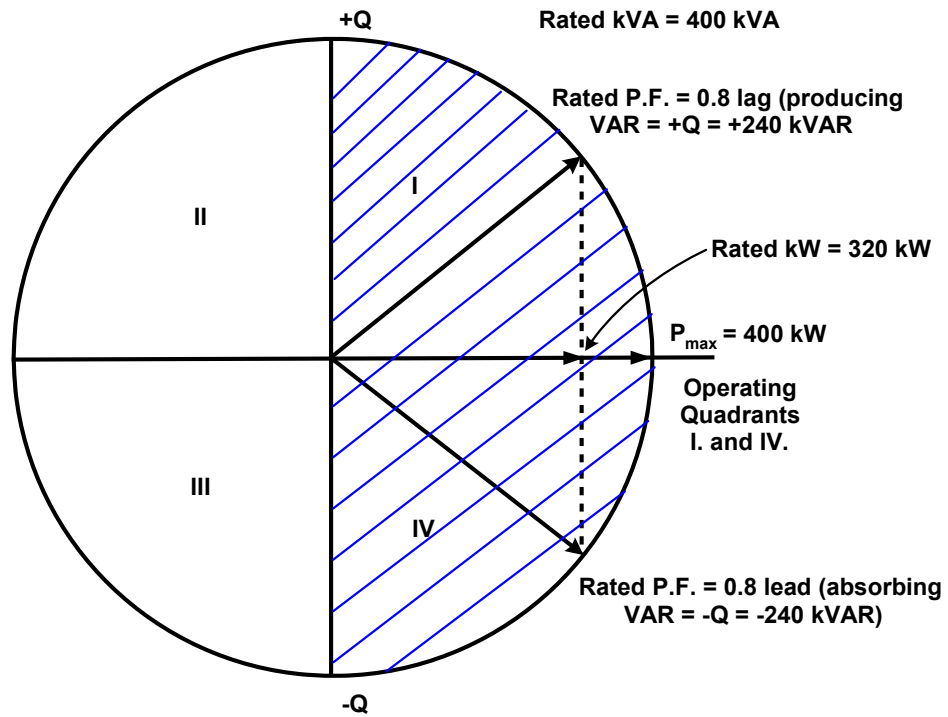
The voltage regulation simulations that were conducted and Strategy 17, which was used for field verification, are outlined in Table 12.



Operating Points

- (a) Points ① and ② is rated kW and rated kVAR
- (b) Point ③ rated kVA and rated lagging P.F.
- (c) Point ④ leading P.F.
- (d) Point ⑤ maximum kW
- (e) Point ⑥ minimum kW and maximum kVAR (synchronous condenser)
- (f) Points ⑦ and ⑧ fixed power factor lagging and leading

Figure 27. DG control strategies for 1000 kW synchronous machine

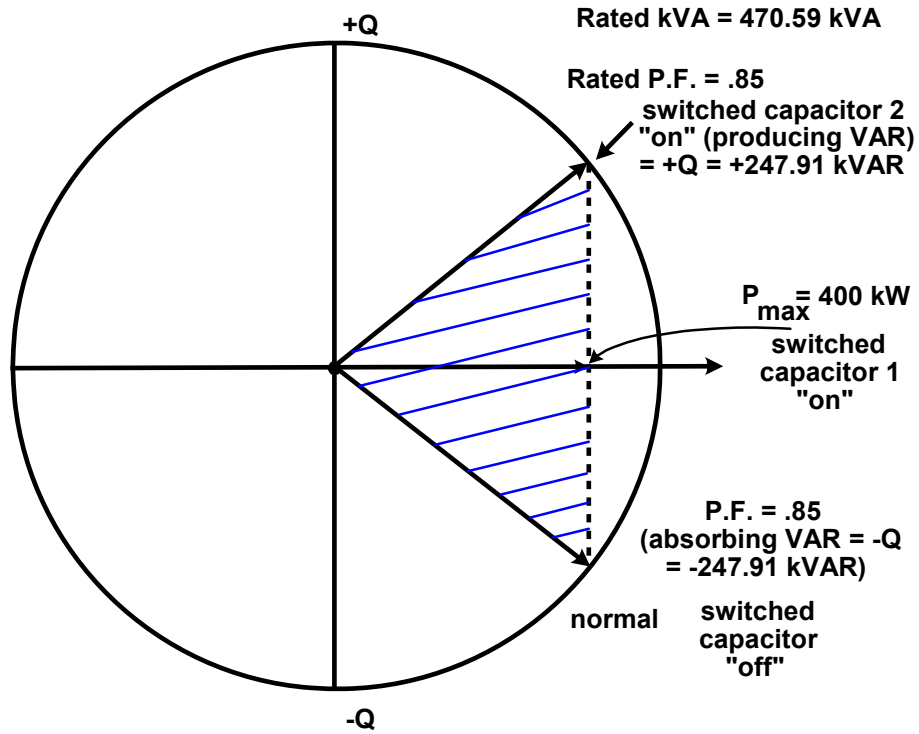


Note (4): DR Control Strategies

- (a) Peak shave, P fixed
- (b) P.F. = unity, P variable
- (c) \pm P.F. constant, P variable
- (d) \pm Q (VAR volt. reg.) P = 0
- (e) $P \pm jQ$ (optimizing) - see synchronous machine
- (f) Frequency Dithering (anti-islanding)

Note (5): (f) not included in model

Figure 28. DG control strategies for 400 kW high-speed generator and inverter in current mode



- (a) Peak shave, P fixed
- (b) P.F. = unity, P fixed
- (c) \pm P.F. constant at P fixed
- (d) \pm Q fixed, P fixed same as (c)

Note (4) Induction machine with inverter is the same as Inverter where the speed is varied to create variable dc output after the rectifier and the ac current output from the inverter are phase shifted (switching) to produce a variable P.F. with respect to the system voltage.

Figure 29. DG control strategies for 400 kW self-excited induction generator

Table 12. Matrix of Voltage Regulation Simulations and Control Strategy 17 for Field Verification

Test Numbers	Reference. Section	Primary Voltage Spread (a)87% (b) 92% (c)93% (d) 95% (e) 98% (f) 105%	Peak Load Day 24 Hourly quantities	Light Load Day 24 Hourly quantities	LTC ± 16 steps & neutral	Line					DR (Synchronous Machine) Locations (1)			
						Regulator		Capacitors			Near End	Midpoint (Actual Site)	Far End	
						#1	#2	#1	#2	#3				
1	I.A.	(a) (d) (f)	x	x										
2	I.B.	(d) (f)	x	x	x									
3	I.C.	(d) (f)	x	x	x	x								
4	I.C. '	(d) (f)	x	x	x	x	x							
5	I.D.	(d) (f)	x	x	x			x						
6	I.D. '	(d) (f)	x	x	x			x	x					
7	I.D. "	(d) (f)	x	x	x			x	x	x				
8	I.E.	(d) (f)	x	x	x	x	x	x	x	x				
9	II.A.	x	x	x							(b) (d) (e)			
10	II.B.	x	x	x							(b) (d) (e)			
11	II.C.	x	x	x								(b) (d) (e)		
12	II.D.	Repeat II.A., II.B., II.C. turn on LTC												
13	II.E.	Repeat II.A., II.B., II.C. turn on LTC, and Regulator (1)												
14	II.F.	Repeat II.A., II.B., II.C. turn on LTC, and Regulator (1) and (2)												
15	II.G.	Repeat II.A., II.B., II.C. turn on LTC, and Regulator (1) and (2) and Cap. (1)												
16	II.H.	Repeat II.A., II.B., II.C. turn on LTC, and Regulator (1) and (2) and Cap. (1), (2)												
17	II.I.	Repeat II.A., II.B., II.C. turn on LTC, and Regulator (1) and (2) and Cap. (1), (2), (3)												
18														
19														
20														
21														
22														
23														
24														
25														
Note (1): DR Control Strategies														
(a.) The DR is operated at fixed real power output and normally is scheduled to run during peak periods when the cost of DR generation is lower than host utility cost. The Q is zero at the PCC. 984 kW rated														
(b.) The DR is operated at unity P.F. with variable power output. 492 kW (50%) to 1050 kW max.														
(c.) DR is operated at a fixed power factor either lead or lag (for example ± 0.8 P.F.) with variable P and Q to not violate voltage criteria.														
(d.) The DR is operated as a synchronous condenser with minimum watts and variable VARs to regulate voltage. 246 kW (25% of rated)														
(e.) DR is operated with variable P and Q and is used to optimize to a specific set of criteria such as minimize real losses, minimize reactive losses, regulate voltage and maximize released capacity.														

Test Numbers	Reference. Section	Primary Voltage Spread (a)87% (b) 92% (c)93% (d) 95% (e) 98% (f) 105%	Peak Load Day 24 Hourly quantities	Light Load Day 24 Hourly quantities	LTC + 16 steps & neutral	Line Regulator					Capacitors			DR (Induction Generator) Locations		
						#1	#2	#1	#2	#3	Near End	Midpoint (Actual Site)	Far End			
1		(a) (d) (f)														
2		(d) (f)														
3		(d) (f)														
4		(d) (f)														
5		(d) (f)														
6		(d) (f)														
7		(d) (f)														
8		(d) (f)														
9	II.A.	x	x	x								(b) (d)				
10	II.B.	x	x	x								(b) (d)				
11	II.C.	x	x	x										(b) (d)		
12	II.D.	Repeat II.A., II.B., II.C. turn on LTC														
13	II.E.	Repeat II.A., II.B., II.C. turn on LTC and Regualator (1)														
14	II.F.	Repeat II.A., II.B., II.C. turn on LTC and Regulators (1) & (2)														
15	II.G.	Repeat II.A., II.B., II.C. turn on LTC, Reg. (1) & (2) and Cap (1)														
16	II.H.	Repeat II.A., II.B., II.C. turn on LTC, Reg. (1) & (2) and Cap (1) and (2)														
17	II.I.	Repeat II.A., II.B., II.C. turn on LTC, Reg (1) & (2) and Cap (1), (2) & (3)														
18	III.	Repeat synchronous and inverter generation														
19	IV.	Repeat synchronous, inverter and induction generation														
20																
21																
22																
23																
24																
25																
26																
27																
28																
29																

Test Numbers	Reference. Section	Primary Voltage Spread (a)87% (b) 92% (c)93% (d) 95% (e) 98% (f) 105%	Peak Load Day 24 Hourly quantities	Light Load Day 24 Hourly quantities	LTC + 16 steps & neutral	Line Regulator					Capacitors			DR (Induction Generator) Locations				
						#1	#2	#1	#2	#3	Near End	Midpoint (Actual Site)	Far End					
														DR (Induction Generator) Locations (a)Peak shave, P fixed (b) P.F.= Unity, P fixed (c) ± P.F. Constant, P fixed (d) ± Q fixed, P fixed same as (c)				
1		(a) (d) (f)																
2		(d) (f)																
3		(d) (f)																
4		(d) (f)																
5		(d) (f)																
6		(d) (f)																
7		(d) (f)																
8		(d) (f)																
9	II.A.	x	x	x									(b) (d)					
10	II.B.	x	x	x									(b) (d)					
11	II.C.	x	x	x												(b) (d)		
12	II.D.	Repeat II.A., II.B., II.C. turn on LTC																
13	II.E.	Repeat II.A., II.B., II.C. turn on LTC and Regualator (1)																
14	II.F.	Repeat II.A., II.B., II.C. turn on LTC and Regulators (1) & (2)																
15	II.G.	Repeat II.A., II.B., II.C. turn on LTC, Reg. (1) & (2) and Cap (1)																
16	II.H.	Repeat II.A., II.B., II.C. turn on LTC, Reg. (1) & (2) and Cap (1) and (2)																
17	II.I.	Repeat II.A., II.B., II.C. turn on LTC, Reg (1) & (2) and Cap (1), (2) & (3)																
18	III.	Repeat synchronous and inverter generation																
19	IV.	Repeat synchronous, inverter and induction generation																
20																		
21																		
22																		
23																		
24																		
25																		
26																		
27																		
28																		
29																		

6.0 Results for Field Verification of Models

This section describes the verification of the models using field test data. The voltage regulation models were developed in Section 3.0 for the LTC transformer at the substation, the bidirectional step regulators, the capacitors, all the distribution circuit transformer connections, and the line sections. In addition, models for synchronous, induction, and inverter-type generators were given.

Field verifications were conducted using the metering equipment defined in Section 4.0, and DG generation control for the 1000 kW synchronous generator was described in Section 5.0. The control strategy used was Strategy 17, in which all three capacitors (1, 2, and 3), the regulator (1), and the substation LTC would be turned on.

Field verification studies were conducted for the circuit peak day July 17, 2006, at 17:43 hours; on July 29, 2006, at 17:11 hours when the 1000 kW DG was running; and on July 31, 2006, at 17:56 hours when the DG was turned off.

6.1 Circuit and Generation Measured Data

The nodes where measured data were taken on the circuit and node D (node 10), where the generation unit is interconnected to the circuit, were shown in Figure 25. Test dates and data collection periods are presented in Table 13.

Table 13. Test Dates and Data Collection Periods

Date	Circuit Start	Circuit Peak	Circuit End	Generation Start (postgeneration start)	Generation End (pregeneration off)
7/17/06	10:42	17:43	23:58	17:28	21:23
7/29/06	00:11	17:11	23:56	17:11	20:16
7/31/06	00:11	17:56	23:56	← generator →	
8/02/06	00:11	17:56	23:56	10:26	12:16

There is a time delay between the initiation of the “start” generator command and the time when the unit is synchronized and carrying load, and a time delay between the initiation of the “stop” generator command and the time when the generator is not carrying load. Therefore, the times given in the Table 13 are the postgeneration start (the time the unit is carrying load) and the pregeneration off (the time the unit is still carrying load but has received the “stop” generator command).

**Illustrative Example of Generation Run Time and
Distribution Circuit Time Stamps for Simulation Studies
and Field Verification**

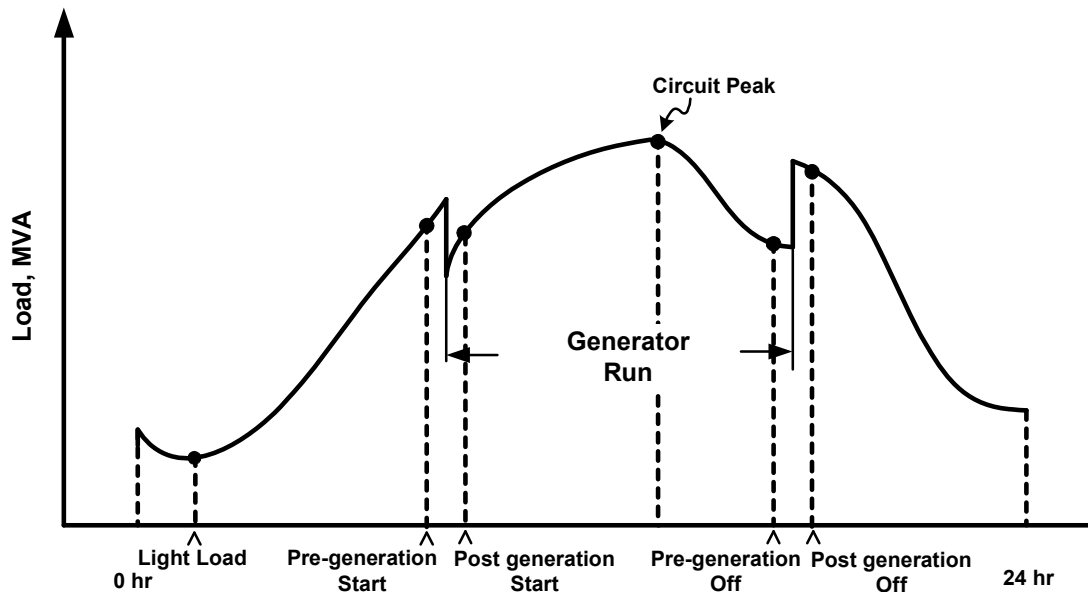


Figure 30. Daily circuit load profile and time stamps

These times are illustrated in Figure 30. As shown in Table 13, there were four days during the summer when tests were conducted and four days when measured data were collected. The first two days, July 17 and 29, 2006, the 1000 kW DG was turned on to offset the circuit peak load, and on July 31, this DG was turned off. This was done to determine whether there was a difference in the variance between simulation and field measured data when the DG was running and when the DG was not running.

Simulations and comparisons with field measured data were not conducted on the last test day, August 2, 2006, because the load of the South Branch of the Milford Circuit DC 8103 had been cut over to a circuit fed from the Page Substation on August 1 at 19:00 hours. This removed approximately 2 MVA load (there was a 15.92 MVA peak before the cutover vs. a 13.98 MVA peak after it) from the Milford Circuit DC 8103. See Table 14.

The time of circuit peak data and generation data are given in Table 14 for the four test days. The measured data consist of :

1. Circuit peak kVA
2. Circuit phase currents at Substation node 1
3. Generation line currents at node 10
4. Generation line-to-line voltages at node 10
5. Generation three-phase power factor at node 10
6. Generation three-phase kW, kVAR, and kVA at node 10.

6.2 Bidirectional Voltage Regulator Measured Data

The bidirectional voltage regulator measured data for the circuit peak time of each test day are given in Table 15 and listed below for each phase regulator at node 9.

1. Load current
2. Load power factor
3. kW load
4. kVA load
5. kVAR load
6. Voltage 120 V base

6.3 Circuit Equipment (Capacitors) and Customer Measured Data

The measured data at the time of circuit peak for each of the three capacitors located at nodes 6, 12, and 13 on the respective test days are given in Table 16, and they consist of the phase currents and phase voltages. Also given in the table are the customer-measured data for node I, consisting of I_a and I_c phase currents; node L, the V_C phase voltage; and node K, the V_A phase voltage.

6.4 Percent Variance Between Simulated and Field Measured Data

Table 17 and Table 18 compare simulated data and field measured data for the two test days when the DG generation unit is running. Table 19 shows similar data when the DG is turned off. The field data for the phase currents, phase voltages, and phase power factors of the circuit, generator, and the VR1 bidirectional regulator are given for node 1, node 10, and node 9, respectively, on the left side of the tables. The corresponding simulation data are shown on the right side of these tables.

The measured phase currents and phase voltages for the three capacitors and their respective simulation data are also given in the tables. However, the simulated voltage data have been reduced by 3.67 V to reduce the measured primary voltage to secondary voltage values. Finally, customer-measured current and voltage data and simulation data for nodes I and L are listed.

Table 20 shows the percent variance between actual and simulated current, voltage, and power factor for each node and summarizes the difference between measured and simulated values. For three-phase quantities, the percent variance is calculated as the absolute value of the sum of the differences between the actual and simulated values divided by three and then dividing by the average of the actual three-phase values. The result is multiplied by 100 to represent the percent difference using the average of the actuals as the base. For single-phase quantities, the percent variance is the absolute value of the difference divided by the actual as the base and multiplying by 100.

Table 14. Circuit and Generation Measured Data

Circuit Generator		Start:	7/17/2006 10:42	End:	7/17/2006 23:58													
Generator Start:		7/17/2006 17:28	End:	7/17/2006 21:23														
Date	Time	Circuit Load Including Generation	Node 1 Circuit Phase Currents			Node 10 Generation Data												
		5 Minute Integrated	15 minute Integrated			Line Current			Line to Line V			120 Volt Base						
		3 phase kVA	Ia	Ib	Ic	3 phase KW	3phase Kvar	3 phase Kva	power factor	Ia	Ib	Ic	Va	Vb	Vc	Va	Vb	Vc
Circuit Start	7/17/2006 10:42	10,101.50	384.00	419.00	442.00	-	-	-	-	-	-	-	-	-	-	-	-	-
Circuit Peak	7/17/2006 17:43	15,257.22	565.00	651.00	637.00	433.00	120.50	449.45	0.96	503.60	474.10	467.60	490.00	490.00	481.00	122.50	122.50	120.25
Circuit Generator		Start:	7/29/2006 00:11	End:	7/29/2006 23:56													
Generator Start:		7/29/2006 17:11	End:	7/29/2006 20:16														
Date	Time	Circuit Load Including Generation	Node 1 Circuit Phase Currents			Node 10 Generation Data												
		5 Minute Integrated	15 Minute Integrated			Line Current			Line to Line V			120 Volt Base						
		3 phase kVA	Ia	Ib	Ic	3 phase KW	3phase Kvar	3 phase Kva	power factor	Ia	Ib	Ic	Va	Vb	Vc	Va	Vb	Vc
Circuit Start	7/29/2006 0:11	7,596.38	270.00	319.00	332.00	-	-	-	-	-	-	-	-	-	-	-	-	-
Circuit Peak	7/29/2006 17:11	14,670.96	562.00	635.00	615.00	166.19	33.75	167.00	0.94	222.00	193.00	188.00	489.00	489.00	483.00	122.25	122.25	120.75
Circuit Generator		Start:	7/31/2006 00:11	End:	7/31/2006 23:56													
Generator Start:		7/31/2006 16:11	End:	7/31/2006 17:11														
Date	Time	Circuit Load Including Generation	Node 1 Circuit Phase Currents			Node 10 Generation Data												
		5 Minute Integrated	15 Minute Integrated			Line Current			Line to Line V			120 Volt Base						
		3 phase kVA	Ia	Ib	Ic	3 phase KW	3phase Kvar	3 phase Kva	power factor	Ia	Ib	Ic	Va	Vb	Vc	Va	Vb	Vc
Circuit Start	7/31/2006 0:11	6,947.16	248.00	301.00	304.00	-	-	-	-	-	-	-	-	-	-	-	-	-
Circuit Peak	7/31/2006 17:56	15,917.42	604.00	696.00	678.00	-	-	-	-	-	-	-	-	-	-	-	-	-
Circuit Generator		Start:	8/2/2006 00:11	End:	8/2/2006 23:56													
Generator Start:		8/2/2006 10:26	End:	8/2/2006 12:16														
Date	Time	Circuit Load Including Generation	Node 1 Circuit Phase Currents			Node 10 Generation Data												
		5 Minute Integrated	15 Minute Integrated			Line Current			Line to Line V			120 Volt Base						
		3 phase kVA	Ia	Ib	Ic	3 phase KW	3phase Kvar	3 phase Kva	power factor	Ia	Ib	Ic	Va	Vb	Vc	Va	Vb	Vc
Circuit Start	8/2/2006 0:11	10,241.28	428.00	408.00	448.00	-	-	-	-	-	-	-	-	-	-	-	-	-
Generator	8/2/2006 12:16	11,277.14	475.00	433.00	469.00	409.00	112.00	424.06	0.97	551.50	500.00	447.00	489.00	489.00	488.00	122.25	122.25	122.00
Circuit Peak	8/2/2006 17:56	13,976.61	601.00	557.00	611.00	-	-	-	-	-	-	-	-	-	-	-	-	-

August 1st moved south branch to Page Substation at 19:00

Table 15. Bidirectional Voltage Regulator Measured Data

Circuit Generator		Start: 7/17/2006 10:42	End: 7/17/2006 23:58					End: 7/17/2006 21:23														
Date	Time	East Regulator Phase A							North Regulator Phase B							South Regulator Phase C						
		Load Current	Load Power Factor	Load Kva	Load KW	Load Kvar	Load Voltage	Load Voltage 120V Base	Load Current	Load Power Factor	Load Kva	Load KW	Load Kvar	Load Voltage	Load Voltage 120V Base	Load Current	Load Power Factor	Load Kva	Load KW	Load Kvar	Load Voltage	Load Voltage 120V Base
Circuit Start	7/17/2006 10:42	132.20	0.98	1,039.00	1,021.00	190.00	7,857.51	123.72	126.90	0.99	998.00	984.00	169.00	7,868.23	123.89	120.50	0.98	946.00	929.00	179.00	7,852.46	123.64
Circuit Peak	7/17/2006 17:43	282.60	0.94	2,216.00	2,088.00	742.00	7841.79	123.48	255.70	0.95	2,009.00	1,913.00	612.00	7855.34	123.69	238.00	0.94	1,877.00	1,772.00	619.00	7887.05	124.19
Circuit Generator		Start: 7/29/2006 00:11	End: 7/29/2006 23:56					End: 7/29/2006 20:16														
Date	Time	East Regulator Phase A							North Regulator Phase B							South Regulator Phase C						
		Load Current	Load Power Factor	Load Kva	Load KW	Load Kvar	Load Voltage	Load Voltage 120V Base	Load Current	Load Power Factor	Load Kva	Load KW	Load Kvar	Load Voltage	Load Voltage 120V Base	Load Current	Load Power Factor	Load Kva	Load KW	Load Kvar	Load Voltage	Load Voltage 120V Base
Circuit Start	7/29/2006 0:11	157.80	0.89	1,248.00	1,110.00	570.00	7,908.95	124.53	138.80	0.90	1,096.00	991.00	468.00	7,896.23	124.33	143.40	0.88	1,133.00	1,000.00	533.00	7,901.98	124.42
Circuit Peak	7/29/2006 17:11	312.30	0.93	2,464.00	2,286.00	917.00	7887.81	124.20	296.60	0.94	2,331.00	2,190.00	798.00	7859.16	123.75	279.70	0.93	2,195.00	2,041.00	806.00	7,847.19	123.56
Circuit Generator		Start: 7/31/2006 00:11	End: 7/31/2006 23:56					End: 7/31/2006 17:11														
Date	Time	East Regulator Phase A							North Regulator Phase B							South Regulator Phase C						
		Load Current	Load Power Factor	Load Kva	Load KW	Load Kvar	Load Voltage	Load Voltage 120V Base	Load Current	Load Power Factor	Load Kva	Load KW	Load Kvar	Load Voltage	Load Voltage 120V Base	Load Current	Load Power Factor	Load Kva	Load KW	Load Kvar	Load Voltage	Load Voltage 120V Base
Circuit Start	7/31/2006 0:11	271.10	0.89	2,139.00	1,903.00	977.00	7,891.57	124.26	256.90	0.90	2,029.00	1,829.00	878.00	7,898.27	124.37	241.10	0.89	1,892.00	1,680.00	871.00	7,851.34	123.63
Circuit Peak	7/31/2006 17:56	369.00	0.94	2,882.00	2,695.00	1,021.00	7811.26	123.00	355.00	0.94	2,813.00	2,640.00	971.00	7924.79	124.78	314.00	0.93	2,486.00	2,317.00	900.00	7897.24	124.35
Circuit Generator		Start: 8/2/2006 00:11	End: 8/2/2006 23:56					End: 8/2/2006 12:16														
Date	Time	East Regulator Phase A							North Regulator Phase B							South Regulator Phase C						
		Load Current	Load Power Factor	Load Kva	Load KW	Load Kvar	Load Voltage	Load Voltage 120V Base	Load Current	Load Power Factor	Load Kva	Load KW	Load Kvar	Load Voltage	Load Voltage 120V Base	Load Current	Load Power Factor	Load Kva	Load KW	Load Kvar	Load Voltage	Load Voltage 120V Base
Circuit Start	8/2/2006 0:11	116.00	0.91	917.00	833.00	384.00	7,907.76	124.52	113.00	0.91	895.00	818.00	361.00	7,914.87	124.63	107.30	0.89	845.00	753.00	383.00	7,873.56	123.98
Generator	8/2/2006 12:16	170.10	0.96	1,334.00	1,287.00	352.00	7,844.62	123.52	154.10	0.98	1,210.00	1,185.00	246.00	7,854.76	123.68	149.40	0.97	1,167.00	1,136.00	267.00	7,811.54	123.00
Circuit Peak	8/2/2006 17:56	259.70	0.93	2,059.00	1,924.00	734.00	7,929.52	124.86	247.60	0.95	1,950.00	1,856.00	595.00	7,873.08	123.97	227.90	0.94	1,794.00	1,691.00	599.00	7,872.60	123.96

August 1st moved south branch to Page Substation at 19:00

Table 16. Circuit Equipment and Customer Measured Data

Date		Time		Node F/6 Capacitor 1 (900 Kvar)						Node G/12 Capacitor 2 (900 Kvar)						Node H/13 Capacitor 3 (1200 Kvar)					
		Phase Currents			Phase Voltages			Phase Currents			Phase Voltages			Phase Currents			Phase Voltages				
		la	lb	lc	Va	Vb	Vc	la	lb	lc	Va	Vb	Vc	la	lb	lc	Va	Vb	Vc		
Circuit Start	7/17/2006	10:42																			
Generator Start	7/17/2006	17:28																			
Circuit Peak	7/17/2006	17:43	48.57	108.20	13.00	118.25	117.75	121.08	51.96	14.00	23.83	120.65	118.40	118.65	65.84	27.09	53.70	117.05	116.93	118.	

Date		Time		Node I			Node K	Node L
		la	lb	lc	Va	Vc		
Circuit Start	7/17/2006	10:42	32.00	-	19.00	-	120.05	
Circuit Peak	7/17/2006	17:43	46.00	-	31.00	-	117.60	

Date		Time		Node F/6 Capacitor 1 (900 Kvar)						Node G/12 Capacitor 2 (900 Kvar)						Node H/13 Capacitor 3 (1200 Kvar)					
		Phase Currents			Phase Voltages			Phase Currents			Phase Voltages			Phase Currents			Phase Voltages				
		la	lb	lc	Va	Vb	Vc	la	lb	lc	Va	Vb	Vc	la	lb	lc	Va	Vb	Vc		
Circuit Start	7/29/2006	0:11	23.82	47.09	8.78			24.69	5.42	10.78				27.23	12.53	31.53					
Circuit Peak	7/29/2006	17:11	50.45	103.25	10.34			54.29	13.02	24.72				50.05	18.57	47.97					

Date		Time		Node F/6 Capacitor 1 (900 Kvar)						Node G/12 Capacitor 2 (900 Kvar)						Node H/13 Capacitor 3 (1200 Kvar)					
		Phase Currents			Phase Voltages			Phase Currents			Phase Voltages			Phase Currents			Phase Voltages				
		la	lb	lc	Va	Vb	Vc	la	lb	lc	Va	Vb	Vc	la	lb	lc	Va	Vb	Vc		
Circuit Start	7/31/2006	0:11	22.12	44.79	7.74			21.23	5.81	10.16				30.38	14.65	31.88					
Circuit Peak	7/31/2006	17:56	51.53	108.84	11.78			49.30	14.93	23.96				62.18	27.37	54.05					

Date		Time		Node F/6 Capacitor 1 (900 Kvar)						Node G/12 Capacitor 2 (900 Kvar)						Node H/13 Capacitor 3 (1200 Kvar)					
		Phase Currents			Phase Voltages			Phase Currents			Phase Voltages			Phase Currents			Phase Voltages				
		la	lb	lc	Va	Vb	Vc	la	lb	lc	Va	Vb	Vc	la	lb	lc	Va	Vb	Vc		
Circuit Start	8/2/2006	0:11	34.58	77.96	10.80			41.65	9.95	18.72				47.89	23.05	52.07					
Generator Start	8/2/2006	12:16	37.82	86.89	12.02			42.15	13.98	18.46				52.82	23.95	50.02					
Circuit Peak	8/2/2006	17:56	52.56	109.82	13.40			51.40	15.32	24.46				52.27	20.09	55.17					

Date		Time		Node K	Node L
		Va	Vc		
Circuit Start	8/2/2006	0:11		-	
Generator Start	8/2/2006	12:16	119.15	-	

Notes

- (1): August 1st moved south branch to Page Substation at 19:00
- (2): Voltage Data At Capacitor Locations Not Available from July 26 until August 22
- (3): All Capacitor Phase Voltages Are Measured On The Secondary Side At The Customer's Meter
- (4): All Capacitor Phase Currents Are Measured On The Primary

Table 17. Field Verification Data – 7/17/06 – DR Generation On

Location	Node	Field Data - 7/17/06 - Circuit Peak 17:43									Simulation								
		Current			Voltage			PF			Current			Voltage			PF		
		A	B	C	A	B	C	A	B	C	A	B	C	A	B	C	A	B	C
Start of Circuit	1	565.00	651.00	637.00	126.00	126.00	126.00	0.95	0.95	0.95	554.54	637.77	619.97	125.86	125.80	125.39	0.93	0.92	0.93
			2.2%			0.3%													
Generator	10	18.31	17.24	17.00	122.50	122.50	120.25	0.96	0.96	0.96	17.49	17.25	17.36	121.68	123.38	122.62	0.96	0.96	0.96
			2.3%			1.1%													
VR 1	9	282.60	255.70	238.00	123.48	123.69	124.19	0.94	0.95	0.94	274.07	246.07	227.56	123.60	123.82	123.62	0.93	0.94	0.93
			3.7%			0.2%													
Cap 1*	6	48.57	108.20	13.00	118.25	117.75	121.08				48.03	104.47	13.77	121.25	121.14	123.29			
			3.0%			0.7%								<i>117.58</i>	<i>117.47</i>	<i>119.62</i>			
Cap 2*	12	51.96	14.00	23.83	120.65	118.40	118.65				52.18	14.87	24.53	120.51	123.09	121.87			
			2.0%			1.5%								<i>116.84</i>	<i>119.42</i>	<i>118.20</i>			
Cap 3*	13	65.84	27.09	53.70	117.05	116.93	118.15				64.44	27.92	50.18	119.04	121.44	120.03			
			3.9%			1.2%								<i>115.37</i>	<i>117.77</i>	<i>116.36</i>			
Node I	16	46.00		31.00							32.73		22.94						
			38.3%																
Node L*	18				117.60									121.42					
						0.1%								<i>117.75</i>					

*The voltage measurements were taken at the customer's meter. Therefore, an average voltage drop of 3.67 V was included to reduce the primary voltage to the secondary voltage for the comparison shown in the table.

Table 18. Field Verification Data – 7/29/06 – DR Generation On

Location	Node	Field Data - 7/29/06 - Circuit Peak 17:11									Simulation								
		Current			Voltage			PF			Current			Voltage			PF		
		A	B	C	A	B	C	A	B	C	A	B	C	A	B	C	A	B	C
Start of Circuit	1	562.00	635.00	615.00							564.59	636.69	616.03	126.46	126.34	125.91	0.91	0.92	0.90
			0.3%																
Generator	10	8.07	7.08	6.84	122.25	122.25	120.75	0.98	0.98	0.98	7.30	7.19	7.22	121.76	123.67	123.17	0.98	0.98	0.98
			5.7%																
VR 1	9	312.30	296.60	279.70	124.20	123.75	123.56	0.93	0.94	0.93	316.35	299.29	284.46	123.92	124.46	124.48	0.92	0.92	0.92
			1.3%																
Cap 1	6	50.45	103.25	10.34							49.80	100.44	11.10						
			2.6%																
Cap 2	12	54.29	13.02	24.72							54.48	13.91	25.46						
			2.0%																
Cap 3	13	50.05	18.57	47.97							49.11	19.56	45.29						
			4.0%																

Table 19. Field Verification Data – 7/31/06 – DR Generation Off

Location	Node	Field Data - 7/31/06 - Circuit Peak 17:56									Simulation								
		Current			Voltage			PF			Current			Voltage			PF		
		A	B	C	A	B	C	A	B	C	A	B	C	A	B	C	A	B	C
Start of Circuit	1	604.00	696.00	678.00							608.76	699.59	678.97	126.26	126.14	125.58	0.92	0.92	0.91
			0.5%																
Generator	10	N/A	N/A	N/A	N/A	N/A	N/A	N/A	N/A	N/A									
VR 1	9	369.00	355.00	314.00	123.00	124.78	124.35	0.94	0.94	0.93	376.11	362.02	324.22	122.93	123.63	123.61	0.93	0.92	0.92
			2.3%																
Cap 1	6	51.53	108.84	11.78							50.82	105.52	12.49						
			2.8%																
Cap 2	12	49.30	14.93	23.96							48.74	15.69	24.55						
			2.2%																
Cap 3	13	62.18	27.37	54.05							60.45	28.03	49.14						
			5.1%																

6.5 Summary of Variance Results

From Table 20, we see that the percent variance between actual field measured data and the simulated data is less than 6% (5.7% actual) for the phase currents throughout the circuit, except for node I, where the percent unbalanced current is very high. The highest percent variance for the phase voltages throughout the circuit is 1.5%, whereas the highest percent variance for the power factor is 5.7% at the start of the circuit. Note that the lowest percent variances occur on the load side of the step regulators, because these regulators are individually phase-controlled and not gang-operated, as the LTC at the substation.

As shown in the percent variance data in Table 20, the simulated data closely match actual field-measured data in most cases; the models developed in Section 3.0 can be used to estimate phase currents, phase voltages, and power factors without the use of extensive circuit metering. However, knowing the phasing of the loads is paramount in accurate data simulation. No significant difference in the percent variance occurred when the variance data were compared for the situation in which the DG is turned on and that in which it is turned off.

**Table 20. Percent Variance Between Actual and Simulated
Currents, Voltages, and Power Factors**

Location	Node	Current	Voltage	P.F.
Test Day 7/17/06 DR Generation Running				
Start of Circuit	1	2.2	0.3	5.7
Generator	10	2.3	1.1	0.0
Voltage Regulator	9	3.7	0.2	2.4
Capacitor 1	6	3.0	0.7	--
Capacitor 2	12	2.0	1.5	--
Capacitor 3	13	3.9	1.2	--
Node I	16	38.3	--	--
Node L	18	--	0.1	--
Test Day 7/29/06 DR Generation Running				
Start of Circuit	1	0.3	--	--
Generator	10	5.7	1.2	0.0
Voltage Regulator	9	1.3	0.5	3.4
Capacitor 1	6	2.6	--	--
Capacitor 2	12	2.0	--	--
Capacitor 3	13	4.0	--	--
Test Day 7/31/06 DR Generation Off				
Start of Circuit	1	0.5	--	--
Generator	N/A	N/A	N/A	N/A
Voltage Regulator	9	2.3	0.5	3.4
Capacitor 1	6	2.8	--	--
Capacitor 2	12	2.2	--	--
Capacitor 3	13	5.1	--	--

7.0 Conclusions and Recommendations

Conclusions

The distribution circuit selected was a 13.2 kV three-phase wye-multigrounded system that serves approximately 76.2% residential, 4.0% commercial, and 19.8% light industrial customers. The load on the summer peak day was 15.3 MVA, and the summer peak day minimum load was 5.91 MVA. A 1000 kW synchronous generator, installed at the midpoint of the circuit, offset the peak load on July 17, 2006, by 449.5 kVA. There were no voltage violations on the circuit. The lowest single-phase measured voltage was 117.60 V on phase C versus a simulated value of 117.75 V.

Models were developed for the 10 MVA LTC delta wye-grounded substation transformer, the 167 kVA bidirectional voltage regulators, the three wye-grounded capacitors, line impedances, and all distribution circuit transformer connections (9 cases).

The line loss model was validated using three line configurations and balanced and unbalanced load conditions. The three line configurations studied were the balanced impedance triangular spacing configuration, or equilateral configuration; the flat configuration nontransposed; and the flat configuration transposed. The purpose of the validation was to show that with a balanced line impedance and balanced load, kW losses are the same in each phase, and the total kW losses are the lowest. In addition, an example was provided to show that even though the kW losses per phase are not correct (owing to the Kron reduction process from a 4x4 matrix to a 3x3 matrix), the total losses for the three phases are in fact correct.

Models were developed for the 1000 kW synchronous generator, the self-excited 400 kW induction generator, and the 400 kW high-speed generator and inverter generator system.

The line, equipment, and generation models were verified with the maximum phase current variance of 3.9% on July 17, 2006, and 5.7% on July 29, 2006, except for node I, where the percent unbalance current was very high. The maximum phase voltage variance was 1.5% on July 17 and 1.2% on July 29. The maximum power factor variance did not exceed 5.7% on July 17 and 3.4% on July 29.

Three voltage control strategies were tested for the 400 kW induction generator and were tested at low and high substation primary voltage for a total of 6 simulations. Three voltage control strategies for the 400 kW inverter-based generation were tested at low and high substation primary voltage, for a total of 6 simulations. And 13 voltage control strategies were simulated for high voltage and 13 for low voltage for the synchronous generator located at the beginning location of the circuit, at the mid-location, and at the end location, for a total of 78 simulations.

The maximum released capacity of 10.44% was achieved with the 1000 kW synchronous generator, with $P = 100\%$ and $Q = 100\%$.

The optimum location for the DG with the highest released capacity of 10.44% is at the source of the circuit, because it directly offsets the load current and load losses of the circuit. The optimum DG location to achieve the greatest loss reduction is at the midpoint location of the circuit, because adding generation here reduces, on a pro rata basis, the load and the length of the circuit, and thus there are reduced losses. There is little difference between locating the DG at the midpoint or end of the circuit to improve the voltage regulation; there is a slightly better improvement at the midpoint for circuits in which the conductor size of the entire three-phase backbone is the same.

Recommendations

Distributed generation can be used to reduce real peak losses and to improve voltage regulation and release capacity. This project used validated circuit models and a validated VDC load model to test 78 synchronous generator voltage control strategies. The voltage-dependent current model best represented the load characteristics of the circuit.

Future research should fund the development of a real-time optimal control of one or more DG units to accomplish the optimum generator voltage control condition, including the control of the substation transformer LTC, the bidirectional step regulators, and the switched capacitors. The cost to perform this development work on the Milford Circuit DC 8103 would be substantially lower than installing DG units and metering equipment on a new circuit, because all the equipment is already installed and tested. Furthermore, the newly developed control strategies can be tested in summer 2008. The estimated cost of this project would be less than \$500,000, and the development, testing, and analysis schedule is estimated to be approximately 1.5 years.

Benefits to California

Models have been developed and validated with measured test data. This project shows that adding DG units to a distribution circuit can reduce peak losses and improve generation capacity (released capacity), and these results can be achieved in 1 year rather than the 7 to 10 years associated with traditional central station generation. Also, improved voltage regulation results in fewer service voltage criteria violations and fewer distribution energy losses (approximately 10%).

8.0 References

Davis, M.W. *Determine the Market Penetration Limits of Distributed Energy Resources (by Distributed Generation Type) by the Year 2015*. Work performed under contract no. ADD-3-33906-01. Golden, CO: National Renewable Energy Laboratory; December 2003.

Davis, M.W.; Krupa, T.J.; Diedzic, M.J. "The Economics of Load Management on the Design and Operation of the Distribution System, Part II, Load Characteristics." *IEEE Transactions on Power Apparatus and Systems*, Vol. PA 8-102, No. 3, March 1983; pp. 654-674.

Kersting, W.H. "The Computation of Neutral and Dirt Currents and Power Losses." *IEEE Power Engineering Society Power Systems Conference and Exposition 2004*, Vol. 1, 10-13, October 2004; pp. 213-218.

REPORT DOCUMENTATION PAGE

Form Approved
OMB No. 0704-0188

The public reporting burden for this collection of information is estimated to average 1 hour per response, including the time for reviewing instructions, searching existing data sources, gathering and maintaining the data needed, and completing and reviewing the collection of information. Send comments regarding this burden estimate or any other aspect of this collection of information, including suggestions for reducing the burden, to Department of Defense, Executive Services and Communications Directorate (0704-0188). Respondents should be aware that notwithstanding any other provision of law, no person shall be subject to any penalty for failing to comply with a collection of information if it does not display a currently valid OMB control number.

PLEASE DO NOT RETURN YOUR FORM TO THE ABOVE ORGANIZATION.

1. REPORT DATE (DD-MM-YYYY) July 2007		2. REPORT TYPE Annual Subcontract Report		3. DATES COVERED (From - To) June 2006-June 2007	
4. TITLE AND SUBTITLE Modeling and Verification of Distributed Generation and Voltage Regulation Equipment for Unbalanced Distribution Power Systems				5a. CONTRACT NUMBER DE-AC36-99-GO10337	
				5b. GRANT NUMBER	
				5c. PROGRAM ELEMENT NUMBER	
6. AUTHOR(S) M.W. Davis, R. Broadwater, and J. Hambrick				5d. PROJECT NUMBER NREL/SR-581-41885	
				5e. TASK NUMBER WW88.2003	
				5f. WORK UNIT NUMBER	
7. PERFORMING ORGANIZATION NAME(S) AND ADDRESS(ES) M. W. Davis, DTE Energy, Detroit, MI; R. Broadwater, Electrical Distribution Design, Inc., Blacksburg, VA; J. Hambrick, Virginia Polytechnic Institute and State University, Blacksburg, VA				8. PERFORMING ORGANIZATION REPORT NUMBER ZAT-5-32616-06	
9. SPONSORING/MONITORING AGENCY NAME(S) AND ADDRESS(ES) National Renewable Energy Laboratory 1617 Cole Blvd. Golden, CO 80401-3393				10. SPONSOR/MONITOR'S ACRONYM(S) NREL	
				11. SPONSORING/MONITORING AGENCY REPORT NUMBER NREL/SR-581-41885	
12. DISTRIBUTION AVAILABILITY STATEMENT National Technical Information Service U.S. Department of Commerce 5285 Port Royal Road Springfield, VA 22161					
13. SUPPLEMENTARY NOTES NREL Technical Monitor: T. Basso					
14. ABSTRACT (Maximum 200 Words) This report summarizes the development of models for distributed generation and distribution circuit voltage regulation equipment for unbalanced power systems. The project also included verification, through actual field measurements, that the models accurately represent the power distribution system. The variance between actual field measurements and model simulation data did not exceed 5.7% for phase currents and 1.5% for phase voltages.					
15. SUBJECT TERMS modeling; distributed generation; unbalanced distribution power systems; voltage regulation equipment; validating distribution circuit models; National Renewable Energy Laboratory; NREL; DTE Energy					
16. SECURITY CLASSIFICATION OF:			17. LIMITATION OF ABSTRACT UL	18. NUMBER OF PAGES	19a. NAME OF RESPONSIBLE PERSON
a. REPORT Unclassified	b. ABSTRACT Unclassified	c. THIS PAGE Unclassified			19b. TELEPHONE NUMBER (Include area code)

Standard Form 298 (Rev. 8/98)
Prescribed by ANSI Std. Z39.18